[illegible] 1917

THE JOURNAL OF CHEMICAL PHYSICS

VOLUME 15 [illegible]

SEPTEMBER, 1947

Published by the
AMERICAN [illegible] OF PHYSICS
[illegible] York

exponents. The solidus (/) should be used wherever possible for fractions.

All illustrations should accompany manuscript and should always be referred to in the text. Line drawings must be made with India ink on plain white paper or on tracing cloth. Coordinate paper is not desirable, but if used must be blue-lined with all coordinates to be reproduced drawn with India ink. Lettering should be of sufficient size to be legible after reduction.

Proof and all correspondence concerning papers in the process of publication should be addressed to the Publications Manager, American Institute of Physics, 57 East 55 Street, New York 22, New York.

Subscription Rates

The United States and Possessions, Canada and Mexico $10.00

Elsewhere 11.00

Back Numbers

Complete set: Vol. 1, 1933—Vol. 14, 1946 (except Vol. 1, No. 1) $140.00

Yearly rate: $11.00.

Single copies: $1.00 each.

Subscriptions and orders for single copies should be addressed to Prince and Lemon Streets, Lancaster, Pennsylvania, or to the American Institute of Physics, 57 East 55 Street, New York 22, New York.

Changes of address should be sent to the Business Manager, American Institute of Physics.

Prince and Lemon Streets, Lancaster, Pennsylvania.

Entered as second-class matter at the Post Office at Lancaster, Pa., under the Act of August 24, 1912. Acceptance for mailing at special rate of postage provided for in paragraph 4, Section 538, P. L. & R.: authorized January 23, 1933.

THE JOURNAL
OF
CHEMICAL PHYSICS

VOLUME 15, NUMBER 9 · SEPTEMBER, 1947

The Relationship between the Brunauer-Emmett-Teller Adsorption Isotherm and the New Isotherm of Jura and Harkins

H. K. LIVINGSTON
Jackson Laboratory, E. I. duPont de Nemours and Company, Wilmington, Delaware

(Received April 28, 1947)

Values for the surface pressure and area of molecules adsorbed on solid surfaces can be calculated from the adsorption equation of Brunauer-Emmett-Teller. Over a wide pressure range these calculated values are in approximate agreement with the two-dimensional equation of state for vapor-condensed films. Since the adsorption equation of Jura and Harkins was derived from this same equation of state, it is concluded that for a great many experimental isotherms, the mathematical agreement between the two adsorption equations is so good that extremely accurate experimental work would be necessary to determine which equation was more nearly correct.

The Brunauer-Emmett-Teller equation gives calculated curves on Gregg-type plots that agree qualitatively with those reported by Gregg for multi-layer adsorptions. Surface-area values obtained from these curves by Gregg's *X*-point method are generally considerably higher than those that would be obtained by the method of Brunauer-Emmett-Teller.

The limiting area occupied by a molecule (i.e., in a mono-molecular layer) as calculated by the method of Harkins and Jura appears to decrease with decreasing energies of adsorption (i.e., decreasing values of c in the Brunauer-Emmett-Teller isotherm). It is suggested that this decrease is artificial, rather than real, and results from the assumption that the constant a in the two-dimensional equation of state does not vary with changes in the nature of the solid adsorbent.

It is not possible at the present time to suggest that one of the isotherms is to be preferred to the other on theoretical grounds. In general, preference should be given to the one which fits experimental data over the broader pressure range.

SYMBOLS

a = constant of the two-dimensional equation of state (2).
b = another constant of Eq. (2).
b' = intercept on the $k_1\pi$ axis of the straight-line equation (18).
c = constant of the Brunauer-Emmett-Teller adsorption isotherm (1).
k = constant used by Jura and Harkins to convert A values to Σ values.
k_1 = constant of straight-line equation (18).
k_2 = another constant of Eq. (18).
m = slope of straight-line equation (18).
p = pressure.
p_0 = saturation pressure.
v = volume of gas adsorbed per gram of adsorbent.
v_m = volume of gas which would correspond to a monomolecular layer on one gram of adsorbent.
v_0 = volume of gas adsorbed at saturation per gram of adsorbent.
A = constant of Jura and Harkins adsorption isotherm (9).
B = another constant of Eq. (9).
M = molecular weight of gas.
N = Avogadro's number.
R = gas constant.
T = absolute temperature.
V = volume of one mole of gas.
α = area occupied by each adsorbed molecule in a monomolecular layer.
π = surface pressure (change in free energy of the solid surface attributable to adsorption).
σ = area per molecule.
Σ = specific surface of adsorbent.

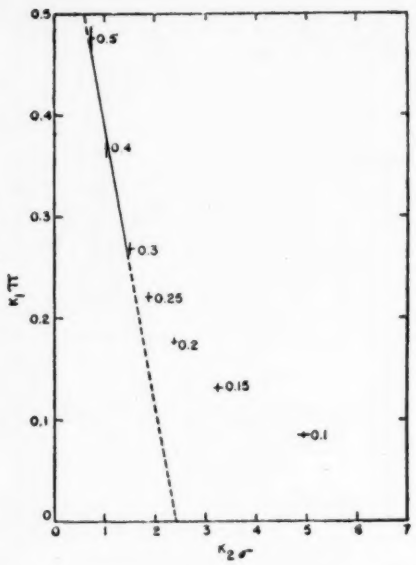

FIG. 1. Pressure-area plot calculated from Brunauer-Emmett-Teller isotherm with $c=2$; the numbers beside the points are relative pressures.

INTRODUCTION

THE multi-molecular adsorption theory of Brunauer, Emmett, and Teller[1] has been found to be in agreement with a great number of experimentally-determined adsorption isotherms over a fairly extensive range of pressures. In a critical evaluation, Brunauer[2] has concluded that the theory has limited accuracy at very low pressures where adsorbents tend to be strongly heterogeneous, and at high pressures where capillary condensation can occur, but in the pressure range where p/p_0 is 0.05 to 0.35 the agreement of theory and experiment is excellent. The basic equation

$$v=cv_m pp_0/(p_0-p)(p_0-p+cp) \qquad (1)$$

has been found by many investigators to fit the observed data within experimental accuracy over the pressure range given by Brunauer. Extensive use has been made[3] of this equation to calculate the specific surface of solids from v_m.

Jura and Harkins[4] later developed an alternate equation for expressing adsorption isotherms. They considered their equation to have a thermodynamic background, since it was derived by combining the two-dimensional equation of state for condensed mono-layers

$$\pi=b-a\sigma \qquad (2)$$

with the thermodynamic relationship derived by Gibbs for adsorption on solid surfaces [Eq. (678) of the "Equilibrium of Heterogeneous Surfaces"][5] which, for a two-component system at constant temperature, is

$$d\pi=(RT/V\Sigma)(v/p)dp. \qquad (3)$$

Since

$$\sigma=\Sigma V/Nv, \qquad (4)$$

differentiation of Eq. (2) gives

$$d\pi=-(a\Sigma V/N)d(1/v). \qquad (5)$$

By combination of Eqs. (3) and (5), followed by integration, the adsorption isotherm of Jura and Harkins is obtained:

$$\ln p=\ln p_0+(a\Sigma^2V^2/2NRT)[(1/v_0^2)-(1/v^2)]. \qquad (6)$$

The constant terms in this equation may be grouped as:

$$A=a\Sigma^2V^2/2NRT, \qquad (7)$$

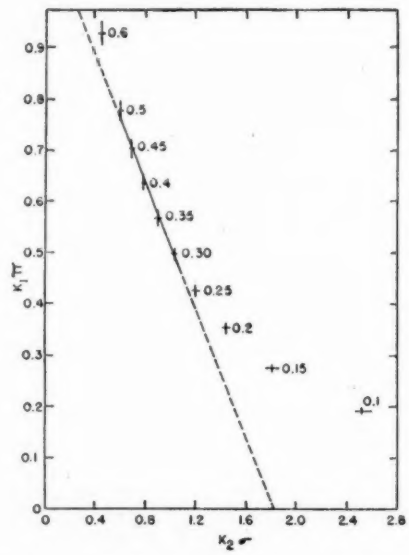

FIG. 2. Pressure-area plot calculated from Brunauer-Emmett-Teller isotherm with $c=5$.

[1] S. Brunauer, P. H. Emmett, and E. Teller, J. Am. Chem. Soc. **60**, 309 (1938).
[2] S. Brunauer, *The Adsorption of Gases and Vapors* (Princeton University Press, Princeton, 1943), Vol I. *Physical Adsorption*.
[3] P. H. Emmett, *Recent Advances in Colloid Science* (Interscience Publishers, Inc., New York, 1942), Vol. I, p. 1.
[4] G. Jura and W. D. Harkins, J. Chem. Phys. **11**, 430 (1943).
[5] *The Collected Works of J. Willard Gibbs* (Longmans, Green and Company, New York, 1928), Vol. I, p. 329.

$$B=\ln p_0+(A/v_0^2), \quad (8)$$

so that

$$\ln p=B-A/v^2. \quad (9)$$

Harkins and Jura[6] found this equation, as well as Eq. (1), to be valid for almost all of the very large number of isotherms that they studied. For nitrogen adsorptions, Eq. (9) generally fits the experimental data over a wider range of pressures than Eq. (1).

Since the specific surface is a factor in the constant A (see Eq. (7)), it can be evaluated from Eq. (9). Harkins and Jura[6] use the relation

$$\Sigma=kA^{\frac{1}{2}} \quad (10)$$

for this evaluation. They suggest that k has a constant value for any adsorbate at any temperature and recommend a value for nitrogen at $-195.8°$ of 4.06. Specific surface values calculated by this method were almost identical with those calculated by the method of Brunauer-Emmett-Teller. Harkins and Jura[6] state that "this is very remarkable when the great difference between the two theories, one kinetic and the other thermodynamic, is taken into consideration." It is the purpose of this paper to discuss the agreement between these theories and the reason for its existence.

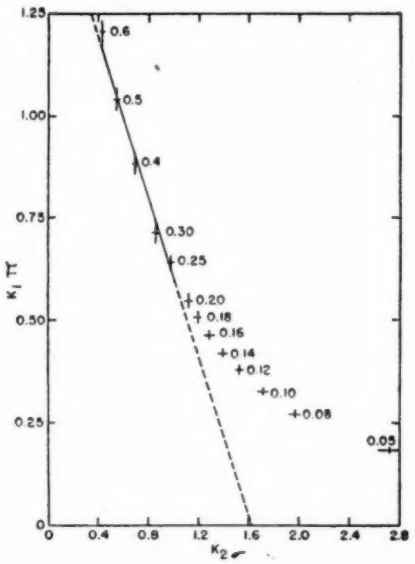

FIG. 3. Pressure-area plot calculated from Brunauer-Emmett-Teller isosherm with $c=10$.

[6] W. D. Harkins and G. Jura, J. Am. Chem. Soc. **66**, 1366 (1944).

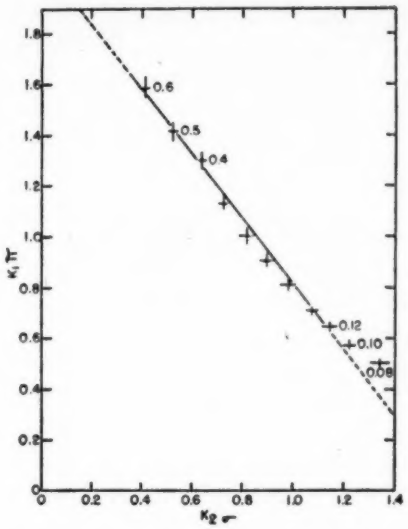

FIG. 4. Pressure-area plot calculated from Brunauer-Emmett-Teller isotherm with $c=25$.

EQUATIONS RELATING THE THEORIES

(Note: A brief summary of this section was published, under the same title as the present paper, in this journal in November, 1944.)[7]

The mathematical relationship between pressure and adsorption developed by Brunauer, Emmett, and Teller, as expressed by Eq. (1), may be substituted into Eq. (3). The result is:

$$d\pi=(RT/V\Sigma)[cv_m p_0/(p_0-p) \times(p_0-p+cp)]dp. \quad (11)$$

The integration of this equation has been shown[8] to give as the result:

$$\pi=(RTv_m/V\Sigma)\ln(p_0-p+cp)/(p_0-p). \quad (12)$$

Data calculated from Eq. (12) for $c=50$ were in agreement with Eq. (2) over a wide pressure range.

It is possible to determine the relationship between π and σ, for isotherms obeying the Brunauer-Emmett-Teller equation with widely varying values of c. A substitution of Eq. (1) in Eq. (4) gives:

$$\sigma=\Sigma V(p_0-p)(p_0-p+cp)/Nv_m cpp_0. \quad (13)$$

The terms in Eqs. (12) and (13) that do not vary with p or c may be combined into two

[7] H. K. Livingston, J. Chem. Phys. **12**, 466 (1944).
[8] H. K. Livingston, J. Am. Chem. Soc. **66**, 569 (1944).

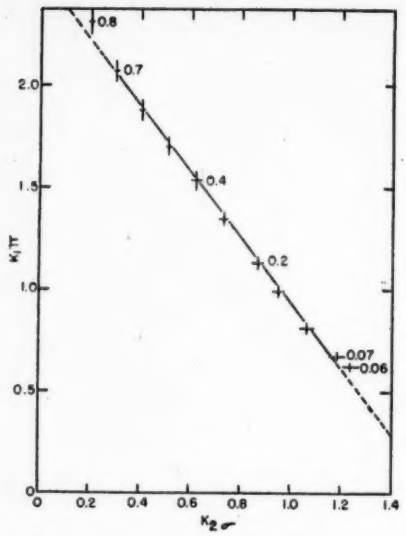

FIG. 5. Pressure-area plot calculated from Brunauer-Emmett-Teller isotherm with $c=50$.

constant terms:

$$k_1 = V\Sigma/(RTv_m \ln 10), \tag{14}$$

$$k_2 = Nv_m/V\Sigma. \tag{15}$$

Then, from Eqs. (12) and (13) the following equations can be formulated:

$$\log(p_0-p+cp)/(p_0-p) = k_1\pi, \tag{16}$$

$$(p_0-p)(p_0-p+cp)/cpp_0 = k_2\sigma. \tag{17}$$

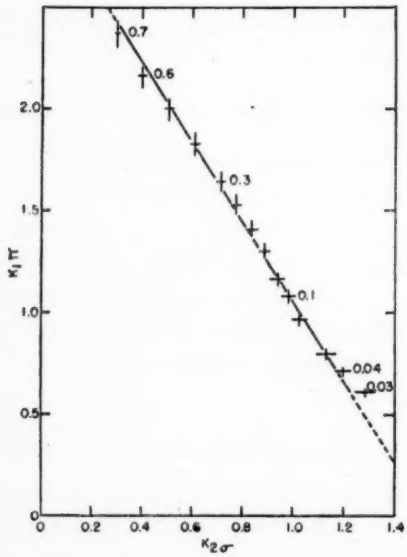

FIG. 6. Pressure-area plot calculated from Brunauer-Emmett-Teller isotherm with $c=100$.

For any given value of c, the solution of Eqs. (16) and (17) for a series of relative pressures will give $k_1\pi$ and $k_2\sigma$ values that can be examined graphically for the existence of the straight-line relationship:

$$k_1\pi = b' - mk_2\sigma. \tag{18}$$

This, of course, is equivalent to Eq. (2). That is, if values of π and σ calculated from the Brunauer-Emmett-Teller equation are in a straight-line relationship, then the basic assumption made in deriving the equation of Jura and Harkins is satisfied, and the pressure-adsorption isotherm can be expressed by either of the two equations.

CALCULATIONS FOR SELECTED VALUES OF c

Values for $k_1\pi$ and $k_2\sigma$ over a wide range of pressures have been calculated for the following values of c: 2, 5, 10, 25, 50, 100, and 250. The results have been plotted in Figs. 1 to 7. In plotting these data, consideration has been given to the accuracy of experimental adsorption data. In practice, the comparison of data determined experimentally with a theoretical equation is made by applying some test of agreement such as a least-square calculation and, using an assumed value for the accuracy of the experimental data, determining the range of agreement.

Since an assumed experimental accuracy would be used in determining the fit of either the Brunauer-Emmett-Teller of Jura and Harkins isotherms, the region where both appeared to be applicable would increase in extent as the assumed error increased. In plotting Figs. 1 to 7, it has been assumed that π and σ are known with an accuracy of ± 3 percent. The position of the calculated points is indicated, then, by a cross whose dimensions in the horizontal and vertical directions represent 6 percent of $k_2\sigma$ and $k_1\pi$, respectively. On each figure an unbroken straight line is drawn which at each point passes within the ellipse whose axes are the indicated cross. The line actually drawn is the longest possible line fulfilling these conditions. In the region where the conditions no longer apply, a broken line is drawn.

As an example, it will be seen from Fig. 7 that within the assumed limits of ± 3 percent, data that rigorously obey the Brunauer-Emmett-

TABLE I.

c	Constants of straight-line equation (18) m	b'	Relative pressures at which the equation fits the data within 3% p/p_0, low value	p/p_0, high value
2	0.28	0.68	0.3	0.5
5	.63	1.13	.26	.52
10	.99	1.59	.24	.60
25	1.29	2.09	.11	.62
50	1.61	2.54	.07	.75
100	1.95	3.01	.04	.72
250	2.33	3.66	.07	.50

(These values are based on a recalculation of those given in reference 7 and should be considered to supercede the earlier results.)

TABLE II.

c	Relative pressures at which the equation fits the data within 0.5% p/p_0, low value	p/p_0, high value
25	0.24	0.36
50	.14	.65
100	.14	.55
250	.07	.19
	.38	.65

Teller equation (1) from $p/p_0=0.07$ to $p/p_0=0.50$, with $c=250$, would be found, insofar as the accuracy would permit judgment, to obey Eq. (2) (and therefore the Jura and Harkins equation (7)). Similarly, data that rigorously obeyed the Jura and Harkins equation (7) over this pressure range, would be found to obey Eq. (1) (if $c=250$) over the same range, and no distinction could be made between the two equations.

A summary of the range of pressures over which the two equations agree within 3 percent, for the seven c values studied, is given in Table I. For those c values for which the range is largest, the range of pressures over which the two equations agree within 0.5 percent has also been determined (Table II). Because of the complex form of the line on which the points of Fig. 7 lie, two sets of limits are given for $c=250$ in Table II. In the Harkins-Jura terminology, this corresponds to the existence of two different condensed phases for the adsorbed vapor.

If accuracy were better than 3 percent, of course, the pressure ranges would be narrowed somewhat. The great majority of experimentally observed c values are from 25 to 250. For these values, the pressure range of agreement is very wide, covering almost all of the range wherein the Brunauer-Emmett-Teller equation is generally found to be valid. Very accurate experimental work would be necessary to determine which equation was more nearly correct in these cases.

COMPARISON OF THESE RESULTS WITH OTHERS RECENTLY PUBLISHED

Gregg[9,10] has considered adsorption isotherms from the standpoint of two-dimensional equations of state, in the same general manner as Jura and Harkins. Gregg's procedure involves the integration of adsorption data and construction of $\pi\sigma$ *vs.* $\pi\Sigma$ plots, for a number of systems for which Σ was unknown. He has constructed such plots for adsorbed films on charcoal, mica, sodium chloride, ferric oxide, copper oxide, and silica gel. For gaseous films, such plots give lines extrapolating to $\pi\sigma=RT$ at $\pi=0$. Gregg assumes, after Schofield and Rideal,[11] that for condensed films the slope of a $\pi\sigma-\pi\Sigma$ curve would be α/Σ.

Gregg has developed two methods for determining surface areas. The first method, applicable to linear plots, depends on the slope being α/Σ, as predicted by Schofield and Rideal. The

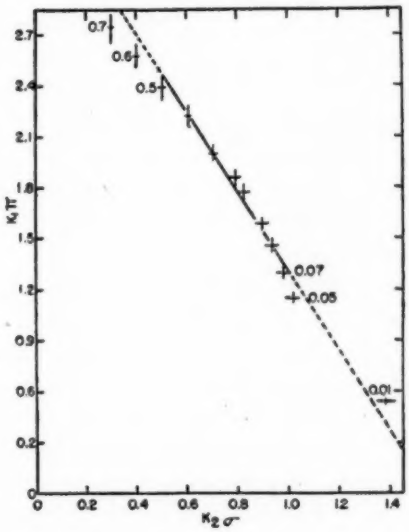

FIG. 7. Pressure-area plot calculated from Brunauer-Emmett-Teller isotherm with $c=250$.

[9] S. Gregg, J. Chem. Soc. 696 (1942).
[10] S. Gregg, *Proceedings of the Conference on Ultra-fine Structure of Coals and Cokes* (British Coal Utilisation Research Assoc., London, 1944), p. 110.
[11] R. Schofield and E. Rideal, Proc. Roy. Soc. **A109**, 57 (1935).

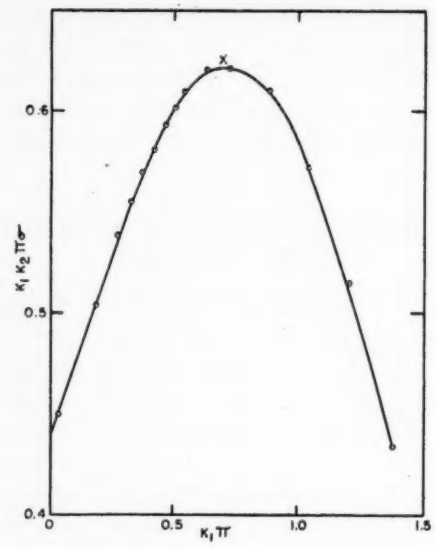

FIG. 8. Gregg-type plot calculated from Brunauer-Emmett-Teller isotherm with $c=10$.

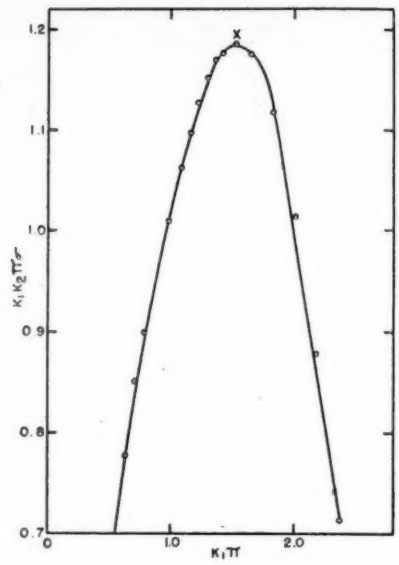

FIG. 9. Gregg-type plot calculated from Brunauer-Emmett-Teller isotherm with $c=100$.

second method is used in those cases where $\pi\sigma$ *vs.* $\pi\Sigma$ plots are not linear. Where multi-layer formations occur, parabolic curves are ordinarily observed. Gregg[10] takes the area corresponding to point X (which is essentially the vertex of the curve) to be α, and suggests that this value is approximately the same as would be calculated from the slope below this point. Maggs[12] has found specific surfaces calculated in this way to agree fairly well with those calculated from Eq. (1) (Emmett's method[2]). Gregg[10] suggests that the integration and plotting of Eq. (1) according to his method gives curves that coincide fairly well with the type obtained for his assumed equations of state.

We have used the data plotted in Figs. 3 and 6 to form a $\pi\sigma$ *vs.* $\pi\Sigma$ plot of the Gregg type. The curves (Figs. 8 and 9) closely resemble several of those that Maggs[12] has calculated from experimental data. Gregg's first method, which assumes that $\sigma=\alpha$, requires that for a plot of $k_1k_2\pi\sigma$ *vs.* $k_1\pi$, the slope be $k_2\sigma(=k_2\alpha=1)$ (see Eq. 19). Since the curves drawn in Figs. 8 and 9 are not straight lines, it is not proper to apply this method, but it can be stated that in neither case is a slope of unity approached by an appreciable linear portion of the section of the curves that is shown. If the second (X-point) method is used, the areas corresponding to the vertex of the curves (indicated by X in Figs. 8 and 9), as obtained from the original $k_1\pi-k_2\sigma$ data, should be $\sigma=\alpha$. Actually, the areas are $\sigma=\alpha/1.16$ for $c=10$ and $\sigma=\alpha/1.29$ for $c=100$. This shows that an estimation of the section area (α) by this method would be appreciably in error for adsorptions that follow the Brunauer-Emmett-Teller equation.

Emmett[13] has recently compared the Brunauer-Emmett-Teller and Jura and Harkins equations directly by solving Eq. (1) for v at various pressures and plotting the results according to Eq. (9) [i.e., $\log p/p_0$ *vs.* $(1/v^2)$]. The calculations were made for the following c values: 2, 5, 10, 25, 50, 100, 250, and 1000. This is equivalent to the operation carried out in the present paper, but Emmett's calculations were made with $p-v$ data rather than $\pi-\sigma$ data. That is, in the present paper, Eq. (1) was integrated (by means of the Gibbs equation) and substituted into Eq. (2), from which the Jura and Harkins equation (9) was derived, while Emmett used Eqs. (1) and (9) in their original forms.

It is interesting to compare the two results, especially since the same c values were used, except for $c=1000$. In both cases curved lines

[12] F. Maggs, *Proceedings of the Conference on Ultra-fine Structure of Coals and Cokes* (British Coal Utilisation Research Assoc., London, 1944), p. 95.

[13] P. H. Emmett, J. Am. Chem. Soc. **68**, 1784 (1946).

were obtained. Emmett has concluded that, inasmuch as curved lines are obtained, the statement in reference 7 that straight lines are obtained within 3 percent is misleading. This is no doubt true, if the significance of the 3 percent limitation (which unfortunately was not stressed in reference 7) is not appreciated. It should be emphasized that the 3 percent error allowed applies to $\pi-\sigma$ data, not $p-v$ data.

Emmett has stated that his data, as plotted in Figs. 1 and 2 of his article, approximately coincide with a straight line over an appreciable pressure range. Within the pressure range $p/p_0 = 0.11$ to 0.40, and for the common c values of 25 to 250, his data show a fairly reasonable agreement to exist between the two isotherms. This leads to the same conclusion arrived at from a consideration of Figs. 1 to 7, namely, that very careful experimental work would be necessary in many cases to determine which isotherm is the more accurate. In comparing Emmett's plots with those given in this paper, consideration must be given to the fact that his method of plotting is much more sensitive to variations in v, since he uses v^{-2} as an abscissa, rather than σ which is a function of v^{-1}.

SPECIFIC SURFACES CALCULATED FROM THE TWO ISOTHERMS

Emmett[13] has made the interesting observation that cross-sectional areas (section areas) of adsorbed molecules calculated from the Jura and Harkins equation vary with c, if they are calculated from the synthetic data obtained by substituting Eq. (1) in Eq. (7). His plot shows the calculated section area of nitrogen to vary from 13 to 20 A^2/molecule as c varies from 30 to 300. This same type of calculation can be made from the data of Table I.

The section area, α, is defined by the equation

$$\alpha = V\Sigma/Nv_m = 1/k_2. \tag{19}$$

It bears a definite relationship to the constants of Eq. (18). This equation may be put in the form

$$\pi = b'/k_1 - (mk_2/k_1). \tag{20}$$

Comparison with Eq. (2) shows that the term (mk_2/k_1) must be equivalent to a. Therefore

$$m = a\alpha k_1 = \frac{a\alpha V\Sigma}{RTv_m \ln 10} = \frac{Na\alpha^2}{RT \ln 10}. \tag{21}$$

If, as was assumed by Harkins and Jura,[6] a is a constant for a given adsorbent at constant temperature, the m values in Table I may be used to calculate α as a function of c. It will be assumed that $\alpha = 16\ A^2$ at $c = 100$ (which is the value read from Emmett's Fig. 3). The results of this calculation are plotted in Fig. 10. While this plot covers a different range of c values than Emmett's Fig. 3, the two seem to be in close agreement.

Emmett reports a trend in experimental α values roughly coinciding with the derived curve. While this may be a generally valid result, it should be pointed out that a may not necessarily be a constant for different c values. Harkins and Jura made this assumption because it is known that insoluble mono-layers on water tend to show no change in a when the pH or electrolyte content of the water sub-phase is changed. Such changes might have much less effect on surface forces than would result from changes in the solid adsorbent that cause large changes in c. Certainly a comparison between adsorptions of the same vapor on two adsorbents differing in c values by a factor of 10 or more might be expected to show appreciably different a values. It would seem likely then, that the values of k given by Harkins and Jura[6] for different ad-

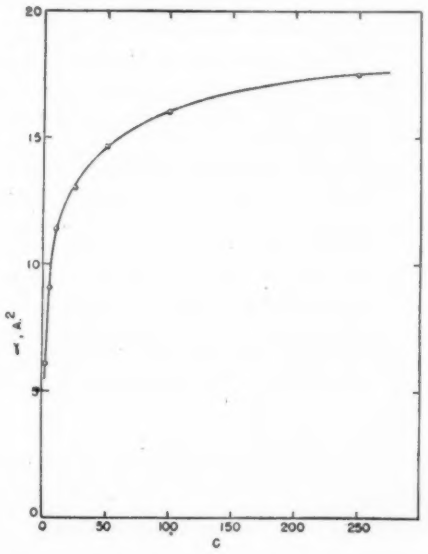

FIG. 10. The cross-sectional area (α) of molecules calculated by the Harkins and Jura method from the slope of Figs. 1–7 (assuming $\alpha = 16$ at $c = 100$).

sorbents might not always have the unique values assigned.

POSSIBILITY OF A CHOICE BETWEEN THE TWO ISOTHERMS

It is conceivable that a mathematical analysis of the two isotherms would suggest a basis for preferring one to the other. No such choice can be made as a result of the present analysis. The fact that the two equations are both equally in agreement with many of the experimental isotherms determined during the past ten years promises to make such a choice particularly difficult. If it is a fundamental property of adsorbed films under these experimental conditions to obey the two-dimensional equation of state of condensed films, then it might be considered fortuitous that the equation derived by Brunauer, Emmett, and Teller, with appropriate constants, expresses the adsorption isotherm over a considerable pressure range. On the other hand, if the kinetic theory of these authors, from which their equation was derived, is an exact expression of the performance of vapors and adsorbents at moderate relative pressures, for a great many systems the surface pressure and area will correspond to the two-dimensional equation of state expressed by Eq. (2), and therefore will be in agreement with the Jura and Harkins isotherm.

The nature of the relationship between the two isotherms has been most recently summarized by Jura and Harkins,[14] who concluded that "it is apparent that there is no conflict." It was predicted that new developments in theoretical and experimental studies of phase transitions would improve the agreement. In investigations of this sort, consideration should be given to the mathematical relationship between the equations that has been demonstrated by Emmett[13] and in the present paper.

[14] G. Jura and W. D. Harkins, J. Am. Chem. Soc. **68**, 1941 (1946).

THE JOURNAL OF CHEMICAL PHYSICS VOLUME 15, NUMBER 9 SEPTEMBER, 1947

The Adsorption of Hydrogen on Tungsten Powders

GEORGE HALSEY AND HUGH S. TAYLOR
Frick Chemical Laboratory, Princeton, New Jersey

(Received May 12, 1947)

An analysis of the extensive experimental data of Frankenburg on the adsorption of hydrogen by metallic tungsten powder between −194 and 750°C has been made, using the Fowler-Guggenheim treatment of adsorption phenomena as the mode of approach. It has not been found possible to interpret the data in terms of interaction between the adsorbed species on a *uniform* adsorbent surface. It is shown that the experimental data can be interpreted on the basis of a non-uniform surface without interaction, the heterogeneity of the surface being specified in terms of an exponential distribution of sites given by the distribution function $N=ce^{-\chi/\chi_m}$, where χ represents the energy difference between the lowest energy state of the gas and the lowest energy of the adsorption complex. Such a distribution function yields the experimentally observed relation $d\ln p/d\ln\theta=$constant at constant temperature. Such a heterogeneity is especially significant in the case of tungsten metal which hitherto has been treated as an essentially uniform surface. The quantity χ_m has been found to vary with the temperature. The significance of this variation has been briefly explored.

A COMPREHENSIVE study of the adsorption of hydrogen on tungsten powders has been recorded by W. G. Frankenburg,[1] and he has presented a series of isotherms between −194° and 750°. Special attention was given to the cleanliness of the metal surface, and the hydrogen was adsorbed rapidly at the temperatures employed. These data form an excellent example of an adsorption equilibrium in a localized mono-layer. Frankenburg's analysis of his data led to an empirical relation, the logarithm

[1] J. Am. Chem. Soc. **66**, 1827 (1944); **66**, 1838 (1944).

of the adsorbed hydrogen varying linearly with the logarithm of the gas pressure. The plot of these isothermal lines, when extrapolated, appears to intersect at a point corresponding to approximately 3150-mm hydrogen pressure.

In the present communication these data are analyzed from the standpoint of statistical mechanics, proceeding from the treatment of such adsorption phenomena by Fowler and Guggenheim.[2] Their treatment of localized mono-layers presents initially a thermodynamic derivation of the Langmuir adsorption isotherm. They emphasize the semiquantitative nature of the equation, becoming in some cases "useless owing to the ignoring of the interaction between adsorbed molecules." Their treatment is therefore modified to include interaction between the molecules which has for its effect an apparently increasing resistance to adsorption as the surface sites are filled, if the interactions are of a repulsive nature.

As a first approximation in solving the interactive case, Fowler and Guggenheim consider the case in which the molecules have a completely random distribution among the sites. This treatment is modified to include the effect of the interactive forces on the equilibrium distribution. This interaction on a uniform surface is rejected by the present authors, in what follows, as an explanation of the isotherms on tungsten powders. We shall consider, therefore, the simple random case, because for the interactive case the refinement lessens the effect of the interaction in the sparsely covered regions of the isotherms. As will presently appear, the interaction is too small even in the more favorable simple case.

INTERACTION ON A UNIFORM ABSORBENT SURFACE

Fowler and Guggenheim derive the equation,

$$p=p_0\frac{\theta}{1-\theta}e^{2\theta w/kT}, \tag{1}$$

where p is the gas pressure, p_0 is a function of the condition of the materials employed, independent of θ, the extent of surface covered. The term w is a measure of the interaction. The differential heat of adsorption (which Frankenburg derives from his data) can be obtained by inserting Eq. (1) in the Clapeyron-Clausius equation (2), which we express in terms of the heat of adsorption, q, per molecule.

$$-q=k\frac{d\ \ln p}{d1/T}=k\frac{d\ \ln p_0}{d1/T}+2\theta w. \tag{2}$$

The heat of adsorption q is, in this case, a linear function of θ. Such a result is not in agreement with the data of Frankenburg who finds a linear relation between $\log\theta$ and q over most of the plot.

If Fowler and Guggenheim's treatment is formulated to include the effect of higher interactions than between pairs of adsorbed species, instead of writing for the energy of interaction, ϵ,

$$\epsilon=N_s(\theta^2 w),$$

where N_s is the total number of sites, one may write

$$\epsilon=N_s(\theta^2 w+\theta^3 v+\cdots),$$

where the higher terms allow for groups of three, etc. That is, the energy of a cluster is not the sum of the energies of all the pairs in the cluster. For the partial potential, μ, Fowler and Guggenheim write

$$\frac{\mu}{kT}=\frac{1}{kT}\left(\frac{\partial F}{\partial N_A}\right)=\ln\frac{\theta}{1-\theta}-\ln a_0+\frac{1}{N_s kT}\left(\frac{\partial\epsilon}{\partial\theta}\right). \tag{3}$$

Here, N_A is the number of occupied sites and a_0 contains the partition function of the materials. Inserting the more general energy of interaction, the absolute activity, λ, is

$$\lambda=e^{\mu/kT}=\frac{\theta e^{(2\theta w+3\theta^2 v+\cdots)/kT}}{(1-\theta)a_0}. \tag{4}$$

The absolute activity of the gas phase is

$$\lambda_g=\frac{p}{kT}\frac{h^3}{(2\pi mkT)^{\frac{3}{2}}j_A}, \tag{5}$$

where j_A is the partition function for vibration and rotation in the gas. Thus,

$$p=p_0\frac{\theta}{1-\theta}e^{(2\theta w+3\theta^2 v+\cdots)/kT}, \tag{6}$$

[2] R. H. Fowler, and E. A. Guggenheim, *Statistical Thermodynamics* (Cambridge University Press, Teddington, England, 1939), Chapter X, p. 421.

where p_0 is of the form

$$p_0=\frac{(2\pi m)^{3/2}(kT)^{5/2}j_G(T)}{h^3 j_s(T)}e^{-\chi_0/kT}, \qquad (7)$$

where χ_0 is the energy difference between the lowest energy states of the gas and the adsorption complex. A discussion of its variability will follow. From the expression for p, Eq. (6),

$$-q=k\frac{d\ln p}{d(1/T)}=k\frac{d\ln p_0}{d(1/T)}+2\theta w+3\theta^2 v+\cdots, \qquad (8)$$

and the slope of $-q$ *versus* θ is given by

$$\frac{-dq}{d\theta}=2w+6\theta v+\cdots \qquad (9)$$

which shows that, when the coverage is low, $-dq/d\theta=2w$. Frankenburg's curve for q *versus* θ has its maximum slope when θ is small and it has no inflexion. It follows, therefore, that w must have a positive value, and the coefficients of the higher terms, v, $\cdots$ must be negative. Up to a rather large value of θ (0.2–0.3) the slope of the curve $-dq/d\theta$ is very large. If higher interactions were suppressed this would be equivalent to having q *versus* θ given by the projected tangent to this early slope. With Frankenburg's data the slope is so large that the heat of adsorption would become negative long before θ reached unity. Actually the tangent would reach zero heat with θ in the neighborhood of 0.1 to 0.2.

Because interactions at low coverage are almost exclusively isolated-pair interactions and because, when all the sites are covered, there are two pair-interactions per atom, it follows that the lowest value of θ at which the tangent to the initial portion of the curve could cross $q=0$ would be, with the help of all the higher order interactions, when $\theta=\frac{1}{4}$. Frankenburg's data could conform to this condition did they involve low energy repulsions. On the contrary, in order to account for the extremely steep initial slope of the $q-\theta$ curve a value of w/kT of ~ 100 or more would be required. The early interactions would involve a term e^{100} in the exact treatment, a condition which renders a poor argument for interaction actually impossible. An alternative statement of this conclusion is that pair-interaction is more than sufficient to prohibit adsorption, which is clearly impossible since vigorous adsorption occurs on the surface at small θ.

This argument is deemed sufficient to show that we cannot interpret the Frankenburg data on the basis of a theory of interaction on a uniform surface. It can further be pointed out that the isotherms yielded by such a theory are clearly not straight lines on a plot of log$p$ *versus* logθ. Nor do they tend to meet in a point as Frankenburg found. Rather, in common with all isotherms with a saturation value, they tend to become asymptotic to a line of constant coverage.

Thus, no interaction theory on a uniform surface can explain a differential heat of adsorption with increased coverage which has an initial slope $dq/d\theta$ greater than $0.25q_{\text{initial}}$. Accordingly, the case of a heterogeneous surface must necessarily be examined.[3] While, in this case, interactions between neighboring molecules undoubtedly exist, it is simpler, at the outset, to begin by considering heterogeneity alone without interactions. It emerges that this ideal case, omitting interaction, is adequate to provide a reasonable basis for the analysis of Frankenburg's isotherms.

THE NON-UNIFORM ADSORBENT SURFACE

Consider a surface with variable energy differences between the lowest energy state of the gas and the lowest energy state of the adsorption complex. For any particular value of χ the Langmuir isotherm is applied:

$$\frac{\theta_\chi}{1-\theta_\chi}=\frac{p}{p_0}=\frac{p}{ae^{-\chi/kT}}. \qquad (10)$$

By setting $p_0=ae^{-\chi/kT}$, the effect of variable χ has been separated from the remainder of the partition-function ratio. The total coverage is given by

$$\theta=\int N_\chi\theta_\chi d\chi, \qquad (11)$$

where N_χ is the distribution function of sites, usually normalized to $\int N_\chi d_\chi=1$. Solving the

[3] There are many such efforts previously made. See Fowler, *Statistical Mechanics* (Cambridge University Press, Teddington, England, 1936), second edition, p. 833. Also, Brunauer, *The Adsorption of Gases and Vapors* (Princeton University Press, Princeton, 1943), p. 74.

Langmuir expression for θ_χ,

$$\theta_\chi = \frac{1}{\frac{a}{p}e^{-\chi/kT}+1} \tag{12}$$

the expression for θ becomes

$$\theta = \int \frac{N_\chi d\chi}{\frac{a}{p}e^{-\chi/kT}+1}. \tag{13}$$

Case 1: N is Constant

To evaluate the integral it is necessary to assume a form for N_χ. One form that permits integration with indefinite limits obtains when N_χ is constant. Then if $\int N_\chi d\chi = 1$, $N = 1/\Delta\chi$ where $\Delta\chi$ is the range of integration, $\chi_{upper} - \chi_0$. Inserting this value in the expression (13) for θ yields

$$\theta = \frac{1}{\Delta\chi}\int \frac{d\chi}{\frac{a}{p}e^{-\chi/kT}+1}$$

$$= 1 + \frac{kT}{\Delta\chi}\ln\frac{1+\frac{a}{p}e^{-(\chi_0+\Delta\chi)/kT}}{1+\frac{a}{p}e^{-\chi_0/kT}}. \tag{14}$$

To compute the differential heat, $-q$, by means of the Clapeyron-Clausius equation (2), the expression for θ must be solved for p. Two approximations, corresponding to the low and high pressure approximations in the simple Langmuir theory can be made. For low pressure the poorest sites are totally vacant, in which case $(a/p)e^{-\chi_0/kT} \gg 1$. The isotherm then becomes

$$1-\theta = \frac{kT}{\Delta\chi}\ln\frac{\frac{a}{p}e^{-\chi_0/kT}}{1+\frac{a}{p}e^{-(\chi_0+\Delta\chi)/kT}}$$

$$= -\frac{kT}{\Delta\chi}\ln\left(\frac{p}{a}e^{\chi_0/kT}+e^{-\Delta\chi/kT}\right). \tag{15}$$

Hence,

$$-q = \frac{kd\ln p}{d1/T} = \text{const.} - \frac{(1-\theta)\Delta\chi e^{-(1-\theta)\Delta\chi/kT} - \Delta\chi e^{-\Delta\chi/kT}}{e^{-(1-\theta)\Delta\chi/kT} - e^{-\Delta\chi/kT}}. \tag{16}$$

At high pressure, $(a/p)e^{-(\chi_0+\Delta\chi)/kT}$ becomes small and the best sites are covered. Then,

$$1-\theta = \frac{kT}{\Delta\chi}\ln\left(1+\frac{a}{p}e^{-\chi_0/kT}\right) \tag{17}$$

and

$$p = \frac{ae^{-\chi_0/kT}}{e^{(1-\theta)\Delta\chi/kT}-1} \tag{18}$$

and

$$-q = \frac{kd\ln p}{d1/T} = \text{const.} - \frac{(1-\theta)\Delta\chi e^{(1-\theta)\Delta\chi/kT}}{e^{(1-\theta)\Delta\chi/kT}-1}. \tag{19}$$

These equations, complex as they are, do not account for Frankenburg's data, unless a number of segments are arbitrarily patched together. It is usual to measure q and assume that this function represents the distribution pattern of the surface. These equations indicate that this procedure is not sound. There is always a complex relationship even in the simple case when N_χ is constant. An exception may be noted in the simplification possible when the two approximations which have been used apply simultaneously. In this case, adsorption has no beginning or end in either direction and the normalization becomes meaningless. It is replaceable by a factor m adjusted to make θ emerge in the proper units.

$$1-\theta = mkT\ln\frac{a}{p}e^{-\chi_0/kT}. \tag{20}$$

Replacing a $e^{-\chi_0/kT}$ by p_0,

$$1-\theta = mkT\ln\frac{p}{p_0}. \tag{21}$$

From this logarithmic isotherm (21), it follows that

$$\ln p = \frac{1-\theta}{mkT} + \ln p_0$$

and

$$-q=\frac{kd\ln p}{d^1/T}=\frac{1-\theta}{m}+\frac{kd\ln p_0}{d(1/T)}.$$

This is a linear relationship between θ and q. In this case, therefore, the distribution and the heat have the same functional form. Whenever the heat function is not linear, as in Frankenburg's results, analysis of the problem with finite limits is difficult. Applicability of the two approximations already employed, permits a more complex function to be used, which, at the same time makes the analysis possible.

Case 2: Exponential Distribution for N

With a distribution of the form

$$N_\chi=ce^{-\chi/\chi_m} \tag{22}$$

over the whole range of χ, positive and negative,

$$\theta=c\int_{-\infty}^{+\infty}\frac{e^{-\chi/\chi_m}}{\frac{a}{p}-e^{-\chi/kT}+1}d\chi. \tag{23}$$

Inserting Z for $(a/p)e^{-\chi/kT}$ the expression can be written

$$\theta=\left(\frac{a}{p}\right)^{-kT/\chi_m}ckT\int_0^\infty\frac{Z^{(kT/\chi_m-1)}}{1+Z}dZ. \tag{24}$$

This integral has the value[4] $\pi\ \mathrm{cosec}\pi kT/\chi_m$. This expression has the approximate value χ_m/kT for large values of this quantity. This expression will not be carried in further equations because other terms involving T are indistinguishable.

In the expression for θ, there are no constants involving p under the integral. Now, if the exponential retarding adsorption in the region of negative $\chi(e^{+\chi/kT})$ increases more rapidly than the available sites (e^{χ/χ_m}), the infinite integral will converge and become independent of the variable. The condition for convergence is $\chi_m/kT>1$. Hence,

$$\theta=ckT\left(\frac{p}{a}\right)^{kT/\chi_m}f(kT/\chi_m), \tag{25}$$

where $f(kT/\chi_m)$ is written for the infinite integral.

From this expression it follows that

$$\ln\theta=\frac{kT}{\chi_m}\ln p+\text{const.} \tag{26}$$

and

$$\frac{d\ln p}{d\ln\theta}=\frac{\chi_m}{kT}, \tag{27}$$

which is the functional relation between p and θ found by Frankenburg. Similarly, as found by Frankenburg for the main portion of his data,

$$-q=\frac{kd\ln p}{d^1/T}=\text{const.}+\chi_m\log\theta. \tag{28}$$

For some value of θ, q is zero. If the value for the constant in the equation for q is independent of temperature, then the value of θ that makes q equal to zero is the same for all temperatures. Extrapolation of Frankenburg's data supports this constancy with respect to temperature. If we select, as a normalization condition, this value as $\theta=1$, the constant becomes zero and

$$-q=\chi_m\log\theta, \tag{29}$$

and

$$\ln p=\frac{\chi_m}{kT}\ln\theta+\ln p_0. \tag{30}$$

When $p=p_0$ all of the isotherms intersect. Frankenburg finds this value by extrapolation to be 3150 mm. At the point of intersection, for powder 9799, θ has the value $S=1000\times10^{-8}$ mole H_2 per g tungsten powder. At this point all of the sites with positive energies would not be filled (unless $T=0°K$) but enough of the sites of negative energy are filled to make the net heat effect zero. Frankenburg did not reach this point experimentally.

Below a certain coverage, $\theta=0.015$, Frankenburg found that the differential heat of adsorption was constant. This indicates a breakdown, in the sparsely covered region, of the hypothesis in the present treatment that the best site is always covered and that, therefore, $-q$ should increase indefinitely. This low pressure region doubtless has an effective χ and can be treated on the basis of a simple Langmuir isotherm.

Granting the validity of the treatment here proposed, it should be pointed out that the slope ($\ln p$ *versus* $\ln\theta$), 2.0–2.06, indicates that the

[4] D. Bierens de Haan, *Nouvelles Tables d'Integrales Definies* (Amsterdam, 1867), Table 16, No. 1.

adsorption is atomic rather than molecular. This is the accepted view. The total effect of this modification is that Eqs. (29) and (30) become, respectively,

$$(p/p_0)^{\frac{1}{2}} = \theta^{\chi_m/kT} \tag{31}$$

and

$$-q = 2\chi_m \ln\theta. \tag{32}$$

The constant χ_m, which is the energy at which the sites are a fraction $1/e$ of those when $\chi = 0$, is a function of temperature which is approximately linear. It is somewhat difficult to reconcile this continuous change in χ_m over the temperature range with the calculations of Frankenburg in which he found q to be constant below 529°C. He himself indicates the reason for the discrepancy when he details the calculation of q, in which the slopes are adjusted on the basis of his modification of the Langmuir treatment.

In Table I are given Frankenburg's average slopes and the variation of χ_m with temperature. The values of χ_m were calculated by use of the formula, based on atomic adsorption,

$$\chi_m = \frac{kT}{2}\frac{d\ln p}{d\ln\theta}. \tag{33}$$

Since χ_m was considered constant with respect to $1/T$ throughout the preceding derivations, the equations will be re-examined in respect to $-q$. The derivation of the isotherm is not impaired; hence, from Eq. (26) it follows that

$$-q = \frac{kd\ln p}{d(1/T)} = \text{const.} + \ln\theta\left(\chi_m - T\frac{\partial\chi_m}{\partial T}\right). \tag{34}$$

The slope of the differential-heat curve plotting $-q$ *versus* $\ln\theta$,

$$\chi_m{}^0 = \frac{d(-q)}{d\ln\theta} = \chi_m - T\frac{\partial\chi_m}{\partial T}, \tag{35}$$

is still independent of θ but now is a function of T. The constancy of q with respect to temperature is so often encountered or implied that it is of interest to deduce the most general law that will yield it. If $\chi_m{}^0$ is a constant, the differential equation

$$-T\frac{\partial\chi_m}{\partial T} + \chi_m = \chi_m{}^0 \tag{36}$$

has the solution

$$\chi_m = \chi_m{}^0 + cT \quad \text{or} \quad -q = \chi_m{}^0 \ln\theta, \tag{37}$$

where c is the constant of integration. If $c = 0$, $\chi_m = \chi_m{}^0$, which is the special case of constant χ_m treated earlier. The data of Frankenburg are not specially suited to this case but are fairly satisfactory over the middle range. The expression

$$\chi_m = 16.6 - 0.005(T - 273°)$$

where the data are given in kcal. per mole and the corresponding expression for the heat of adsorption, Q, per mole,

$$-Q = 2.3\times 16.6\log\theta,$$

conform more closely but not entirely satisfactorily to the Frankenburg data. The form that appears to fit the data best is

$$\chi_m = \chi_m{}^0 + c\ln T, \tag{38}$$

whence

$$-q = \chi_m{}^0 - c(\ln T + 1)\ln. \tag{39}$$

Numerically, in kcal. per mole and °K, the expression becomes

$$\chi_m = 4.45 - 5.0\log\frac{T}{300}.$$

Hence, the numerical expression for Frankenburg's data over the main portion of his iso-

TABLE I. Variation of $d\ln p/d\ln\theta$ and χ_m with temperature.

Temperature °K	$\frac{d\ln p}{d\ln\theta}$	χ_m kcal.
99	(67.4)	6.65
200	(24.1)	4.83
273	16.63	4.54
373	10.81	4.01
473	7.58	3.58
573	5.60	3.21
673	4.17	2.84
773	3.06	2.37
873	2.31	2.02
973	1.85	1.80

therms, would be

$$\frac{p_{\text{mm}}}{1350}=\left(\frac{m_{H_2}}{1.00\times10^{-5}}\right)^{\frac{[9.90-10\log(T/300)]}{RT}}.$$

In this expression, m_{H_2} is moles H_2 per gram of tungsten, powder No. 9799, which was used in the high temperature runs. For powder No. 9798 the term 1.00×10^{-5} must be replaced by 0.360×10^{-5} because of the smaller surface per gram of this powder.

The variation of χ_m with temperature indicates that it is not alone χ which varies from site to site on the surface of the tungsten. A term in χ proportional to T is to be associated with a varying entropy of adsorption over the surface. The exact meaning of an entropy term may not be immediately apparent. If the term in the adsorption equation that varies over the surface is not $e^{-\chi/kT}$ but an expression of the form

$$e^{a\chi}e^{-\chi/kT}=e^{-\chi(1-aT)/kT}, \tag{40}$$

then the expression for $\ln\theta$ becomes

$$\ln\theta=\frac{kT}{m(1-cT)}\ln p. \tag{41}$$

If χ is independent of the temperature, as just assumed, a variation in χ_m such as was found necessary in the preceding must result. Taking the values found for the constants into account, it means that when the energy of adsorption changes by 16.6 kcal., the change in the entropy of adsorption is 5 entropy units or 0.3 entropy unit per kcal. change in energy of adsorption.

ACKNOWLEDGMENT

The authors wish to thank Dr. Walter G. Frankenburg for his cooperation in providing supplementary information and advice in the analysis of his extensive data, and Professor Walter Kauzmann for a critical examination of the manuscript.

THE JOURNAL OF CHEMICAL PHYSICS VOLUME 15, NUMBER 9 SEPTEMBER, 1947

Contribution to the Study of Electronic Spectra of Bent Triatomic Molecules

JULES DUCHESNE* AND B. ROSEN
Department of Chemical Physics and Institute of Astrophysics, University of Liége, Liége, Belgium

(Received June 9, 1947)

The electronic absorption spectra of the SO_2, SeO_2, and TeO_2 molecules have been studied under widely varied experimental conditions. The vibrational analysis of the ultraviolet absorption region of SO_2 with center of gravity near 2000A reveals that it is formed by at least two electronic systems with the following vibrational constants:

System $\alpha_1 \cdots \nu_0 = 42{,}170$ cm^{-1}, $\nu_1' = 963$ cm^{-1}, $\nu_2' = 379$ cm^{-1}, $x'\nu_2' = 2$ cm^{-1}.
System $\alpha_2 \cdots \nu_0 = 44{,}236$ cm^{-1}, $\nu_1' = 775$ cm^{-1}, $\nu_2' = 375$ cm^{-1}.

The presence in the same region of a third electronic system, with $\nu_2' = 360$ cm^{-1} and $\nu_1' = 845$ cm^{-1}, seems highly probable.

The character of the vibrational structure of the band systems and a preliminary analysis of the rotational structure of several bands have enabled us to obtain some information about the molecular structure of the excited states.

The vibrational analysis of the *c*-system of SeO_2 in the visible, and the TeO_2 bands in the visible and ultraviolet, have enabled us to correlate the electronic states of the three similar molecules.

INTRODUCTION

A CONSIDERABLE amount of work has been done in the last few years, chiefly by Mulliken and his collaborators, in the field of electronic spectra of triatomic molecules. During the war we were engaged on similar problems and started inyestigations on the electronic spectra of the SO_2, SeO_2, and TeO_2 molecules. The wartime conditions prevented us from publishing our results, with the exception of one paper on the *b*-system of SeO_2.[1] The present paper deals with the analysis of the *a*-system of SO_2, in the far ultraviolet (center of gravity near 2000A), the *c*-system of SeO_2 in the visible, and with TeO_2 bands in the visible and near ultraviolet.

HISTORICAL CONSIDERATIONS

The *a*-system of SO_2 was first studied in absorption by V. Henri and by Wieland.[2] They correlated the observed bands with three fundamental frequencies of the ground level and assigned the frequencies 960 and 379.5 cm^{-1} to the upper level. In 1933, Chow[3] performed a new analysis and suggested that the bands belong to three electronic systems, each of them being characterized by a frequency of about 750–770 cm^{-1} in the upper evel.

Chow's analysis was criticized in 1938 by Price and Simpson[4] who considered that all the most prominent bands in the region 2300–2000A form a single progression with $\nu_2' = 380$ cm^{-1}.

The *a*-system of SO_2 was observed by Chow[3] in emission as well as in absorption. Later, Lotmar[5] studied the monochromatically-excited resonance spectra in SO_2 vapor and Kornfeld[6] extended the emission spectra, using electrodeless excitation.

While Chow and Lotmar interpreted the system using an asymmetrical vibration, ν_3'', Kornfeld succeeded in arranging the observed bands using only symmetrical frequencies in both states. In view of the application of the selection rules and the discussion of molecular configurations, these divergencies must be cleared up. On the other hand, the values for the band heads given by different authors are in some cases widely divergent, so that new measures of this system seemed to be of interest. For the present study, we were able to use some spectra taken by V. Henri in 1922 and 1930. The dispersion

* Associate fellow of the Belgian National Foundation of Scientific Researches.

[1] J. Duchesne and B. Rosen, Physica **8**, 540 (1941).

[2] V. Henri, *The Structure of Molecules*, edited by P. Debye (Blackie and Son Limited, London, 1932), p. 121; K. Wieland, Nature **130**, 847 (1932).

[3] Tung-Ching Chow, Phys. Rev. **44**, 638 (1933).

[4] W. C. Price and D. M. Simpson, Proc. Roy. Soc. **A165**, 272 (1938).

[5] W. Lotmar, Zeits. f. Physik **83**, 765 (1933).

[6] G. Kornfeld, Trans. Faraday Soc **32**, 1487 (1936).

was either 2A/mm or 5A/mm at 2200A, the pressure varied from 0.5 to 100 mm, and the temperature from −80° to 500°. The absorption lengths varied from 5 cm to one meter.

VIBRATIONAL ANALYSIS

In the first column of Table I we give the mean value for the band heads obtained on a series of plates taken at −80°C and corresponding to widely varied conditions of pressure and absorption paths. The dispersion was 2A/mm at 2200A, and the difference between individual measures did not exceed 3 cm^{-1}. Some additional band heads measured only on low dispersion plates, and marked with an asterisk, are also included. For these bands the precision is not so good. This is also the case for the last bands situated towards the ultraviolet, where accurate measures of our high dispersion plates are no longer possible.

TABLE I.

D. and R.		Chow	D. and R.		Chow	D. and R.		Chow	D. and R.		Chow
42,170(?)	α_1		44,663	α_1	44,663	46,218	α_3	46,217			47,707
42,183(?)			44,677		44,674	46,227					47,742
			44,885	α_1		46,353	α_3	46,348			47,889
42,576	α_1	42,575									47,922
42,589		42,589	44,966*	α_2	44,978			46,444			47,965
		42,759	44,980		44,987			46,464			48,000
42,955	α_1	42,954	45,032	α_1	45,030	46,471*	α_2	47,472	48,015*	α_2	48,005
42,968		42,966	45,046			46,484		46,482			48,083
		43,018	45,160(?)			46,574	α_3	46,570			48,121
43,138	α_1	43,137	45,247*	α_1				46,697			48,355
43,148		43,145	45,337	α_2	45,333	46,704*	α_3	46,704	48,390*	α_2	48,375
43,332	α_1	43,329	45,354		45,351	46,820*	α_2	46,818		α_2	48,724
43,343		43,340	45,399	α_1	45,393			46,829		α_2	48,781
		43,407	45,413			46,866	α_2	46,865		α_2	49,133
43,539	α_1	43,538	45,499	α_3		46,878		46,874		α_2	49,477
43,552		43,550	45,601*	α_1	45,572	46,925*	α_3			α_2	49,550
43,701	α_1				45,672	47,057*	α_3	47,052		α_2	49,910
43,713		43,714			45,686			47,074		α_2	50,248
43,919	α_1	43,918	45,710	α_2	45,706			47,198		α_2	50,302
43,930		43,929	45,726		45,725			47,223			
44,086	α_1	44,085	45,759	α_1	45,757			47,232			
		44,100		α_2							
			45,858	α_3	45,859	47,257*	α_2	47,246			
44,236	α_2	44,236	45,869					47,391			
44,293	α_1	44,293			45,923			47,548			
44,306		44,305			46,077			47,576			
44,491(?)	α_1		46,085*	α_2	46,084			47,623			
44,543(?)		44,570	46,106	α_2	46,104	47,627*	α_2	47,636			
44,603	α_2	44,603	46,122		46,118						

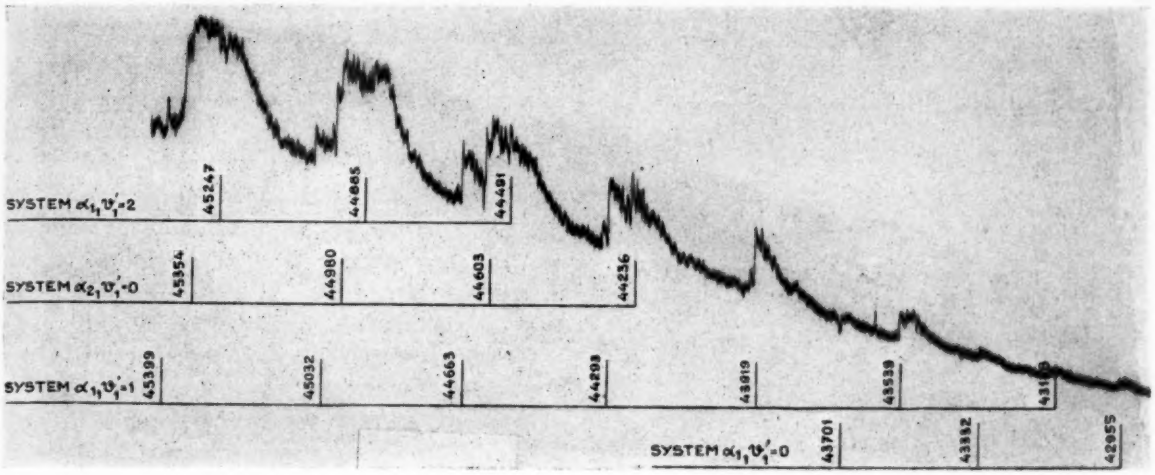

FIG. 1.

The third column of Table I contains the band heads observed by Chow[3] at room temperature. The two sets of values are in general in quite satisfactory agreement.

In 1931, V. Henri[2] pointed out that he had observed 120 band heads between 2445 and 2100A. A systematic study of our plates reveals, however, that many of these band heads are, in fact, sub-heads in the fine structure. This point will be discussed in detail below. In any case, the bands given in the first column of Table I are by far the most characteristic of the whole system. The analysis of the spectrum shows that the occurrence of the 380 cm^{-1} ν_2' frequency is beyond any doubt, but we cannot agree with the statement of Price and Simpson[4] that all the prominent bands are members of a single ν_2' progression.

The microphotometer record of Fig. 1, corresponding to the long wave-length end of the spectrum, shows clearly that there are at least three superposed series with characteristic intensity distribution around a single maximum. Moreover, intensity-temperature variations indicate definitely that the observed series cannot arise from excited vibrational levels in the normal state. Thus, the distance between the corresponding members of two series must be correlated either to a frequency (fundamental or combination) of the upper level or to the distance between two neighboring electronic states.

The essential results of our new interpretation are summarized in Tables II to V. In Table II the columns represent v_2' series with $\nu_2' \sim 380$ cm^{-1}. Taking into account the constant difference of about 963 cm^{-1} between bands of the first

TABLE II. System α_1.

v_2' \ v_1'	0			1			2
0	42,170 (?) 968 42,183 (?) 965			43,138 (3) 43,148 (2)			
	406			402			
1	42,576 (2) 963 42,589 (1) 963			43,539 (4) 43,552 (3)		952	44,491
	379			379			394
2	42,955 (3) 964 42,968 (2) 962			43,919 (5) 43,930 (4)		966	44,885
	376			375			362
3	43,332 (3) 961 43,343 (2) 963			44,293 (5) 44,306 (4)		954	45,247
	370			370			354
4	43,701 962 43,713 964			44,663 (5) 44,677 (4)		938	45,601
	373			369			
5	— 44,086 (1) 960			45,032 (3) 45,046 (2)			
				367			
6				45,399 (2) 45,413 (1)			
				360			
7				45,759 (1) —			

TABLE III. System α_2.

v_2' \ v_1'	0	1	2	3	4	5	6
0	— 44,236 367						
1	— 44,603 377						
2	44,966 44,980 (779) 373	— 45,759 363					
3	45,337 (769) 45,354 (768) 372	46,106 46,122 363					
4	45,710 (761) 45,726 (758) 375	46,471 46,484 395	(780) 47,257 (758) 370	48,015 (766) 375	48,781* (769) 352	49,550* (752) 360	50,302*
5	46,085 (781) — 359	46,866 46,878	(755) 47,627 (763)	48,390 (743) 334	49,133* (777) 344	49,910* 338	
6	(46,444)* (46,464)* 356			48,724* (753)	49,477* (771)	50,248*	
7	— 46,820						

* Measured by Chow only.

two columns of Table II, we obtain the second characteristic frequency mentioned by V. Henri and correlated with ν_1'. All the values 963 ± 380 cm^{-1} are of course alternative values for ν_1'. All the bands in the first two columns seem to have the same fine structure. For instance, they are all doublets with the same mean separation of about 13 cm^{-1}.

The first band in the second column of Table II shows irregular behavior inasmuch as its distance from the next one has an abnormally high value of 402 cm^{-1}. On the other hand, the doublet separation is definitely smaller than for the other bands (it is only 8 cm^{-1} according to Chow's measure). Both kinds of irregularities result probably from a perturbation affecting the first level of the second series (the first doublet of the first series is too faint and accurate measures are impossible; thus it is not possible to state definitely whether this level is also perturbed). The other levels seem regularly spaced, indicating an anharmonicity $x'\nu_2'$ of about 2 cm^{-1}.

The distribution of intensity in the first two columns of Table II is very regular around a single maximum occurring for $v_2'=2$ or 3. The intensities indicated (between brackets) are rough visual estimations, valid only when comparing bands in the same column. It must be noted that bands of the first column appear only at pressures about 10 times larger than those necessary to observe the bands of the second one.

A third group of bands can be fitted into the scheme of Table II as a $v_1'=2$ series. They are blended by strong bands of other series (see Fig. 1) and it is rather difficult to estimate their intensity. Nevertheless, it seems that the maximum intensity for the bands of Table II is reached for the $(1'v_2'0)$ series, and this seems normal in view of the assumed ratio ν_1'/ν_1''

$=963/1151$. The following series could not be observed because their position coincides with strong bands belonging to another electronic transition.

The first column of Table III contains a very strong series, with nearly the same characteristic frequency difference of about 375 cm^{-1}. It also consists of doublets but, contrary to the first two series of Table II, the strongest head is situated towards the ultraviolet, and the doublet separation is larger (17 cm^{-1} on the average).

The series given in the second column of Table III is not so regular, and at first sight it seems that it could form a continuation of the first one, the bands 46106–46122 following the bands 45710–45726. This arrangement, which would suppose some perturbations, cannot be definitely ruled out. But several arguments can be advanced against it. First of all, the characters of the bands in the first and second columns are somewhat different, the latter being less regular, for instance in regard to the relative intensity in the doublets. The fine structure seems also to be different, and the structures of the bands in the second column are on the whole more complex, probably as a consequence of superpositions of at least two series. A possible confirmation of this point of view is given by the observations made by Chow (at room temperature) of 4 bands at 46444, 46464, 46472, and 46482 cm^{-1}, instead of two bands 46471–46484 observed by us. These 4 bands can be interpreted as nearly superposed doublets belonging to two series. It is to be noted that the first doublet cannot be interpreted as arising from excited vibrational levels of the lower state. It is included (between brackets) in the first column of Table III.

Assuming the existence of two separate series, it is possible to interpret two additional bands which otherwise cannot be easily fitted in the scheme (bands 46085 and 46820 cm^{-1}).

The constant $\Delta\nu$ difference of about 770 ± 370 cm^{-1} between the first two columns of Table III must correspond to the frequency ν_1'. We admit with Chow that the most probable value is $\nu_1'=770$ cm^{-1}. The next columns of Table III contain further bands measured towards the ultraviolet, as well as the most characteristic bands measured by Chow. In this region the characteristic frequency difference of about 770 cm^{-1} is clearly visible on the records given in Chow's paper. It is predominant further to the ultraviolet, according to Herreng,[7] and to not yet published results obtained in our laboratory by P. Migeotte.**

TABLE IV. System α_3.

	0		1		2
0	45,499	(854)	46,353	(845)	47,198*
	359				
1	{45,858 / 45,869	(846)	46,704	(844)	47,548*
	359				
2	{46,218 / 46,227	(839)	47,057	(832)	47,889*
	356				
3	46,574				
	351				
4	46,925				

* Measured by Chow.

For the system of Table III, the ν_1' series are much more developed than for the system of Table II corresponding to the decreasing ν_1'/ν_1'' ratio.

TABLE V. Absorption bands of SO_2 arising from excited vibrational levels of the ground state.

ν	Arising from:	Corresponding band arising from (0″0″0″)	$\Delta\nu$
{41,620 / 41,633	(2″0″0″)	{43,919 / 43,930	2,299 / 2,297
41,807	(1″0″0″)	42,955	1,148
{41,987 / 41,998	(1″0″0″) / (1″0″0″)	{43,138 / 43,149	1,151 / 1,151
{42,059 / 42,073	(0″1″0″) / (0″1″0″)	{42,576 / 42,589	517 / 516
{42,249 / 42,387	(1″1″0″) / (1″0″0″)	43,919 / 43,539	1,670 / 1,152
{42,766 / 42,776	(1″0″0″) / (1″0″0″)	{43,919 / 43,930	1,153 / 1,154
43,020	(0″1″0″)	43,539	519

Mean values: $\nu_1''=1,151.5$ cm^{-1} from infra-red[8] $\nu_1''=1,151.38$; $\nu_2''=517.3$; $\nu_2''=517.84$

[7] P. Herreng, Rev. d'optique **15**, 413 (1936).

** According to preliminary results of P. Migeotte, it seems probable that a new electronic transition is responsible for bands in the 1900–1800A region.

The two schemes of Tables II and III contain nearly all the strong bands observed by us and by Chow, with the exception of the bands denoted α_3 in the Table I. On account of their great relative intensity, it is difficult to correlate the latter with an asymmetrical frequency. For this reason, the possibility that they belong to a third electronic system must be taken into consideration. For this hypothetical third system, the scheme of Table IV with $\nu_1' = 845$ and $\nu_2' = 360$ cm^{-1} seems to be the most probable one.

The third column of Table IV corresponds to bands observed by Chow only. They cannot be explained as arising from excited vibrational levels of the ground state. A study further to the ultraviolet is of course necessary before reaching definite conclusions concerning the reality of this system.

Under the conditions of our experiments, bands corresponding to excited vibrational levels of the ground state are practically lacking at $-80°$, but they are easily observed at 20°. An accurate measure of these bands is possible only on the long wave-length side of the $(0'0'0') - (0''0''0'')$ band of the α_1 system, and the mean values obtained for several bands at temperatures ranging up to 335° are given in Table V. For ν_1'' and ν_2'' the mean values obtained are in good agreement with the values given by Barker[8] on the basis of infra-red analysis. $\Delta\nu$ values for the first two bands of Table V indicate a small but definite anharmonicity for ν_1''.

ROTATIONAL STRUCTURE

The dispersion used did not allow a complete resolution of the fine structure, but some very characteristic features of this structure were observed. For instance, the coarse K-structure was analyzed for several bands situated at the long wave-length end of the spectrum, where blendings are less frequent than in other parts of the spectrum.

It can be seen easily that the structure of all bands in the first two columns of Table II is similar, thus reinforcing our previous assumption that these bands belong to the same electronic transition. On the other hand, we have observed two series of sub-bands (p and r) in the K-structure of several α_1 bands; this indicates that they belong to the perpendicular type. Using the second differences, we obtain $C' - C'' = -0.7 \pm 0.10$ cm^{-1}. Taking into account the value $C'' = 1.8$ cm^{-1}*** and the fact that the K-structure is degraded towards the red, it can be stated that $C' = 1.1 \pm 0.10$ cm^{-1}.

With the dispersion used, the J-structure remains completely unresolved, but there are indications that the convergence is slow.

For this reason, it can be reasonably admitted that the change of B correlated with the electronic transition is small; even the sense of the degradation in the J-structure is not clear, but it seems to be rather degraded in the same direction as the K-structure, i.e., toward the red. This statement is enhanced by the lack of marked absorption on the short wave-length side of the K-heads, even at high pressure.

It should be of great interest to resolve the fine structure of the α_2 bands given in the first two columns of Table III. All that can be said for the time being is that it seems to be very different from the structure of the α_1 bands (Table II). Our previous arguments in favor of separating the observed bands into at least two electronic systems are thus reinforced.†

INTERPRETATION OF THE RESULTS

The molecular orbitals for C_{2v} symmetry are distributed among four classes, following the symmetry of the wave functions with respect to the planes of symmetry of the molecule. These classes have been described by Mulliken as a_1, a_2, b_1, and b_2. On this basis and by the application of the molecular orbital theory, Mulliken[9] has proposed a scheme of the electronic levels of angular molecules and particularly of SO_2. He has given a preliminary interpretation of the observed electronic spectra of this molecule and

[8] E. F. Barker, Rev. Mod. Phys. **14**, 198 (1942).

*** In our previous letter (Nature **157**, 692 (1946)) we had erroneously given the value $C'' = 1.6$ cm^{-1}. This error does not affect our results.

† It must be stated, however, that the alternative arrangement, according to which the bands of Table II and Table III form a single electronic system, though rather improbable cannot be definitely ruled out. In fact, from a strictly numerical point of view it would be possible to consider the first two columns of Table II and the columns of Table III as consecutive v' series with ν_1' increasing from 965 ± 380 to 1062 ± 375 and reaching 1150 ± 370 cm for $v_1' = 2$.

[9] R. S. Mulliken, Rev. Mod. Phys. **14**, 204 (1942).

has considered the a-system as resulting from an allowed transition $3b_2 \rightarrow 5a_1$.

In the first part of this paper we have explained that the "a-system" must be divided into at least 2 electronic transitions corresponding to Tables II and III and described, respectively, as α_1 and α_2.

The molecular constants of the upper state of the two systems are the following:

$\alpha_1 \cdots \nu_1' = 963 \text{ cm}^{-1}$, $\nu_2' = 379 \text{ cm}^{-1}$,
$x'\nu_2' = 2 \text{ cm}^{-1}$, $\nu_0 = 42{,}170 \text{ cm}^{-1}$.
$\alpha_2 \cdots \nu_1' = 775 \text{ cm}^{-1}$, $\nu_2' = 375 \text{ cm}^{-1}$,
$\nu_0 = 44{,}236 \text{ cm}^{-1}$.

The high transition probability for both systems and the lack of antisymmetrical vibrations indicate that they are presumably due to allowed transitions; it must be stated however that the α_2 bands are much more intense than the α_1 bands. As already remarked, the α_1 bands appear to be of perpendicular type; according to group theoretical rules they must thus correspond to one of the three transitions: $a_1 - a_1$, $a_1 - b_1$, and $a_2 - b_2$. The first assignment is partially in agreement with the theoretical scheme proposed by Mulliken.†† In fact this scheme predicts two transitions in the 2000A region, one of them corresponding to $4a_1 - 5a_1$ ($\perp$ type), the other to $3b_2 - 5a_1$ ($\parallel$ type). It seems thus possible to correlate α_1 with the first and α_2 with the second one. The relative intensities of both systems are also in agreement with Mulliken's prediction. This interpretation, however, cannot be definitely accepted because Mulliken predicts $\Delta\alpha > 0$ for the $4a_1 - 5a_1$ transition, while, as we shall see below, we have deduced $\Delta\alpha < 0$ from our analysis of rotational structure.

It is also to be noticed that, while the α_1 system is weak relatively to α_2, it is much stronger than the b-system at 3000A, corresponding to $1a_2 - 2b_1$; this seems also contrary to Mulliken's predictions.

For this reason, the other possibilities mentioned above cannot be disregarded.

As the transition $a_1 - b_1$ has already been correlated with the c-system (λ max$\sim$3700A),[9] we have to emphasize only the third one, i.e., $1a_2 - 4b_2$. However this would require, according to Mulliken's scheme, 10 ev, instead of about 5 ev, according to our analysis. But it must be noted that even the energetic position of $3b_2$ has not been determined with certainty experimentally and that according to Mulliken all the calculations have not much more than a qualitative meaning. If α_1 corresponds really to $1a_2 - 4b_2$, it should be necessary to reconsider theoretically the variation of $4b_2$ with respect to the apex angle α of the molecule.

On the other hand, we have said that B' must be nearly equal to B'' while C' is very different from C''. If so, we have a case already discussed by Metropolis[10] and related to $\Delta\alpha < 0$ and $\Delta r \sim 0$. Then from the variation of C and B, we can conclude that the angle α has decreased by about 20°, while r_e has slightly increased by excitation.

These conclusions are in complete agreement with the general considerations of Metropolis[10] and would explain the fact that the α_1 system is not well developed toward high v_1' values.

For the α_2 system, the lack of rotational data prevents a more extensive analysis. A transition such as $3b_2 \rightarrow 5a_1$, as proposed by Mulliken for the whole a-system, seems not to be excluded and would give rise to parallel bands. In any event, the angle α cannot be determined by the analysis of the vibrational potential function of the excited state as it has been done by Metropolis[11] for the b-system. The reason lies in the fact that the value of α is very sensitive to the cross terms for angular molecules and, as it has been proved by one of us,[12] the cross terms cannot be neglected in such molecules. Furthermore, as the parallel character of the bands in the b-system must be considered with caution, we shall understand that the assigned transition ($1a_2 \rightarrow 2b_1$) cannot be considered as being established with certainty. The full discussion of the scheme proposed by Mulliken must thus be postponed until new experimental data farther to the ultraviolet will be available. On the other hand, it seems that the α_2 system is much more developed in the sense of high v_1' values than the α_1 system, and this indicates that in the

†† We are very indebted to Professor Mulliken for his valuable suggestion concerning this possibility, erroneously neglected by us in our previous letter (Nature **157**, 692 (1946)).

[10] N. Metropolis, Phys. Rev. **60**, 283 (1941).
[11] N. Metropolis, Phys. Rev. **60**, 295 (1941).
[12] J. Duchesne, Mémoires Soc. Roy. Sci. (Liége) **1**, fasc. 2, 429 (1943).

former r_e must be modified by excitation as well as α.

Before new steps in the interpretation of the SO_2 spectrum can be undertaken, it would be important to check the reality of the third α_3 system of Table IV, to get more information concerning the distribution of intensity in the bands, and to have more reliable data concerning bands in the 2000–1800A region.

P. Migeotte in our laboratory is now engaged on such experiments.

SeO_2

Introduction

The electronic diffraction patterns of SeO_2 vapor, studied by Palmer and Elliott,[13] indicate an angular symmetrical structure of the SeO_2 molecule, with a Se−O distance of 1.61A. The diffraction patterns being relatively insensitive to the apex angle, its value has not yet been determined.

The SO_2, SeO_2, and TeO_2 molecules belong to the same class of 18-electron molecules, and their comparative spectroscopic study presents, therefore, considerable interest. Up to now, three electronic systems of SeO_2 have been reported between 2000 and 5000A. Preliminary descriptions of these systems were given by several authors,[14] and in a recent paper[1] we have analyzed in some detail the vibrational structure of the *b*-system situated between 2300 and 3300A. In the present paper we deal with the vibrational study of the *c*-system situated in the visible, and we will try to develop some general conclusions regarding the electronic structure of the excited states. The analysis of the *a*-system in the farther ultraviolet is now in progress and will be published later.

Vibrational Analysis

For the present study we have used a two-prism Bourguel spectrograph for the visible, giving a dispersion of about 30A/mm at 4500A, and a Jobin quartz spectrograph giving a dispersion of about 15A/mm at 3000A. The source of background radiation was an Osram Nitra tungsten-strip filament bulb. The absorption of the SeO_2 vapor was investigated in 4-meter, 25-cm, and 2-cm absorption cells at temperatures varying between 300 and 500°C.

The SeO_2 crystals were carefully purified by repeated distillations in vacuum and introduced in a side tube sealed to the main absorption cell. This side tube could be heated independently from the furnace heating the main cell, and thus the vapor pressure could be varied in the usual manner independently of the temperature. We used pressures between 50 and 450 mm.

By varying the conditions of pressure and temperature, the SeO_2 absorption spectrum was investigated between 5000 and 3400A. In this region about 100 bands were measured, and the measurements are in general in agreement with those of Evans and of Choong-Shin Piaw.[14] These authors have reported (especially in the ultraviolet part of the spectrum) more bands than we. Some of them must probably be correlated with rotational structure, as we have already noted in the case of the *b*-system.[1]

The absorption in the bands of the *c*-system is considerably weaker than in the bands of the *a*- and *b*-systems. The number of molecules needed to reveal absorption in the visible is at least 10 times greater than the number needed to provoke absorption in the ultraviolet.

A characteristic feature of the *c*-system is the diffuseness of the bands in the central region and the increased sharpness toward both ends. On both extremes, the bands are relatively well defined and the majority of the heads can be measured with good precision, although errors up to 20 cm^{-1} cannot be excluded for fainter bands. In the central region, heads cannot be measured at all, and we have determined the position of the maxima of intensity on microphotometric records. Another striking feature of the *c*-system is provided by long series of bands extending through all the spectrum with the characteristic periodicity of about 200 cm^{-1}. These series are given in the columns of Table VI. The 200-cm^{-1} progression must surely be correlated with the bending frequency ν_2' of the excited state. The presence of long v_2' progressions indicates a considerable change of the apex angle of the molecule. The apparent lack of

[13] K. J. Parlmer and N. Elliott, J. Am. Chem. Soc. **60**, 1389 (1938).

[14] S. F. Evans, Nature **125**, 528 (1930); Choong-Shin Piaw, C. R. Acad. Sci. Paris **202**, 127 (1936); *ibid.* **203**, 239 (1936); Ann. de physique **10**, 191 (1938).

TABLE VI.

$v_1'v_2'v_3'$ \ $v_1''v_2''v_3''$	0		1		2		3		4
0	—		20,940						
			178						
1	—		21,118	917	20,201				
			206						
2	—		21,324						
			210						
3	—		21,534*	919	20,615				
			210		205				
4	—		21,743	923	20,820				
			192		215				
5	22,855	920	21,935	900	21,035				
	203		208		203				
6	23,058	915	22,143	905	21,238				
	201		198		210				
7	23,259	918	22,341	893	21,448				
	203		199		207				
8	23,462	922	22,540	885	21,655				
	192		193		188				
9	23,650	917	22,733	890	21,843				
	184		197		207				
10	23,834	904	22,930	880	22,050*				
	190		206		190				
11	24,030	894	23,136	896	22,240				
	200		209		174				
12	24,230	885	23,345	931	22,414				
	192		165		216				
13	24,422*	912	23,510	880	22,630		21,680		
	200		194		163		192		
14	24,622	918	23,704	911	22,793	921	21,872		
	198		185		198		200		
15	24,820	931	23,889	898	22,991	919	22,072	897	21,176
	182		201		202		211		215
16	25,002	912	24,090	897	23,193	910	22,283	892	21,391
	203		204		197		199		194
17	25,205	911	24,294*	904	23,390	908	22,482	897	21,585
	185		186		182		214		198
18	25,390	910	24,480	908	23,572	876	22,696*	913	21,783*
	245		210		190		198		
19	25,635	945	24,690	928	23,672	868	22,894		
	181		212		197		208		
20	25,816	914	24,902	947	23,955	853	23,102	919	22,183
					208		208		
21					24,163	855	23,310		
					205				
22					24,368				
					196				
23					24,564*				
					211				
24					24,775				
					188				
25					24,963				

* The underlined bands correspond to intensity maxima in the series.

TABLE VII.

$\Delta G_{v_1}''$	b-system mean values	c-system weighted values
0–1	894	911
1–2	893	898
2–3	907	889
3–4	902	903
0–4	3,596	3,601

stretching frequencies means that the valency bond remains practically unchanged. It seems, however, not excluded that some fainter bands in the ultraviolet part of the spectrum are due to a weak excitation of the valence frequency.

The first column of Table VI contains the most prominent bands of the whole system, and must, therefore, undoubtedly be correlated to the zero level of the normal state. The intensity distribution in this series is regular, and the maximum occurs at about 24,500 cm^{-1}. The assignment of the other series to definite vibrational levels cannot be done without some ambiguity. This is due to lack of regularity in the intensity distribution and to frequent irregularities in the distances between neighboring bands. From a strictly numerical point of view, several arrangements are possible; however, the scheme given in Table VI seems to us to be by far the most reliable; in particular, it gives for the ground level a frequency of about 900 cm^{-1}, already assigned to the stretching frequency of normal SeO_2 on the basis of our analysis of the b-system.

It is important to check this last conclusion by comparing the mean values of $\Delta G''$ resulting from the study of the b- and the c-systems. The agreement of the mean $\Delta G''$ values, corresponding to both systems and given in Table VII, can be considered as satisfactory and is even improved if we consider only those bands which can be measured with good accuracy. In doing so we obtain for the symmetrical stretching frequency in the ground level of SeO_2 the value of $\nu_1'' = 910$ cm^{-1}.

In adopting the vibrational scheme of Table VI for the c-system, we must admit that the irregularities in the progressions are due to some kind of perturbation. On the other hand, the occurrence of two intensity maxima observed in the bands of the second and third columns of Table VI (underlined bands) must be correlated either with the special form of potential energy surfaces or with the superposition of at least two series.

We have already noted that the band edges become increasingly sharper toward both ends of the spectrum; whereas on the long wave-length side the bands are shaded toward the red, they are shaded to the opposite sense at the other extremity of the spectrum. In the central part, the sense of the shading is not well defined; however the change of shading can be approximately located at 22,000 cm^{-1}.

A similar anomaly in the shading was observed by us in the TeO_2 bands, as will be reported in detail in the last part of this paper. On the other hand, the bands of all known SO_2 band systems are uniformly degraded toward the red (if we neglect the J-structure which has not been observed in the spectra of SeO_2 and TeO_2). It seems to us that the above-mentioned behavior of the SeO_2 and TeO_2 spectra must be explained as due to an isotopic shift and can be correlated with the fact that Se and Te have several abundant isotopes, whereas S has practically only one. We give in Table VIII the isotopic constitution of selenium:

TABLE VIII. Isotopic constitution of selenium.

Atomic weights	74	76	77	78	80	82
Abundance	0.9	9.5	8.3	24	48	9.3

Table VIII shows that the center of gravity of the isotopic group lies on the side of greater atomic weights. Thus the groups of isotopic bands are apparently shaded toward the red on the long wave-length side with respect to the origin, and toward the violet at the opposite extremity. In conformity with this point of view the change in the sense of degradation occurs at about 22,000 cm^{-1}, and coincides with the origin of the system according to the proposed vibration scheme.

Interpretation of Results

The present data do not permit stating whether the c-bands of SeO_2 correspond to an allowed or to a forbidden transition. The intensity distribution in the vibrational series indicates strongly that the electronic excitation does

not change appreciably the Se−O distance, whereas the apex angle is considerably modified.

We have already noted that most of the bands are rather diffuse, and this could presumably be due to the fact that the J- and K-structures are shaded in opposite directions. Not much more can be said for the moment about the structure of the molecule in the upper level.

It is worth while pointing out that no analogy can be established between this system and the c-system of the SO_2 molecule, studied by Metropolis and Beutler.[15] For the former, $\Delta r \cong 0$ and $\Delta\alpha \neq 0$, while for the latter $\Delta r \neq 0$ and $\Delta\alpha \cong 0$. On the contrary, the c-system of SO_2 is much more similar in regard to these properties to the b-system of SeO_2 for which we have previously proved[1] that r_e is the only parameter to change appreciably.

As Metropolis remarked,[10] the ratio of the moments of inertia I_c/I_b is practically constant ($\sim$1.17) in the normal state of a series of angular molecules such as SO_2, NO_2, and ClO_2. If we extend the validity of this rule to SeO_2, it provides an apex angle of about 130°. On the other hand, we observe that the ratio of the antisymmetrical and symmetrical frequencies of the same molecules also follows such a sort of regularity and equals approximately 1.17. Though the identity of the constants seems purely fortuitous, the extrapolation of this rule to SeO_2 gives us the possibility to locate ν_3'' at about 1060 cm^{-1}. The bending frequency ν_2'' can also be approximately estimated; in fact the apparent disappearance of this vibration in the spectrum may be explained by assuming that the fundamental frequency ν_2'' is a multiple of ν_2', the most probable value being $\nu_2'' = 400$ cm^{-1}. If this estimation is correct, the columns of Table VI could result from a superposition of several types of progressions, and the apparent lack of the 400-cm^{-1} progression, as well as the anomalies of intensity referred to above, could be satisfactorily explained.

With the three fundamental frequencies thus obtained (910, 400, and 1060 cm^{-1}) and by using a valence-deformation force field, we compute an apex angle of about 160°. The reason for the divergency with respect to 130°, which seems much more plausible, could be explained by the neglect of the cross terms in the potential function. The introduction of a small stretch-stretch cross term (f_{12}) of about -0.4×10^5 dyne/cm is sufficient to remove the divergency. On the other hand, by taking into account a stretch-deformation cross term (g_e) only, the best value equals about $+0.4\times10^5$ dyne/cm, and it is impossible to obtain quite satisfactory results. However, in order to obtain such results, it is sufficient to add in the potential function a slightly negative value of f_{12}. Thus, as we have no reason to believe that f_{12} has a considerable value, while $g_e = 0$ (or the reverse), it seems established that f_{12} and g_e have opposite signs, the former being negative and the latter positive, with numerical values smaller than 0.4×10^5 dyne/cm. Furthermore, the presence of the cross terms proves that the apex angle of molecules like SeO_2 and SO_2 cannot be determined by assuming a valency force field, contrary to the assumption by Metropolis for the case of the c-system of SO_2.

TeO_2

The TeO_2 absorption bands were first studied by Choong-Shin Piaw.[16] He arranged a part of the observed bands in a vibrational scheme according to the formula:

$$\nu = 25636 + 545v_1' - v_1'^2 + 206v_2' - 3v_2'^2 + 675v_3' - 2.7v_3'^2.$$

Several objections can be raised against this analysis:

1—It seems quite abnormal that at the high temperature used, the frequencies of the ground level do not appear in the spectrum.

2—only about 60 percent of the observed bands fit into the scheme.

3—the selection rules are not respected. It thus seemed necessary to re-investigate the TeO_2 spectrum before any attempt to compare it with the SO_2 and SeO_2 band systems could be undertaken.

Experimental Procedure

The TeO_2 vapor reacts with quartz at high temperatures necessary to obtain sufficient vapor

[15] N. Metropolis and H. Beutler, Phys. Rev. **57**, 1078 (1940).

[16] Choong-Shin Piaw, C. R. Paris **201**, 1181 (1935); Thesis, Paris (1937).

pressure. The absorption was therefore studied in thin open porcelain tubes filled with carefully purified TeO_2 crystals. The tube with TeO_2 was introduced into the electric furnace after the desired temperature was attained. We have thus operated in conditions far from equilibrium and contrary to the experiments concerning the SO_2 and SeO_2 absorption we were not able to vary the pressure independently of the temperature. In some cases, it was necessary to avoid excess oxygen and then the absorption tube was provided with water-cooled quartz windows and filled with nitrogen to prevent rapid distillation of TeO_2 outside the high temperature zone.

TABLE IX. Intensity maxima in the bands of the *b*-system of TeO_2.

ν_{max}	ν_{max}	ν_{max}
21,950	24,680	29,460
22,130	24,810	29,490
22,240	25,000	29,515
22,380	25,150	29,650
22,390	25,170	29,675
22,400	25,190	29,700
22,560	25,340	29,870
22,570	25,470	29,950
22,580	25,525	30,080
		30,165 a
22,650	25,620	30,320
22,665	25,640	30,400 a
22,680	25,660	30,515
	25,825	30,610 a
	26,000	30,750
22,750	26,080	30,790
22,765	26,160	30,830 a
22,780	26,280	30,960 b
	26,460	31,050 a
	26,640	31,160 b
22,920	26,820	31,250 a
22,930	26,920	31,385 b
22,940	27,070	31,450 a
	27,095	31,580 b
23,060	27,120	31,660 a
	27,260	31,800 b
23,200	27,460	31,865 a
	27,550	32,000 b
23,385	27,730	32,090 a
	27,880	32,205 b
23,550	27,910	32,275 a
23,575	27,940	32,410 b
23,600	28,125	32,500 a
	28,210	32,620 b
23,710	28,570	32,700 a
23,730	28,385	32,830 b
23,750	28,400	33,040 b
	28,540	
23,870	28,860	
24,000	29,020	
24,020	29,030	
24,040	29,045	
24,200	29,190	
24,360	29,345	
24,375		
24,400		
24,540		

The dispersion used was the same as in the case of SeO_2. For the bands situated near 4000A, it was possible to use a multiple-prism Jobin spectrograph in Littrow mounting, either with 5 quartz prisms giving a dispersion of about 9A/mm, or with 5 glass prisms with a dispersion of about 2A/mm at 4000A.

Vibrational Analysis

The most characteristic band system of TeO_2 is situated in the blue and near ultraviolet, between 3000 and 4550A, with a maximum near 3550A. In the conditions of our experiments (absorbing layer of a few centimeters, rapid distillation from the middle of the furnace towards the end) it appears at about 900°. At about the same temperature, we have observed very strong absorption bands in the region of 2000A, but owing to the presence of O_2, it has been up to now impossible to investigate these in detail. It is not even excluded that this absorption is due to impurities. Choong Shin-Piaw observed in the ultraviolet above 3000A only continuous absorption. At somewhat higher temperatures (about 1000°C) very weak and diffuse absorption bands appear in the region between 2450–2650A†††). It may belong also to some impurities. At a temperature of about 1100°, some weak and very diffuse bands appear between 4650 and 5100A. We shall refer to them at the end of this paper. At still higher temperature, the TeO_2 bands gradually disappear, and they are replaced by TeO absorption bands which will be discussed in detail elsewhere. In this paper we will deal chiefly with the main system between 3000–4550A, which will be designed as the *b*-system.

In the *b*-system, the bands situated in the blue are sharp and shaded towards the red. Towards the ultraviolet they gradually become more diffuse, and even the sense of degradation is reversed in the extreme ultraviolet end of the spectrum. This change of shading is probably due to an isotopic effect in the same way as

††† The wave numbers of the band heads, which are shaded toward ultraviolet, are the following: 40740, 40260, 39760, 39400, 39260, 39060, 38920, 38740, 38580, 38420, 38240, 38080 cm^{-1}.

described for the corresponding case occurring in SeO_2. In fact, the proportion of the different isotopes of Te is such that the general character of the isotopic shift is the same in both cases.

The general character of the *b*-system of TeO_2 has many common features with the *b*-system of SeO_2. As in the case of SeO_2, it is rather difficult to locate the heads accurately, owing to the diffuse character of most bands. The spectra taken with great dispersion show a very complicated sub-structure which, even at the dispersion of 2A/mm, is not resolved into lines. The present data are not sufficient to decide whether this observed structure is due to isotopic effect or represents sub-bands in the coarse structure of the system. Probably both kinds of substructure interfere and explain the complicated character of the whole system.

The positions of the most prominent band heads are in good agreement with those given by Choong Shin-Piaw, but for the reason given above these figures must be considered with caution. For the vibrational analysis, we preferred to use chiefly the measures of the band maxima given in Table IX.

As in the case of the *b*-system of SeO_2, the TeO_2 *b*-system is characterized mainly by long series of bands with a periodicity of about 650 cm^{-1}. Several irregularities are observed in the distances between neighboring bands; these irregularities are less marked if we use band maxima instead of band heads. With small dispersion the complicated structure of the bands resolves into very characteristic doublets, with irregular doublet separation. As this doubling is presumably due to some kind of perturbations, we have used the mean values for the vibrational analysis. In the Table IX these doublets are joined by brackets. The vibrational analysis finally adopted is reproduced in Table X. Most of the bands of Table IX are fitted into this scheme with only one characteristic frequency in each state; both are to be considered as symmetrical valency frequencies $\nu_1' = 670$ and $\nu_1'' = 810$ cm^{-1}.

It is worth while to note that the value $\nu_1'' = 810$ cm^{-1} for the valency frequency of the ground state of TeO_2 is nearly equal to the vibrational frequency $\omega'' = 796$ of TeO given by

TABLE X. *b*-system of TeO_2.

ν_1'' \ ν_1'	0		1		2		3		4		5		6		7		8		9		10		11		12		13
0	24,020	660	24,680	660	25,340	660	26,000	640	26,640	620	27,260	650	27,910	630	28,540	650	29,190										
	820		810		800		830		835		800		815		810		805										
1	23,200	670	23,870	670	24,540	630	25,170	655	25,825	635	26,460	635	27,095	635	27,730	655	28,385	645	29,030	645	29,675	645	30,320	640	30,960		
	810		810		810		795		825		820		815		810		835		820		815		830		795		
2	22,390	670	23,060	670	23,730	645	24,375	625	25,000	640	25,640	640	26,280	640	26,920	630	27,550	660	28,210	650	28,860	630	29,490	675	30,165	625	30,790
					800		800		800		830		810		840												
3					22,930	645	23,575	625	24,200	610	24,810	660	25,470	610	26,080												
					800		810		815																		
4					22,130	635	22,765	620	23,385																		
							815		815																		
5							21,950	620	22,570																		

Choong-Shin-Piaw.[16] ‡ The same relation is correspondingly valid for the valency frequencies of SeO_2 and SO_2 (910 and 1152) as compared with those of SeO and SO (909 and 1124). Although at present, no theoretical considerations supply a basis for such a relation, it seems nevertheless that the parallelism in the behavior of the six molecules constitutes a further argument in favor of our analysis. The scheme of Table X contains nearly all bands observed between 22,000 and 30,000 cm^{-1}. In the ultraviolet end of the spectrum, however, there are two rather long series of faint bands which appear only when the absorption in the central part is complete and which cannot be fitted in the scheme. These bands are marked *a* and *b* in Table IX and form two progressions with a characteristic frequency of about 200 cm^{-1}. On the other hand, some of the weaker bands farther to the visible, which cannot be fitted in the scheme of Table X, are situated at about 200 cm^{-1} on the violet side of strong bands belonging to the main series. It seems reasonable to admit that 200 cm^{-1} represents the deformation frequency of the upper state and that each v_1' level is combined with a series of v_2' levels. This statement cannot, however, be considered as definitive, as the possibility that the 200-cm^{-1} progression belongs to a separate electronic transition cannot be ruled out. If all the bands belong to a single system, it would mean that the corresponding transition is accompanied not only by considerable change of the apex angle α but also of the Te−O distance.

After having established the analogy existing between the *b*-systems of SeO_2 and TeO_2, we have searched for a system of TeO_2 situated farther toward the red in analogy with the *c*-system of SeO_2. At the highest pressure obtainable, corresponding to temperature above 1100°C, some weak and diffuse bands, without marked heads, appear between 4650 and 5100A on microphotometer records; we have measured the following maxima: 21,520, 21,030, 20,560, 20,150, 19,750 cm^{-1}. These bands bear no analogy with the *c*-system of SeO_2.

Our best thanks are due to Professor R. S. Mulliken for valuable criticism. Some of the spectra used in this investigation were taken and measured by R. Migeotte and A. Robert; we wish to express to them our thanks for their effective help.

‡ According to the new analysis of TeO bands (not yet published) by one of us, $\omega'' = 790$ cm^{-1}.

THE JOURNAL OF CHEMICAL PHYSICS VOLUME 15, NUMBER 9 SEPTEMBER, 1947

Restricted Rotator Thermodynamic Properties from the Old Quantum Theory

J. O. HALFORD
Department of Chemistry, University of Michigan, Ann Arbor, Michigan
(Received May 7, 1947)

Accurate partition functions and free energies are calculated for the hindered internal rotator from the old quantum theory based upon the quantization rule of Wilson and Sommerfeld. The description of the system is incomplete and the energy levels may even be incorrectly placed, but the partition functions are surprisingly close to those now accepted as correct. In the course of the development the lowest energy state of the harmonic oscillator turns up in its correct position at the half-quantum level.

HIGH precision can be achieved in calculating the contributions of vibration and pure rotation to thermodynamic properties by methods which omit most of the detail of the energy states of the molecule. Vibrations are taken to be harmonic, interactions are assumed to be negligible, and the contributions are expressed by simple equations involving not more than one molecular constant for each degree of freedom.

Before these simplifications could be used with confidence they had to be justified mathematically or by reference to experimental data. For example, Mayer, Brunauer, and Mayer[1] derived the energy levels of the unsymmetrical three-dimensional rotator and the free internal rotator of the ethane type from the wave mechanics, and showed that the partition functions could be represented by summations involving only moments of inertia and fundamental constants. Their partition functions proved to be the same as those obtained by the classical statistics. Consequently, it was possible for Kassel[2] to use the classical method when he developed the general case for the rigid framework with attached symmetrical rotators in extension of the important generalization of Eidinoff and Aston.[3] Kassel's result proved for practical purposes to be the same as had been predicted by the writer.[4]

Another less sweeping simplification is applicable to the rotator in regions where the classical statistics are no longer accurate. Here the energy levels based upon the old quantum theory give the same partition functions as those derived from the wave mechanics. For the harmonic oscillator the old quantum theory may be used in spite of the fact that the energy levels are incorrectly located. Consequently, except for restricted internal rotation, it appears that the finer details of the wave mechanics contribute nothing of practical significance to the ordinary calculation of thermodynamic properties.

In this paper it will be shown that a simplified method may also be used for the internal rotator. The old quantum theory based upon the Wilson-Sommerfeld quantization rule yields partition functions which do not differ significantly from those obtained by more detailed methods. The description of the energy states is incomplete and the individual levels may be in incorrect positions, but the partition functions and, therefore, the thermodynamic properties always assume values very close to those now accepted as correct.

The old quantum theory handles this problem without any assistance and leads to a minor uncertainty only in the region of close approach to free rotation. The uncertainty in the free energy, however, remains within about 0.02 cal./mole/deg., and only a small and unimportant part of the tables of thermodynamic properties is affected.

Even the half-quantum of energy in the ground state of the harmonic oscillator is revealed correctly by the old quantum theory of the hindered internal rotator. This unexpected result is a consequence of the necessity for establishing a consistent scale of quantum numbers to be used

[1] J. E. Mayer, S. Brunauer, and M.G. Mayer, J. Am. Chem. Soc. **55**, 37 (1933).
[2] L. S. Kassel, J. Chem. Phys. **4**, 276 (1936).
[3] M. L. Eidinoff and J. G. Aston, J. Chem. Phys. **3**, 379 (1935).
[4] J. O. Halford, J. Chem. Phys. **2**, 694 (1934).

in both the vibrational and the rotational regions. Thus one of the major faults of the method disappears during the present application.

It is doubtful if any procedure which had been so successful in its day has ever been more completely discarded than the Wilson-Sommerfeld quantization method. Confidence in its results has reached such a low point that nearly everyone, including the writer, would be unwilling to trust its application to the restricted rotator if tabulations derived by methods accepted as more rigorous were not available for comparison. As far as thermodynamic functions are concerned, the present study indicates that it has not been wise to discard this useful tool so completely.

It becomes possible to calculate the thermodynamic properties of a compound, except in very unusual cases, without recourse to the detail of the wave mechanics. This statement has valuable practical implications, because it is evident that the complications inherent in the solution of the Schroedinger equation can constitute a serious obstacle and may lead the user into making approximations which tend to nullify the advantages of the method.

The effect of varying the assumed potential energy can now be studied in a simpler manner than the one outlined by Pitzer and Gwinn.[5] There appears to be some theoretical justification for a function of the form

$$V=(V_0/2)[1+\cos n\theta+k(1-\cos 2n\theta)],$$

which corresponds roughly to curve C in their Fig. 2. Calculations are now in progress to determine whether a detailed study of this function would be justified.

RESULTS

Table I shows the differences between the free energies of Pitzer and Gwinn and those obtained in this study at twenty-seven points distributed over the entire useful range of the variables V/RT and $1/Q_f$. A positive difference means that F/T or $(F-F_f)/T$ is greater than the Pitzer and Gwinn value. V is the height of the simple cosine potential barrier, R the gas constant (1.9869), T the absolute temperature, Q_f the partition function of the free rotator,

$$Q_f=2.8148(10^{38}IT)^{\frac{1}{2}}/n, \qquad (1)$$

and I is the reduced moment of inertia.

TABLE I. Deviation of old quantum theory free energies (cal./mole/deg.) from the results of Pitzer and Gwinn.

V/RT \ $1/Q_f$	0	0.1	0.2	0.4	0.55	0.60	0.80
0.4	+0.0007	−0.004	−0.003	+0.002	−0.003		
1.0	−0.0004	+0.002	+0.006	−0.002	−0.011		
4.0	+0.0006	−0.002	+0.003	+0.002		+0.005	
9.0	−0.0002	0.000	−0.001	0.000		+0.001	0.00
16.0	−0.0003	−0.001	−0.001	0.000		0.000	0.000

The largest difference appears at $1/Q_f=0.55$ and $V/RT=1.0$. At this point an adjustment of the zero state to insure asymptotic approach to the free rotator, as described later, becomes most uncertain, but the spread of reasonable adjustments should not cause deviations larger than 0.02 in the column for $1/Q_f=0.55$, 0.015 for $1/Q_f=0.50$, and 0.01 for $1/Q_f=0.45$. Within each column, it has been found by calculations not included in the table that the deviations decrease rapidly from the maximum as V/RT is changed in either direction.

For further application of the old quantum theory it would be permissible to adjust the values in this region toward those of Pitzer and Gwinn. For the present, however, they are left as they are in order to show what the method produces without assistance from other sources. In any case the deviations are unimportant in relation to the errors of thermodynamic data, the arbitrary selection of the potential function and the probability that the region of the largest deviations will not be used unless methyl alcohol proves to have an unexpectedly low potential barrier.[6]

It is obvious without further calculation that the other thermodynamic properties will be close to those found by Pitzer and Gwinn.

ENERGY LEVELS

The total energy E is expressed as the sum of the kinetic and potential energies by the equation

$$2E=I\dot{\theta}^2+V(1-\cos n\theta), \qquad (2)$$

in which θ is a rotational coordinate and n is the symmetry number or the number of potential minima in the cycle. The momentum p, equal to

[5] K. S. Pitzer and W. D. Gwinn, J. Chem. Phys. **10**, 428 (1942).

[6] J. O. Halford, J. Chem. Phys. **15**, 364 (1947).

$I\dot{\theta}$, becomes

$$p = I^{\frac{1}{2}}[2E - V(1-\cos n\theta)]^{\frac{1}{2}} = (IV)^{\frac{1}{2}}[2(E/V-1)+(1+\cos n\theta)]^{\frac{1}{2}}. \quad (3)$$

For states with energy less than V, $E/V-1$ is equal to $-(1+\cos n\theta_0)/2$, where θ_0 is the amplitude of vibration.

The Wilson-Sommerfeld rule requires that

$$rh = \oint p\,d\theta = (IV)^{\frac{1}{2}} \oint [2(E/V-1) + (1+\cos n\theta)]^{\frac{1}{2}} d\theta, \quad (4)$$

with r to have only integral values. The symmetry number can be factored out of the integral by the substitution $\varphi = n\theta$. Limits are then assigned for a complete cycle in φ to give

$$rh = 2(IV)^{\frac{1}{2}}/n \int_0^{\pi} [2(E/V-1) + (1+\cos\varphi)]^{\frac{1}{2}} d\varphi. \quad (5)$$

This equation states that the rotational quantum number at a given total energy is one nth of the quantum number for the same energy in the single minimum case and means that only each nth rotational doublet is to be counted. The corresponding point in the Pitzer and Gwinn development is the assignment of one state to each of the regions delimited by their theory. In Eq. (5), for convenience, the integration is performed over half the cycle and the result is multiplied by two.

The quantum number obtained in this manner gives the mean position of the rotational doublet. If the integration is performed in the vibrational region strictly according to the rule, the upper limit is changed to the amplitude, φ_0, and the length of the cycle is doubled. Here, to keep rotations and vibrations on the same number scale, the doubling is omitted and the rotational scale is retained into the vibrational region, where each quantum number r now gives the mean position of two vibrational states. But in the harmonic oscillator limit the individual states are equally spaced on both the energy and number scales. The two number scales, vibrational and rotational, become consistent if the vibrational states are placed at $r = 1/4, 3/4, 5/4, \cdots$, corresponding to the vibrational quantum numbers $1/2, 3/2, 5/2, \cdots$. In this way the harmonic oscillator acquires an energy $h\nu/2$ in the ground state by an argument based upon the Wilson-Sommerfeld quantization rule.

The key to the use of the old quantum theory in the internal rotation problem is to retain under all conditions the rule that the rotational quantum number r is the arithmetical mean of the quantum numbers of the two components of the doublet.

The manner of arriving at Eq. (5) suggests that it should give a solution for the energy levels in the single minimum case when there is no over-all rotation of the molecule around the axis of the internal motion. This interpretation is in qualitative agreement with diagrams published by Koehler and Dennison[7] for the methanol case in illustration of their general solution for the energy levels with the simple cosine potential function.

For states entirely in the rotational region the theory fails to designate the doublet separation. This is known, however, at the top of the barrier, and can be reasonably assumed to approach zero for high energy levels, a situation that can be approximately represented by assigning the positions $r \pm V/4E$. Because of a tendency toward cancellation of the errors introduced by this assumption, its effect is felt only in those cases where the first doublet is at a short distance above the top of the barrier.

The integration of Eq. (5) has been performed graphically at chosen values of φ_0 or E/V. At

TABLE II. Energy of the internal rotator in terms of the quantum number index.

E/V	A (radians)	ρ
0.03016	0.06724	0.008539
0.1170	0.26385	0.033505
0.2500	0.5746	0.07297
0.4132	0.9749	0.12348
0.5868	1.4305	0.18165
0.7500	1.9005	0.24134
0.8830	2.3344	0.29644
0.9700	2.6729	0.3394
1.00	2.8284	0.3592
1.10	3.2550	0.4133
1.25	3.7267	0.4732
1.50	4.3689	0.5548
2	5.4026	0.6861
3	7.0071	0.8898
5	9.4175	1.1959
9	12.9503	1.6445

[7] J. S. Koehler and D. M. Dennison, Phys. Rev. **57**, 1006 (1940).

TABLE III. δ (Eq. (9)) as a function of ρ.

ρ	δ
0.008539	0.00002
0.033505	0.00024
0.07297	0.00098
0.12378	0.00215
0.18165	0.00235
0.24134	0.00000
0.29644	−0.00863

each point from twenty to forty ordinates were calculated and the area was approximated for the separation $\Delta\varphi$ and the ordinates y_0, y_1, $\cdots$, y_n, according to the equation

$$A=\Delta\varphi[(y_0+y_n)/2+y_1+\cdots+y_{n-1}]. \quad (6)$$

Apparent areas A for several values of $\Delta\varphi$ were plotted against $\Delta\varphi$ and extrapolated to $\Delta\varphi=0$. For this purpose, if the number of ordinates is chosen conveniently, only one addition is necessary. For example, with forty ordinates the first total is based upon y_0, y_8, etc. To this are added y_4, y_{12}, etc., to give the second total for half the spacing first used. The rest of the process is evident. Simpson's one-third rule might have been used, but the writer is a little suspicious of it and preferred the method just described. In a few tests the error made with Simpson's rule for a given $\Delta\varphi$ proved to be about equal to that made with Eq. (6) for $\Delta\varphi/2$. Any advantage of Simpson's rule is partly offset by the extra work of adding the ordinates in new combinations and the need for enough ordinates to provide three points for the extrapolation.

As the ratio E/V increases above 1.0 the area rapidly approaches that of a rectangle erected on the ordinate at $\varphi=\pi/2$ and can be obtained accurately with quite large spacing of the ordinates. At the top of the barrier the integration is carried out analytically to give an area of $2^{\frac{1}{2}}$ radians and provide a check on the accuracy of the graphical method. The difference appears in the fifth digit beyond the decimal point. Incidentally the classical picture of a vibration at this point is rather amusing. At the maximum amplitude the restoring force is zero, suggesting that the period should be infinite and the frequency zero.

Equation 5 is combined with the equation

$$Q_f=(8\pi^3IkT)^{\frac{1}{2}}/nh \quad (7)$$

to give Eq. (8), in which ρ is a convenient quantity that may be called the quantum number index.

$$r/[Q_f(V/RT)^{\frac{1}{2}}]=A/(2\pi^3)^{\frac{1}{2}}=\rho. \quad (8)$$

Since the relation between E/V and A or ρ is the same for all systems within the range of the variables a single curve or its equivalent in tables and equations will summarize the results of the quantization.

Table II shows in successive columns the related values of E/V, the integral A, and the quantum number index ρ.

The information in Table II can be expressed in equations to be used with tables of differences. For E/V between zero and 0.75 the equation is

$$E/V=3.545\rho-1.812\rho^2+\delta \quad (\rho<0.24), \quad (9)$$

for which δ is shown in Table III.

At higher levels the equation

$$E/V=\pi\rho^2+0.5+\Delta \quad (\rho>0.24) \quad (10)$$

is valid. The values of Δ appear in Table IV. For interpolation in Tables III and IV it is convenient to use the graphical method.

It is evident that the curve of E/V against ρ is asymptotic to the harmonic oscillator line $E/V=2\pi^{\frac{1}{2}}\rho$ in the low energy limit, and approaches the parabola $E/V=\pi\rho^2+0.5$ at high energies. The latter limit is consistent with the statement by Koehler and Dennison that the high levels approach the free rotator energies plus $V/2$. The relation to the harmonic oscillator and the limiting rotator is illustrated in Fig. 1.

In terms of the variables used here the equations for the harmonic oscillator and the free rotator take particularly simple forms. For the oscillator the expressions $E=2rh\nu$ and

TABLE IV. Δ (Eq. (10)) as a function of ρ.

ρ	Δ
0.1817	−0.01683
0.2413	+0.06703
0.2964	0.10695
0.3394	0.10792
0.3592	0.09471
0.4133	0.06325
0.4732	0.04641
0.5548	0.03303
0.6861	0.02132
0.8898	0.01259
1.1959	0.00695
1.6445	0.00371

$\nu = n(V/2I)^{\frac{1}{2}}/2\pi$ are combined with Eqs. (7) and (8) to give $E = 2\pi^{\frac{1}{2}}\rho V$. For the free rotator, the relation $E = (nrh)^2/8\pi^2 I$ together with Eqs. (7) and (8) yields $E = \pi\rho^2 V$. Although ρ becomes infinite as V approaches zero, the energy remains definite for all finite values of the quantum number r.

To find the allowed energies for a given rotator, the quantum numbers $r \pm \frac{1}{4}$ and $r \pm V/4E$, where r is an integer, are divided by the product $Q_f(V/RT)^{\frac{1}{2}}$ (which is independent of the temperature) to give the required values of the index ρ, after which the energy ratios E/V are determined from Eqs. (9) and (10) and Tables III and IV. The sum of the quantities $e^{-(E/V - E_0/V)(V/RT)}$ is then the required partition function.

This simple procedure gives highly accurate partition functions and free energies for all cases for which three or more individual energy levels lie within the potential valley, and covers practically all situations for which the thermodynamic properties would probably be needed. The special treatment used between this point and the free rotation limit is considered in a separate section.

HIGH TEMPERATURE LIMIT

When $1/Q_f$ approaches zero the spacing of the energy states becomes infinitesimal and the partition function may be expressed by means of the following integral:

$$Q = 2\int_0^\infty e^{-E/RT} dr = 2Q_f(V/RT)^{\frac{1}{2}} \int_0^\infty e^{-E/RT} d\rho. \quad (11)$$

As Pitzer[8] originally found, the ratios Q/Q_f and the corresponding free energy differences are finite, although the partition functions themselves are not.

The integral from $\rho = 0$ to $\rho = 0.24$ was found by the graphical method in the manner described above in connection with the quantizations. The remainder of the integral was evaluated closely enough by a rapid procedure which enlisted the aid of tabulated values of the probability integral

$$P_1 = (2/\pi^{\frac{1}{2}}) \int_0^{x_1} \exp(-x^2) dx, \quad (12)$$

found in Mellor's *Higher Mathematics*.[9]

[8] K. S. Pitzer, J. Chem. Phys. **5**, 469 (1937).

[9] J. W. Mellor, *Higher Mathematics for Students of Chemistry and Physics* (Dover Publications, New York, 1946), p. 621.

The integral between the limits x_1 and x_2 is $P_2 - P_1$, and for our purposes takes the form

$$P_2 - P_1 = (2a/\pi^{\frac{1}{2}}) \int_{a\rho_1}^{a\rho_2} \exp[-a^2\rho^2] d\rho \quad (13)$$

from which, if $a = (\pi V/RT)^{\frac{1}{2}}$, the fraction of the partition function of a free rotator which comes from the region between ρ_1 and ρ_2 is given directly by $P_2 - P_1$ as found in the table for $x_1 = a\rho_1$ and $x_2 = a\rho_2$. If ρ_1 and ρ_2 are not far apart, the correction Δ of Table IV may be regarded as constant, and the contribution of the region to Q/Q_f will be given by

$$[Q/Q_f]_{\rho_1}^{\rho_2} = (P_2 - P_1) e^{-(0.5+\Delta)V/RT}. \quad (14)$$

As the energy ratio approaches the limit $E/V = \pi\rho^2 + 0.5$, the fractions may be taken over increasingly wide intervals. The result is nearly as accurate as the direct graphical integration when only twelve areas are summed in this manner. The procedure is equivalent to replacing the E/V curve by a series of parabolic sections parallel to the free rotator curve before performing the integration.

APPROACH TO FREE ROTATION

In the harmonic oscillator limit the ground state is found at the position $r_0 = \frac{1}{4}$ or $\rho_0 = 1/[4Q_f(V/RT)^{\frac{1}{2}}]$. If this relation were applied in the region of close approach to free rotation,

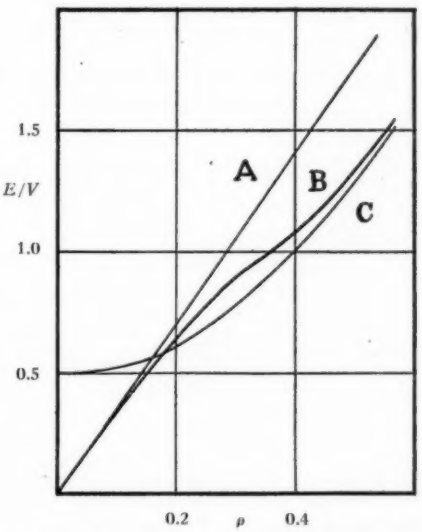

FIG. 1. Ratio of energy to barrier height as a function of the rotational quantum number index. *A*, harmonic oscillator. *B*, restricted rotator. *C*, limiting rotator.

TABLE V. Energy levels of methyl alcohol for $V=770$ cm^{-1}.

E/V (K and D) Min.	Max.	r	ρ	E/V (this study)
0.2482	0.2506	0.25	0.07594	0.2598
0.6784	0.7187	0.75	0.22782	0.7144
0.9644	1.1697	1.25	0.37970	1.0329
1.2152	1.6766	1.85	0.56196	1.5241

with Q_f constant and V/RT approaching zero, the zero state would appear to emerge from the potential valley at a finite value of V/RT, and the ratio E_0/V would increase indefinitely as the barrier decreased toward zero. It is easily shown that in the limit the energy would be one-sixteenth that of the first rotational doublet, and that when the zero state was above $V/2$, the partition function would exceed the free rotation value.

It is, therefore, necessary to adjust the zero state downward if an asymptotic approach to free rotation is to be achieved. While it is obvious that the zero-point energy must disappear in the limit, there is no evident reason why the partition function should not exceed the free rotation value through some limited range of very low potential barriers.

An examination of the graphical illustrations of Koehler and Dennison raises the same question in connection with the region over which the zero state may roam in the triple-minimum problem as the potential barrier decreases toward zero. The answer would come from a detailed study of the combined partition function of the coupled internal and external rotations, and will be sought at some future date when time permits.

For the present it is assumed that the zero state will remain low enough to insure an asymptotic approach of the partition function to the free rotator limit from lower values. An adjustment is made according to the arbitrary relation

$$\alpha\rho_0^{\beta}+\rho_0=1[4Q_f(V/RT)^{\frac{1}{2}}]=\rho_1/4. \quad (15)$$

There appears to be no way to determine α and β uniquely, but satisfactory evaluations can be made by considering the behavior of the function in two limiting regions. It is required, if r is to be at the mean position of the doublet, that the first term of Eq. (15) shall become negligible when the first doublet is entirely within the potential valley, where the separation is fixed by the quantization over the vibrational cycle. For this situation ρ_0 is 0.072, and an error of about 0.0004 can be made without introducing a significant uncertainty into the partition function. If β is assigned, the corresponding α is determined by this assumed error. The behavior of the function near free rotation for various values of β is next examined. It is assumed that at $1/Q_f=0.55$ and $V/RT=0.10$ the partition function will be below and very close to the free rotator value, and the lowest integral value of β is taken for which this is true. The equation then takes the form

$$7.7\times10^6\rho_0^9+\rho_0=\rho_1/4. \quad (16)$$

Actually the deviations in Table I are smaller for the next higher power of ρ_0. A change in the permissible uncertainty at $\rho_0=0.072$ will alter the selection of α and β without producing much change in the size of the corrective term. The procedure is quite arbitrary, but no reasonable change in the assumptions produces serious differences in the partition functions and free energies.

For ρ_1 greater than 0.29, Eq. (16) is used to find the position of the ground state. If the energy at $r_0+1/2$ falls within the barrier, the lower component of the first doublet is placed at this point and the second component is moved upward to $3/2-r_0$ in order to keep ρ_1 for $r=1$ at the mean position. When $r_0+1/2$ is in the rotational region the doublet components are placed at $r=1\pm V/4E$.

As might be expected, the largest deviations of Table I occur near the midpoint, on the ρ_0 scale, of the region spanned by Eq. (16).

METHYL ALCOHOL

The energy levels given by the old quantum theory can be compared with those calculated by Koehler and Dennison for methyl alcohol with an assumed potential barrier of 769.43 cm^{-1}. They have described the first four levels in detail, showing exactly how the components of each triplet change in position with the quantum number of the external rotation about the axis of the methyl top. In Table V, the first and second columns show the ratio E/V for the

minimum and maximum positions of the states within each triplet, and the third, fourth, and fifth give the values of r, ρ, and E/V obtained in this study. The reduced moment of inertia was calculated from other constants in their paper to be 1.116×10^{-40}.

At the upper levels the old quantum theory result appears alternatively toward the upper or lower end of the region delimited by the wave mechanics. At the same end of each region, when the external quantum number is zero, is found a component of a separated doublet derived from a rotational state whose quantum number in the complete system of levels is a multiple of 3, or, more generally, a multiple of n. The Wilson-Sommerfeld rule, therefore, gives an average position weighted toward the true level taken by a component of each nth state when there is no external rotation. The upward displacement of the odd numbered states, on the vibrational scale of quantum numbers, is greater than the downward displacement of the even numbered states.

For the same zero level the old quantum theory would lead to a lower partition function than the one obtained from the mean positions of the regions derived from the wave mechanics. In Table V, however, the zero state is a little high, and our experience indicates that it is just high enough in general to compensate for the different description of the higher levels and lead to the correct partition functions.

THE JOURNAL OF CHEMICAL PHYSICS VOLUME 15, NUMBER 9 SEPTEMBER, 1947

Statistical Properties of Networks of Flexible Chains

HUBERT M. JAMES
Purdue University, West Lafayette, Indiana

(Received May 12, 1947)

A Gaussian network is defined as a network of flexible chain segments, linked to each other and to a system of fixed points, in which each unbranching chain segment can take on a number of configurations which is a Gaussian function of the distance between its ends. Real molecular networks, such as those of rubber, can under certain circumstances be treated as Gaussian networks. The present paper carries out a systematic mathematical discussion of the statistical properties of Gaussian networks: the total number of possible configurations of the network as a function of the fixed-point coordinates, the probability of finding a given element of the network in a given position, or of finding two elements of the network in given relative positions, and so on. All probability-density functions appear as exponentials of quadratic forms, with constants explicity expressible in determinant form. An explicit reduction to a sum of squares is given for all quadratic forms occurring in the theory of coherent Gaussian networks, and an explicit general formula is found for integrals of the form

$$\int_{-\infty}^{+\infty} dX_1 \int_{-\infty}^{+\infty} dX_2 \cdots \int_{-\infty}^{+\infty} dX_q \exp\left\{-\sum_i^n \sum_j^n \gamma_{ij} X_i X_j\right\}.$$

There is described a mechanical analog of a Gaussian network, by consideration of which the statistical properties of the Gaussian network can be determined. The method is applied to the discussion of the statistical properties of a Gaussian network with the connectivity of a regular cubic lattice.

RUBBER-LIKE materials consist of molecular networks formed by the random bonding together of long flexible molecular chains.[1] In developing the theory of rubber-like elasticity it is necessary to study the statistical properties of these networks—to determine how the total numbers of configurations possible for the network depends on the external constraints, to compute the probability that a given element of the network is in a given position, or that a given pair of elements are in given relative positions, and so on. It has been shown elsewhere [1] that for such purposes it is a reasonable approximation (in the case of soft rubber) to assume that each unbranched chain segment in the network can take on a number of configurations which is a Gaussian function of the separation of its ends, and this independently of the

[1] H. M. James and E. Guth, J. Chem. Phys. 11, 455 (1943).

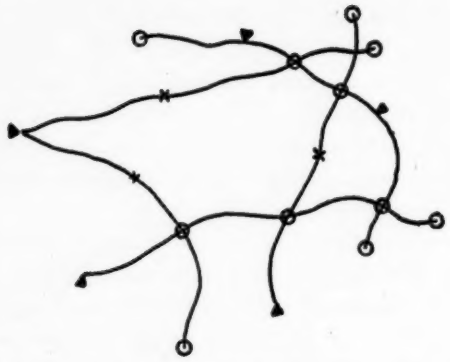

FIG. 1. Terminology. ▲—fixed points; ○—points necessarily treated as "junctions" in the present paper; ×—points which can be treated as junctions.

configurations assumed by other segments. Such chain segments will be termed Gaussian segments, and the networks will be called Gaussian networks. Attention will be confined in the present paper to the statistical properties of Gaussian networks.

In real molecular networks the molecular chains cannot take on all configurations independently of each other; they are subject to mutual constraints which, for instance, determine the volume occupied by the material. It is a consequence of these constraints that the most probable positions of all elements of the networks do not lie at the same point (as they would for an unconstrained Gaussian network), but are distributed with uniform average density through the material; some elements of the network are found always near the surface of the material, some deep in the interior. It would be exceedingly difficult to take detailed account of these constraints. Instead, one can[2] represent the real system by a model consisting of a corresponding Gaussian network of which certain elements—those corresponding to elements of the real system that lie near the surfaces of the material—are constrained to lie at fixed points on the bounding surface of the model. Change in the macroscopic form of the material thus corresponds to displacement of these fixed points of the model.

The networks to be considered in the present paper are Gaussian networks which extend between a set of fixed points. The problem at hand is to determine the statistical properties of these networks as they depend on the nature of the network and on the positions of the fixed points. The subject will here be developed systematically from an almost purely mathematical point of view; physical applications will be found in papers quoted here and in others now in preparation.

[2] This point will be discussed in more detail in a forthcoming paper.

I. TERMINOLOGY AND NOTATION

The networks to be considered are formed when long chains are bonded to each other and to fixed points. The points at which the chains are bonded together are usually called junctions of the network, and the chains are considered to be divided into segments by the points of bonding and the fixed points.

In the present paper it will be convenient to extend the meaning of the terms "segment" and "junction." A chain will be considered to be divided into segments at points of bonding, at fixed points, and at any other points which it may be desired to single out for consideration. The term "junction" will be applied to all points at which segments are terminated; it will thus include points of bonding, the arbitrarily chosen points of divisions of a chain into segments, and the free ends of chains (see Fig. 1). Since the division of an unbranching chain into segments can be made arbitrarily, the term junction can be made to apply to any chosen point of the network. In the theory to be developed, attention will be focused on the junctions and fixed points of the network, each of which is connected by an unbranched Gaussian chain to one or more other junctions or fixed points. It is to be remembered that the statistical properties of "junctions" thus derived will be properties shared by all points of the network.

The fixed points of the network will be distinguished by Greek subscripts $\alpha, \beta, \cdots$, the junctions by Roman subscripts $i, j, k, \cdots$; the Greek letters τ, μ, ν will apply to both types of points. Thus $\sum_\alpha$ will indicate a sum over all fixed points, $\sum_i$ a sum over all junctions, and $\sum_\tau$ a sum over all points of both types. The positions of these points will be specified by the Cartesian coordinates x_τ, y_τ, z_τ, or by the vector $\mathbf{r}_\tau$.

The number of configurations possible for the chain segment linking the points τ and ν will be

expressed, as a function of the separation of these points, by the Gaussian *segment-configuration function*.

$$c(N_{\tau\nu}, |\mathbf{r}_\tau - \mathbf{r}_\nu|) = k_{\tau\nu} \exp\{-(3/2l^2 N_{\tau\nu})|\mathbf{r}_\tau - \mathbf{r}_\nu|^2\}. \quad (1\cdot1)$$

If the segment can take on finite numbers of configurations when the ends occupy points from a discrete set in space—as in some models convenient for the discussion of physical problems—then the segment-configuration function can give directly the number of possible configurations. If the configurations of the segment are continuously variable and the ends can take on all positions in space, then $c(N_{\tau\nu}, |\mathbf{r}_\tau - \mathbf{r}_\nu|)$ can give only the *relative* number of configurations possible for the segment. The configuration function c is expressed in the form derived (as an approximation) for a segment of $N_{\tau\nu}$ independent links of fixed length l. The parameter l will be the same for all segments; each segment will be characterized by the parameter $N_{\tau\nu}$, which may be regarded as the effective number of links in the segment. The constants $k_{\tau\nu}$ will be of no further interest.

When the points τ and ν are not directly connected by a segment, one may set $1/N_{\tau\nu}=0$. The nature of the network is completely specified by giving the complete symmetric matrix $(1/N_{\tau\nu})$; this, and the positions of the fixed points, $\mathbf{r}_\alpha$, will determine all the quantities in which we shall be interested.

Let the fixed points and junctions of the network have definite positions (x_τ, y_τ, z_τ). The relative number of possible configurations of the entire network, consistent with these specified positions, is simply the product of the number of possible configurations assumed independently by the component segments of the network. This is

$$C(\mathbf{r}_\alpha, \mathbf{r}_\beta, \cdots \mathbf{r}_i, \mathbf{r}_j, \cdots) = K \exp\{-(3/2l^2) \sum_{\tau>\nu}\sum (1/N_{\tau\nu})[(x_\tau - x_\nu)^2 + (y_\tau - y_\nu)^2 + (z_\tau - z_\nu)^2]\}. \quad (1\cdot2)$$

This function of the coordinates of all fixed points and junctions will be called the *primary configuration function* of the network.

From the primary configuration function one can derive the total number of configurations of the network consistent with given positions of the fixed points by summing over all possible positions of the junctions. In the continuous case, to which attention will here be restricted, the corresponding integral over the coordinates of all junctions is

$$\mathfrak{C}(\mathbf{r}_\alpha, \mathbf{r}_\beta, \cdots) = \int dV_i \int dV_j \cdots C(\mathbf{r}_\alpha, \mathbf{r}_\beta, \cdots \mathbf{r}_i, \mathbf{r}_j, \cdots). \quad (1\cdot3)$$

The relative number of configurations of the network consistent with given positions of the fixed points and of some one of the junctions, say the ith, can be obtained by integrating C over the coordinates of all junctions *except* the ith. Denoting such an integration by $\int dV_i'$, we have for this *configuration function for the junction i*

$$\mathfrak{C}_i(\mathbf{r}_\alpha, \mathbf{r}_\beta, \cdots; \mathbf{r}_i) = \int dV_i' C(\mathbf{r}_\alpha, \mathbf{r}_\beta, \cdots \mathbf{r}_i, \mathbf{r}_j, \cdots). \quad (1\cdot4)$$

The physical importance of this configuration function is the following. If a molecular network is effectively Gaussian and its potential energy is independent of its configuration, then the probability dP of finding the ith junction with coordinates in the ranges x_i to x_i+dx_i, y_i to y_i+dy_i, z_i to z_i+dz_i, will be proportional to the number of configurations of the network consistent with this position of the ith junction, $\mathfrak{C}_i(\mathbf{r}_\alpha, \cdots; \mathbf{r}_i)dx_i dy_i dz_i$. We define the *probability density function for the junction i*,

$$P_i(\mathbf{r}_\alpha, \mathbf{r}_\beta, \cdots; \mathbf{r}_i),$$

such that this probability is

$$dP = P_i(\mathbf{r}_\alpha, \mathbf{r}_\beta, \cdots; \mathbf{r}_i)dx_i dy_i dz_i. \quad (1\cdot5)$$

P_i differs from $\mathfrak{C}_i$ only by a normalizing factor determined by the condition that

$$\int dV_i P_i(\mathbf{r}_\alpha, \mathbf{r}_\beta, \cdots; \mathbf{r}_i) \equiv 1. \quad (1\cdot6)$$

Since

$$\int dV_i \mathfrak{C}_i(\mathbf{r}_\alpha, \mathbf{r}_\beta, \cdots; \mathbf{r}_i) = \mathfrak{C}(\mathbf{r}_\alpha, \mathbf{r}_\beta, \cdots), \quad (1\cdot7)$$

we have

$$P_i(\mathbf{r}_\alpha, \mathbf{r}_\beta, \cdots; \mathbf{r}_i) = \mathfrak{C}_i(\mathbf{r}_\alpha, \mathbf{r}_\beta, \cdots; \mathbf{r}_i)/\mathfrak{C}(\mathbf{r}_\alpha, \mathbf{r}_\beta, \cdots). \quad (1\cdot8)$$

This probability density function describes the fluctuations in the coordinates of the ith junction of the thermally agitated network; its use to determine the time-averaged mean values of the coordinates, their average deviation from these mean values, and so on, will need no description here.

In the same way one can obtain a configuration function for the junctions i and j by integrating the primary configuration function C over the coordinates of all junctions except the ith and jth:

$$\mathfrak{C}_{ij}(\mathbf{r}_\alpha, \mathbf{r}_\beta, \cdots; \mathbf{r}_i, \mathbf{r}_j) = \int dV_{ij}'' C(\mathbf{r}_\alpha, \mathbf{r}_\beta, \cdots \mathbf{r}_i, \mathbf{r}_j, \cdots). \quad (1\cdot9)$$

This gives the relative number of configurations of the network consistent with the specified positions of the fixed points and the two junctions. From it one can obtain the probability density function

$$P_{ij}(\mathbf{r}_\alpha, \cdots; \mathbf{r}_i, \mathbf{r}_j) = \mathfrak{C}_{ij}(\mathbf{r}_\alpha, \cdots; \mathbf{r}_i, \mathbf{r}_j)/\mathfrak{C}(\mathbf{r}_\alpha, \mathbf{r}_\beta, \cdots), \quad (1\cdot10)$$

such that

$$dP = P_{ij}(\mathbf{r}_\alpha, \mathbf{r}_\beta, \cdots; \mathbf{r}_i, \mathbf{r}_j) dx_i dy_i dz_i dx_j dy_j dz_j \quad (1\cdot11)$$

is the probability that junctions i and j of the thermally-agitated flexible network will simultaneously have coordinates in the indicated ranges.

From P_{ij} one can determine the probability that the relative coordinates of the two junctions,

$$\xi = x_i - x_j, \quad \eta = y_i - y_j, \quad \zeta = z_i - z_j, \quad (1\cdot12)$$

lie in given ranges. Let P_{ij} be expressed as a function of $\mathbf{r}_j$ and ξ, η, ζ, instead of as a function of $\mathbf{r}_j$ and $\mathbf{r}_i$. The probability that these coordinates will lie within ranges of magnitudes $dx_j, dy_j, dz_j, d\xi, d\eta, d\zeta$, respectively, is easily shown to be

$$dP = P_{ij}(\mathbf{r}_\alpha, \mathbf{r}_\beta, \cdots; \mathbf{r}_j, \xi, \eta, \zeta) dx_j dy_j dz_j d\xi d\eta d\zeta. \quad (1\cdot13)$$

The probability that ξ, η, ζ will lie in the given ranges, without regard for the values of the other variables, is

$$dP' = R_{ij}(\mathbf{r}_\alpha, \mathbf{r}_\beta, \cdots; \xi, \eta, \zeta) d\xi d\eta d\zeta, \quad (1\cdot14)$$

where

$$R_{ij}(\mathbf{r}_\alpha, \cdots; \xi, \eta, \zeta) = \int dV_j P_{ij}(\mathbf{r}_\alpha, \cdots; \mathbf{r}_j, \xi, \eta, \zeta) \quad (1\cdot15)$$

is the probability density function for the relative coordinates ξ, η, ζ.

In the same way one can derive from the primary configuration function other configuration functions for larger sets of junctions, and from these can obtain other probability density functions, by normalization and integration over unwanted coordinates. Only the functions defined above will be of immediate interest here.

The integrals defined above, and in particular the integral of Eq. (1·3), will not all exist if it is possible to remove any part of the network from the system without breaking any chains. For example, if the network includes a set of junctions linked by chain segments to each other, but not to any other junctions or to any fixed points, then one can increase the coordinates of all these junctions together indefinitely without increasing the separation of any linked junctions, or decreasing the value of the primary configuration function C. Integration over the coordinates of these junctions, as in Eq. (1·3), will then lead to non-convergent integrals. A network in which every junction is linked to a fixed point by at least one continuous path in the network will be termed a *coherent network*. In this paper attention will for the most part be restricted to coherent networks, for which the integrals thus far defined always exist.

II. TRANSFORMATION OF THE PRIMARY CONFIGURATION FUNCTION

For many purposes it is convenient to express the primary configuration function C in terms of new variables—the Cartesian coordinates X_i, Y_i, Z_i of each junction relative to its most probable position.

Let x_{0i}, y_{0i}, z_{0i} be the coordinates of the junctions which, taken all together, make C an absolute maximum. (It will be shown in Section

V that these are also the mean and the most probable positions of the several junctions of the network.) These quantities depend upon the coordinates of the fixed points in a way which we shall now determine.

The quantities x_{0i}, y_{0i}, z_{0i} are the values of x_i, y_i, z_i, respectively, which solve the equations

$$\partial C/\partial x_i = \partial C/\partial y_i = \partial C/\partial z_i = 0 \qquad (2\cdot1)$$

for all i. If we write for the fixed-point coordinates

$$x_\alpha = x_{0\alpha}, \qquad (2\cdot2)$$

Eq. (2·1) becomes, by Eq. (1·2),

$$\left.\begin{aligned} \textstyle\sum_\tau (1/N_{\tau i})(x_{0\tau}-x_{0i}) &= 0, \qquad (2\cdot3a)\\ \textstyle\sum_\tau (1/N_{\tau i})(y_{0\tau}-y_{0i}) &= 0, \qquad (2\cdot3b)\\ \textstyle\sum_\tau (1/N_{\tau i})(z_{0\tau}-z_{0i}) &= 0. \qquad (2\cdot3c)\end{aligned}\right\} \text{for all } i.$$

Let

$$\left.\begin{aligned} \gamma_{\tau\tau} &= \sum_{\nu\neq\tau} 1/N_{\tau\nu},\\ \gamma_{\tau\nu} &= -1/N_{\tau\nu}, \quad \tau\neq\nu.\end{aligned}\right\} \qquad (2\cdot4)$$

Then Eq. (2·3a) can be written as

$$\textstyle\sum_j \gamma_{ij} x_{0j} = -\sum_\alpha \gamma_{i\alpha} x_\alpha, \qquad (2\cdot5)$$

with similar equations in the y's and z's. The terms on the left involve the unknowns x_{0j}, whereas the terms on the right involve the known coordinates of the fixed points. These linear equations can be solved by Cramer's rule to determine the x_{0j} in terms of the x_α. To give explicit form to this solution it will be convenient to use a determinant notation which will later be employed extensively.

Let Γ be the determinant of the coefficients γ_{ij}, with one row and column for each of the n junctions in the network:

$$\Gamma = \begin{vmatrix} \gamma_{11} & \gamma_{12} & \cdots & \gamma_{1n} \\ \gamma_{21} & \gamma_{22} & \cdots & \cdots \\ \cdots & \cdots & \cdots & \cdots \\ \gamma_{n1} & & \cdots & \gamma_{nn} \end{vmatrix}. \qquad (2\cdot6)$$

(Note that the fixed points of the network are not represented by rows and columns in this determinant.) Let Γ_{ij} be the cofactor of γ_{ij} in Γ —that is, $(-1)^{i+j}$ times the determinant obtained by striking out of Γ the ith row and jth column. Let Γ_{ij}^{kl} be $(-1)^{i+j+k+l}$ times the determinant obtained by striking out of Γ rows i and j, columns k and l. Let $\Gamma^{j\to\alpha}$ be the determinant obtained by replacing the jth column of Γ by the column of constants $\gamma_{1\alpha}, \gamma_{2\alpha}, \cdots \gamma_{i\alpha}, \cdots$, and let $\Gamma^{j\to x}$ be the determinant obtained by replacing the jth column of Γ by the column of quantities $\sum_\alpha \gamma_{1\alpha}x_\alpha, \sum_\alpha \gamma_{2\alpha}x_\alpha, \cdots, \sum_\alpha \gamma_{i\alpha}x_\alpha, \cdots$. It is evident that

$$\Gamma^{j\to x} = \textstyle\sum_\alpha x_\alpha \Gamma^{j\to\alpha}. \qquad (2\cdot7)$$

The Cramer's rule solution of Eqs. (2·5) is, in this notation,

$$x_{0i} = -\Gamma^{i\to x}/\Gamma. \qquad (2\cdot8)$$

Proof that the determinant Γ cannot vanish will be given in Section III. To make more explicit the dependence of the x_{0i} on the fixed-point coordinates, one can write

$$x_{0i} = \textstyle\sum_\alpha c_{i\alpha} x_\alpha, \qquad (2\cdot9a)$$

and similarly,

$$y_{0i} = \textstyle\sum_\alpha c_{i\alpha} y_\alpha. \qquad (2.9b)$$

$$z_{0i} = \textstyle\sum_\alpha c_{i\alpha} z_\alpha, \qquad (2\cdot9c)$$

where

$$c_{i\alpha} = -\Gamma^{i\to\alpha}/\Gamma. \qquad (2\cdot10)$$

Thus the x_{0i}, y_{0i}, z_{0i} are linear functions of the x_α, y_α, z_α, respectively, with coefficients $c_{i\alpha}$ which depend only on the $N_{\tau\nu}$: a change in the position of any fixed point of a Gaussian network will produce a proportional change in the mean position of any other element of the network. It should be noted that the same constants appear in Eqs. (2·3a), (2·3b), and (2·3c) and hence in Eqs. (2·9a), (2·9b), and (2·9c). It follows that a shift of a fixed point of a Gaussian network in any direction will produce a shift of the mean position of any other element of the network, in the same direction, and with magnitude the same for all directions of shift.

The coordinates of the junctions relative to their mean positions are

$$X_i = x_i - x_{0i}, \quad Y_i = y_i - y_{0i}, \quad Z_i = z_i - z_{0i}; \qquad (2\cdot11)$$

for the fixed points, $X_\alpha = Y_\alpha = Z_\alpha = 0$. In terms of the variables $x_{0\tau}$, $y_{0\tau}$, $z_{0\tau}$, and X_τ, Y_τ, Z_τ, the primary configuration function C becomes, by use of Eqs. (2·3),

$$C = K \exp\{-(3/2l^2) \sum_{\tau>\nu}\sum (1/N_{\tau\nu})[(x_{0\tau}-x_{0\nu})^2+(y_{0\tau}-y_{0\nu})^2+(z_{0\tau}-z_{0\nu})^2]\}$$
$$\times \exp\{-(3/2l^2) \sum_{\tau>\nu}\sum (1/N_{\tau\nu})[(X_\tau-X_\nu)^2+(Y_\tau-Y_\nu)^2+(Z_\tau-Z_\nu)^2]\}. \qquad (2\cdot12)$$

The first exponential is a constant determined by the positions of the fixed points; the second exponential depends only on the coordinates of the junctions relative to the points $\mathbf{r}_{0i}$, and is, aside from a normalizing constant, just the probability density function for these relative coordinates. A useful alternative form for C employs the constants $\gamma_{\tau\nu}$ of Eq. (2·4):

$$C=K\exp\{-(3/2l^2)\sum_\tau\sum_\nu\gamma_{\tau\nu}[x_{0\tau}x_{0\nu}+y_{0\tau}y_{0\nu}+z_{0\tau}z_{0\nu}]\}\times\exp\{-(3/2l^2)\sum_i\sum_j\gamma_{ij}[X_iX_j+Y_iY_j+Z_iZ_j]\}. \quad (2\cdot13)$$

As is indicated by the subscripts, the sums in the first exponential are sums over all fixed points and junctions, whereas the sums in the second exponential are over the junctions only.

In terms of the variables x, y, z, we have correspondingly

$$C=K\exp\{-(3/2l^2)\sum_\tau\sum_\nu\gamma_{\tau\nu}[x_\tau x_\nu+y_\tau y_\nu+z_\tau z_\nu]\}. \quad (2\cdot14)$$

III. INTEGRATION OF THE PRIMARY CONFIGURATION FUNCTION

We must now consider the problem of integrating C over some, but not all, of the variables X_i, Y_i, Z_i or x_i, y_i, z_i. The integrations over the X's, the Y's, and the Z's can be considered separately and offer identical problems. They are easily accomplished by the use of the following basic formula:

Theorem I. Let the constants γ_{ij} form a symmetrical matrix Γ. Let $D^{(0)}=1$, and let $D_{ij}^{(p)}$ denote the p-rowed minor of $|\Gamma|$, obtained by striking out all rows but the first to the $(p-1)$st and the ith, and all columns but the first to the $(p-1)$st and the jth:

$$D_{ij}^{(p)}=\begin{vmatrix}\gamma_{11} & \gamma_{12} & \cdots & \gamma_{1,p-1} & \gamma_{ij}\\ \gamma_{21} & \gamma_{22} & \cdots & \gamma_{2,p-1} & \gamma_{2j}\\ \cdots & \cdots & \cdots & \cdots & \cdots\\ \gamma_{p-1,1} & \gamma_{p-1,2} & \cdots & \gamma_{p-1,p-1} & \gamma_{p-1,j}\\ \gamma_{i1} & \gamma_{i2} & \cdots & \gamma_{i,p-1} & \gamma_{ij}\end{vmatrix}. \quad (3\cdot1)$$

Then

$$\int_{-\infty}^{+\infty}dX_1\int_{-\infty}^{+\infty}dX_2\cdots\int_{-\infty}^{+\infty}dX_q\exp\left\{-\sum_i^n\sum_j^n\gamma_{ij}X_iX_j\right\}=[(\pi^{q/2})/\{D_{qq}^{(q)}\}^{\frac{1}{2}}]\exp\left\{-[1/D_{qq}^{(q)}]\sum_{i>q}^n\sum_{j>q}^n D_{ij}^{(q+1)}X_iX_j\right\}, \quad (3\cdot2)$$

provided only that $D_{ii}^{(i)}>0$ for $i\leq q$. Otherwise the integral does not converge.

Proof of this theorem involves partial rearrangement of the quadratic form in the exponent of the integrand into a sum of squares, with repeated use of the relation

$$D_{ij}^{(p)}D_{pp}^{(p)}-D_{pi}^{(p)}D_{pj}^{(p)}=D_{ij}^{(p+1)}D_{p-1,p-1}^{(p+1)}. \quad (3\cdot3)$$

It will be noted that the determinants on the left of Eq. (3·3) are (except for possible interchange of rows and columns) first minors of $D_{ij}^{(p+1)}$ obtained by striking out the rows p or i and the columns p or j; $D_{p-1,p-1}^{(p-1)}$ is the second minor obtained by striking out rows p and i, columns p and j. The truth of Eq. (3·3) then follows from a well-known relation of a determinant to its adjoint.[3]

[3] M. Bôcher, *Introduction to Higher Algebra* (The Macmillan Company, New York, 1929), p. 33.

Rearrangement of the quadratic form proceeds as follows: On completing the square of the terms in X_1, one finds

$$\sum_i\sum_j\gamma_{ij}X_iX_j=\gamma_{11}\{X_1+(1/\gamma_{11})\sum_{j>1}\gamma_{1j}X_j\}^2+\sum_{i>1}\sum_{j>1}[\gamma_{ij}-(\gamma_{1i}\gamma_{1j}/\gamma_{11})]X_iX_j$$
$$=(D_{11}^{(1)}/D^{(0)})\left\{X_1+\sum_{j>1}(D_{1j}^{(1)}/D_{11}^{(1)})X_j\right\}^2+\sum_{i>1}\sum_{j>1}(D_{2j}^{(2)}/D_{11}^{(1)})X_iX_j. \quad (3\cdot4)$$

On completion of the square of the terms in X_2, the last sum on the right becomes

$$\sum_{i>1}\sum_{j>1}(D_{ij}^{(2)}/D_{11}^{(1)})X_iX_j=(D_{22}^{(2)}/D_{11}^{(1)})\{X_2+\sum_{j>2}(D_{2j}^{(2)}/D_{22}^{(2)})X_j\}^2+\sum_{i>2}\sum_{j>2}(D_{ij}^{(3)}/D_{22}^{(2)})X_iX_j, \quad (3\cdot5)$$

when use is made of the fact (Eq. (3·3)) that

$$(D_{ij}^{(2)}/D_{11}^{(1)})-(D_{2i}^{(2)}D_{2j}^{(2)}/D_{11}^{(1)}D_{22}^{(2)}) = D_{ij}^{(3)}/D_{22}^{(2)}. \quad (3\cdot6)$$

Continuation of this process leads to no difficulty if all $D_{ii}^{(i)}\neq 0$; one finds

$$\sum_i^n\sum_j^n \gamma_{ij}X_iX_j = \sum_{i=1}^{p}(D_{ii}^{(i)}/D_{i-1,\,i-1}^{(i-1)})\left\{X_i+\sum_{j>i}^{n}(D_{ij}^{(i)}/D_{ii}^{(i)})X_j\right\}^2 + \sum_{i>p}^{n}\sum_{j>p}^{n}(D_{ij}^{(p+1)}/D_{pp}^{(p)})X_iX_j, \quad (3\cdot7)$$

if $D_{ii}^{(i)}\neq 0$ for $i\leq p$. When p takes on its maximum value, n, the second sum on the right disappears, and one obtains

$$\sum_i^n\sum_j^n \gamma_{ij}X_iX_j = \sum_i^n(D_{ii}^{(i)}/D_{i-1,\,i-1}^{(i-1)})\left\{X_i+\sum_{j>i}^{n}(D_{ij}^{(i)}/D_{ii}^{(i)})X_j\right\}^2, \quad (3\cdot8)$$

valid if all $D_{ii}^{(i)}\neq 0$. The possibility of such a reduction of a quadratic form to a sum of squares and the coefficient of the last term in X_n are well known,[4] but the full form of the reduction is not easily found in the literature.[5] Let us now consider the integral

$$I=\int_{-\infty}^{+\infty}dX_1\int_{-\infty}^{+\infty}dX_2\cdots\int_{-\infty}^{+\infty}dX_q\exp\{-\textstyle\sum_i\sum_j\gamma_{ij}X_iX_j\} \quad (3\cdot9)$$

over the first q coordinates X_i. By Eq. (3·7), with $p=q$, this becomes

$$I=\exp\left\{-(1/D_{qq}^{(q)})\sum_{i>q}\sum_{j>q}D_{ij}^{(q+1)}X_iX_j\right\} \times\int_{-\infty}^{+\infty}dX_1\int_{-\infty}^{+\infty}dX_2\cdots\int_{-\infty}^{+\infty}dX_q\prod_{i=1}^{q}\exp\left\{-(D_{ii}^{(i)}/D_{i-1,\,i-1}^{(i-1)})\left[X_i+\sum_{j>i}(D_{ij}^{(i)}/D_{ii}^{(i)})X_j\right]^2\right\}, \quad (3\cdot10)$$

if $D_{ii}^{(i)}\neq 0$ for $i\leq q$. The integration over X_1 can be carried out at once, since this variable appears in only one exponential factor. If $D_{11}^{(1)}>0$, the integral of this factor over X_1 converges:

$$\int_{-\infty}^{+\infty}dX_1\exp\left\{-D_{11}^{(1)}\left[X_1+\sum_{j>1}(D_{ij}^{(2)}/D_{11}^{(1)})X_j\right]^2\right\} = \{\pi/D_{11}^{(1)}\}^{\frac{1}{2}}. \quad (3\cdot11)$$

After this integration the integrand involves X_2 only through a single factor; integration over X_2 replaces this factor by the constant factor $\{\pi D_{11}^{(1)}/D_{22}^{(2)}\}^{\frac{1}{2}}$, if $D_{22}^{(2)}>0$. Integration over X_3 then replaces an exponential factor by the constant $\{\pi D_{22}^{(2)}/D_{33}^{(3)}\}^{\frac{1}{2}}$, and so on. Integration over all q variables yields

$$I=[\pi^{q/2}/\{D_{qq}^{(q)}\}^{\frac{1}{2}}] \times\exp\left\{-(1/D_{qq}^{(q)})\sum_{i>q}\sum_{j>q}D_{ij}^{(q+1)}X_iX_j\right\}, \quad (3\cdot12)$$

if $D_{ii}^{(i)}>0$ when $i\leq q$; otherwise the integral does not exist. This completes the proof of Theorem I. Similar use of Eq. (3·8) yields

$$I=[\pi^{q/2}/\{D_{qq}^{(q)}\}^{\frac{1}{2}}]\prod_i\exp\left\{-(D_{ii}^{(i)}/D_{i-1,\,i-1}^{(i-1)})\left[X_i+\sum_{j>i}(D_{ij}^{(i)}/D_{ii}^{(i)})X_j\right]^2\right\}, \quad (3\cdot13)$$

valid if $D_{ii}^{(i)}>0$ when $i\leq q$ and $D_{ii}^{(i)}\neq 0$ when $i>q$.

The possibility of applying Theorem I in all cases in which we are interested is assured by

Theorem II. The constants γ_{ij} of a coherent network form a symmetric matrix such that $|\Gamma|$ and all its principal minors have positive values.

The truth of this theorem follows easily from the theorem:[6] The principal minors of a determinant $|A|$ of a generalized quadratic form that

[4] M. Bôcher, *Introduction to Higher Algebra* (The Macmillan Company, New York, 1929), p. 140.

[5] The author is indebted to Professor A. E. Ross for calling to his attention that this is a known result: See, for instance, W. Tartakowsky, Bull. Akad. Sci. U.R.S.S. **7**, 111 (1929). He wishes to acknowledge other helpful discussions with Professor Ross on the material of this section.

[6] See, for instance, H. W. Turnbull and A. C. Aitken, *An Introduction to the Theory of Canonical Matrices* (Blackie and Sons, Ltd., London, 1945), p. 91.

is positive definite are all positive. The quadratic form

$$\sum_\tau \sum_\nu \gamma_{\tau\nu} x_\tau x_\nu + \kappa x_\alpha^2 = \sum_{\tau>\nu}\sum (1/N_{\tau\nu})(x_\tau - x_\nu)^2 + \kappa \sum_\alpha x_\alpha^2 \quad (3\cdot14)$$

is positive definite, if the γ's are the constants defined for a coherent network, x_α is the coordinate of fixed point α, and κ is a positive constant. It is obvious that this quantity can vanish only if $x_\alpha = 0$. For every junction or fixed point in the network directly connected to some fixed point α, there will be a term $(1/N_{\tau\alpha})(x_\tau - x_\alpha)^2$ on the right of Eq. (3·14); this can vanish only if $x_\tau = x_\alpha = 0$. Similarly, there will be a term $(1/N_{\tau\nu})(x_\tau - x_\nu)^2$ for every junction or fixed point ν directly connected to one of the junctions or fixed points τ; vanishing of the quadratic form will require that for all of these $x_\nu = x_\tau = 0$. By extension of this argument it follows that the quadratic form can vanish only if $x_\nu = 0$ for every junction or fixed point that can be reached from some fixed point α by a path through the network. Since the network is coherent this includes every junction and fixed point; the quadratic form can vanish only if every variable in it vanishes, and it is thus a positive definite form. The corresponding determinant $|A|$ is a determinant with a row and column for every junction and fixed point in the network; its elements are the $\gamma_{\tau\nu}$, except that the diagonal element corresponding to fixed point α is $\gamma_{\alpha\alpha} + \kappa$. By the theorem, every principal minor of $|A|$ is positive. Since the determinant $|\Gamma|$, with which we are concerned, is a principal minor of $|A|$, obtained by striking out the rows and columns corresponding to all fixed points, the truth of Theorem II follows immediately.

These theorems can now be applied in the integration of the configuration function C over the coordinates of any chosen set of junctions of the network. If these junctions are numbered 1 to q, the integration of C, as given by Eq. (2·13), yields

$$\int dV_1 \int dV_2 \cdots \int dV_q C(\mathfrak{r}_\alpha, \mathfrak{r}_\beta, \cdots; \mathfrak{r}_1, \mathfrak{r}_2, \cdots \mathfrak{r}_n) = K(2\pi l^2/3)^{3q/2}[D_{qq}^{(q)}]^{-\frac{1}{2}} \exp\{-(3/2l^2)\sum_\tau \sum_\nu \gamma_{\tau\nu}[x_{0\tau}x_{0\nu} + y_{0\tau}y_{0\nu} + z_{0\tau}z_{0\nu}]\} \times \exp\{-(3/2l^2)[D_{qq}^{(q)}]^{-1} \sum_{i>q}\sum_{j>q} D_{ij}^{(q+1)}[X_iX_j + Y_iY_j + Z_iZ_j]\}. \quad (3\cdot15)$$

To obtain the configuration function of any given junction of a Gaussian network one has only to assign this the highest number, n, in numbering the junctions, and then to apply Eq. (3·15) with $q = n-1$. Similarly, to obtain a configuration function for an arbitrary pair of junctions one can number these as junctions $n-1$ and n, and apply Eq. (3·15) with $q = n-2$; the other junctions can be numbered arbitrarily.

IV. TOTAL NUMBER OF CONFIGURATIONS POSSIBLE FOR A GAUSSIAN NETWORK

To determine $\mathfrak{C}$, the total number of configurations possible for a Gaussian network, as a function of the positions of the fixed points, it is necessary to integrate the primary configuration function C over all the coordinates X_i, Y_i, Z_i or x_i, y_i, z_i. The most compact result is found by applying Theorem I in integrating C, as given by Eq. (2·14), over all x_i, y_i, z_i. This yields

$$\mathfrak{C}(\mathfrak{r}_\alpha, \mathfrak{r}_\beta, \cdots) = K_1 \exp\{-(3/2l^2)(1/|\Gamma|)\sum_\alpha \sum_\beta \Gamma_{\alpha\beta}[x_\alpha x_\beta + y_\alpha y_\beta + z_\alpha z_\beta]\}, \quad (4\cdot1)$$

where

$$\Gamma_{\alpha\beta} = \begin{vmatrix} \gamma_{11} & \cdots & \gamma_{1n} & \gamma_{1\alpha} \\ \cdots & \cdots & \cdots & \cdots \\ \gamma_{n1} & & & \gamma_{n\alpha} \\ \gamma_{\beta 1} & \gamma_{\beta 2} & \cdots & \gamma_{\beta\alpha} \end{vmatrix} \quad (4\cdot2)$$

is the determinant $|\Gamma|$ bordered by the column of constants $\gamma_{i\alpha}$ and the row of constants $\gamma_{\beta j}$.

A useful alternative form expresses this result in terms of the mean coordinates $x_{0\tau}$, $y_{0\tau}$, $z_{0\tau}$ of the junctions and fixed points. It is evident from Eq. (2·12) that integration over the coordinates X_i, Y_i, Z_i yields

$$\mathfrak{C}(\mathfrak{r}_\alpha, \mathfrak{r}_\beta, \cdots) = K_1 \exp\{-(3/2l^2)\sum_{\tau>\nu}\sum (1/N_{\tau\nu})[(x_{0\tau} - x_{0\nu})^2 + (y_{0\tau} - u_{0\nu})^2 + (z_{0\tau} - z_{0\nu})^2]\}. \quad (4\cdot3)$$

If the network is coherent the constant K_1 has the form shown in Eq. (3·15) with $q=n$. If the network is not coherent it can be divided into a coherent network and unattached material. The presence of the unattached material will increase K_1 by a factor equal to the number of configurations which it can take on, but will not change the exponential in Eq. (4·3). Further, for any pair of junctions τ and ν in the unattached material, one has $x_{0\tau}=x_{0\nu}$; $y_{0\tau}=y_{0\nu}$, $z_{0\tau}=z_{0\nu}$. Thus Eq. (4·3) has the same form for non-coherent as for coherent networks; the same is true for all other results given in this section.

A case of special interest is that in which the system of fixed points can be subjected to a homogeneous deformation. For example, in the simple model for a cube of rubber subjected to unilateral stretch[1] the fixed points of the network are constrained to lie on the surface of a rectangular parallelopiped with edges of length L_x, L_y, L_z in such a way that

$$x_\alpha=x_\alpha^{(0)}L_x, \quad y_\alpha=y_\alpha^{(0)}L_y, \quad z_\alpha=z_\alpha^{(0)}L_z. \tag{4·4}$$

By Eq. (2·9), the mean coordinates are then also proportional to L_x, L_y, L_z:

$$x_{0i}=x_i^{(0)}L_x, \quad y_{0i}=y_i^{(0)}L_y, \quad z_{0i}=z_i^{(0)}L_z, \tag{4·5}$$

where

$$x_i^{(0)}=\sum_\alpha c_{i\alpha}x_\alpha^{(0)}, \quad y_i^{(0)}=\sum_\alpha c_{i\alpha}y_\alpha^{(0)}, \quad z_i^{(0)}=\sum_\alpha c_{i\alpha}z_\alpha^{(0)}, \tag{4·6}$$

are the mean coordinates of the ith junction when $L_x=L_y=L_z=1$. The number of configurations possible for the network then depends only on L_x, L_y, L_z; Eq. (4·3) becomes

$$\mathfrak{C}(L_x, L_y, L_z) = K_1 \exp\{-(K_xL_x^2+K_yL_y^2+K_zL_z^2)\}, \tag{4·7}$$

where

$$K_x=(3/2l^2)\sum_{\tau>\nu}\sum(1/N_{\tau\nu})(x_\tau^{(0)}-x_\nu^{(0)})^2,$$
$$K_y=(3/2l^2)\sum_{\tau>\nu}\sum(1/N_{\tau\nu})(y_\tau^{(0)}-y_\nu^{(0)})^2, \tag{4·8}$$
$$K_z=(3/2l^2)\sum_{\tau>\nu}\sum(1/N_{\tau\nu})(z_\tau^{(0)}-z_\nu^{(0)})^2.$$

The number of configurations possible for any coherent Gaussian network is thus a Gaussian function of the parameters L_x, L_y, L_z which determine the external dimensions of the system.

If the network is isotropic on the average, then $K_x=K_y=K_z$; one can write

$$\mathfrak{C}(L_x, L_y, L_z) = K_1 \exp\{-K_2(L_x^2+L_y^2+L_z^2)\}, \tag{4·9}$$

with

$$K_2=(1/2l^2)\sum_{\tau>\nu}\sum(1/N_{\tau\nu})[(x_\tau^{(0)}-x_\nu^{(0)})^2+(y_\tau^{(0)}-y_\nu^{(0)})^2+(z_\tau^{(0)}-z_\nu^{(0)})^2]. \tag{4·10}$$

A variant form of Eq. (4·10) has been noted elsewhere.[7] Let the vector extension of the $\tau\nu$-segment be denoted by

$$\mathbf{E}_{\tau\nu}=\mathbf{i}(x_\tau-x_\nu)+\mathbf{j}(y_\tau-y_\nu)+\mathbf{k}(z_\tau-z_\nu). \tag{4·11}$$

It will be shown in Section V that the average of this vector over all configurations of the network is

$$\langle\mathbf{E}_{\tau\nu}\rangle_{Av}=\mathbf{i}(x_{0\tau}-x_{0\nu})+\mathbf{j}(y_{0\tau}-y_{0\nu})+\mathbf{k}(z_{0\tau}-z_{0\nu}). \tag{4·12}$$

The "vector-mean fractional extension" of this segment is the magnitude of this vector divided by the "total length" $N_{\tau\nu}l$ of the segment. Let the value of this vector-mean fractional extension, when $L_x=L_y=L_z=1$, be

$$\lambda_{\tau\nu}^{(0)}=[(x_\tau^{(0)}-x_\nu^{(0)})^2+(y_\tau^{(0)}-y_\nu^{(0)})^2+(z_\tau^{(0)}-z_\nu^{(0)})^2]^{\frac{1}{2}}/N_{\tau\nu}l. \tag{4·13}$$

Then one has simply

$$K_2=\tfrac{1}{2}\sum_{\tau>\nu}\sum N_{\tau\nu}[\lambda_{\tau\nu}^{(0)}]^2. \tag{4·14}$$

The significance of this form of the result is discussed elsewhere.[8]

V. PROBABILITY DENSITY FUNCTION FOR A SINGLE JUNCTION

It is easy to show, without entering into detailed calculations, that the probability density function for any element of a Gaussian network is a Gaussian function about a mean or most probable position:

$$P_i(\mathbf{r}_i)=\{3/2\pi l^2\mathfrak{N}_i\}^{\frac{3}{2}}\exp\{-(3/2l^2\mathfrak{N}_i)|\mathbf{r}_i-\mathbf{r}_{0i}|^2\}. \tag{5·1}$$

[7] H. M. James and E. Guth, J. App. Phys. **15**, 294 (1944).
[8] H. M. James and E. Guth, J. Chem. Phys. **15**, 669 (1947).

This function involves two parameters: $\mathbf{r}_{0i}$, the mean position of the junction, and $\mathfrak{N}_i$, which determines the breadth of the probability distribution about this point. The constant $\mathfrak{N}_i$ is the number of links in a chain which has a configuration function [Eq. (1·1)] of the same form; in other words, the function $P_i(\mathbf{r}_i)$ is the same as the probability density function for the positions of one end of a chain of $\mathfrak{N}_i$ links, when the other end of the chain is fixed at the point $\mathbf{r}_{0i}$. We can now determine these quantities in terms of the quantities previously discussed.

It follows at once from Eqs. (1·8) and (3·15) that

$$P_n(\mathbf{r}_n)=\{(3/2\pi l^2)(D_{nn}{}^{(n)}/D_{n-1,\,n-1}^{(n-1)})\}^{\frac{1}{2}}\exp\{-(3/2l^2)(D_{nn}{}^{(n)}/D_{n-1,\,n-1}^{(n-1)})(X_n{}^2+Y_n{}^2+Z_n{}^2)\}. \quad (5\cdot2)$$

Thus

$$\mathfrak{N}_n=D_{n-1,\,n-1}^{(n-1)}/D_{nn}{}^{(n)}=\Gamma_n{}^n/\Gamma. \quad (5\cdot3)$$

Since any junction can be taken as the nth, it follows that

$$\mathfrak{N}_i=\Gamma_i{}^i/\Gamma. \quad (5\cdot4)$$

(It will be observed that only the notation introduced after Eq. (2·6) is suited for this generalization.)

Equation (5·2) shows that the mean and most probable values of X_n, Y_n, and Z_n are zero. It follows that the mean and most probable values of x_i, y_i, and z_i are the quantities x_{0i}, y_{0i}, z_{0i} defined by Eq. (2·1) and discussed in previous sections. Thus in Eq. (5·1), $\mathbf{r}_{0i}=(x_{0i}, y_{0i}, z_{0i})$. From this the truth of Eq. (4·12) follows without difficulty.

The parameter $\mathfrak{N}_i$ depends on the N_{rv}—on the structure of the network—but not at all on the positions of the fixed points. When a fixed point of a Gaussian network is shifted, the mean position of each junction undergoes a proportionate shift, but there is no change in the fluctuation of the junction coordinates about their mean values.

It should be noted that Eqs. (2·1) will determine the same values of x_j, y_j, z_j for $j\neq i$, whether one treats x_i, y_i, z_i as variables of the problem or assigns to them the fixed values x_{0i}, y_{0i}, z_{0i}. In other words, one can fix any chosen junction of a Gaussian network *at its mean position* without thereby altering the mean position of any other junction. On the other hand, this conversion of a junction into a fixed point will change the values of some of the $\mathfrak{N}_i$; it will reduce the fluctuation of the coordinates of at least some of the other elements of the network.

VI. PROBABILITY DENSITY FUNCTION FOR A PAIR OF JUNCTIONS

The probability density function for the $(n-1)$st and nth junctions of a Gaussian network is easily found by application of Eq. (3·15). It factors into three parts of identical form, depending on the X's, the Y's, and the Z's, respectively. Each of these factors is itself a probability density function for the coordinates involved. The X dependent function is

$$P_{n,\,n-1}(X_{n-1}, X_n)=(3/2\pi l^2)\{D_{nn}{}^{(n)}/D_{n-2,\,n-2}^{(n-2)}\}^{\frac{1}{2}}\exp\{-(3/2l^2)(1/D_{n-2,\,n-2}^{(n-2)})[D_{n-1,\,n-1}^{(n-1)}X_{n-1}{}^2+2D_{n,\,n-1}^{(n-1)}X_nX_{n-1}+D_{nn}{}^{(n-1)}X_n{}^2]\}. \quad (6\cdot1)$$

In the Γ-notation this becomes, for an arbitrary pair of junctions,

$$P_{ij}(X_i, X_j)=(3/2)\pi l^2\{\Gamma/\Gamma_{ij}{}^{ij}\}^{\frac{1}{2}}\exp\{-(3/2l^2)(1/\Gamma_{ij}{}^{ij})(\Gamma_j{}^jX_i{}^2-2\Gamma_i{}^jX_iX_j+\Gamma_i{}^iX_j{}^2)\}. \quad (6\cdot2)$$

It should be noted that $D_{n,\,n-1}^{(n-1)}$ corresponds to $-\Gamma_i{}^j$, not to $+\Gamma_i{}^j$, and that

$$\Gamma_i{}^j\geq0 \quad (6\cdot3)$$

for all i and j. If the two junctions under consideration are numbered as the $(n-1)$st and nth, one obtains $D_{n,\,n-1}^{(n-1)}$ by striking out the nth row and $(n-1)$st column of $\mathfrak{C}$. If these junctions are numbered as the ith and jth, with a corresponding increase in the numbering of other

junctions, one obtains $(-1)^{i+j}\Gamma_i{}^j$ on striking out the ith row and jth row column of Γ. These two determinants differ, however, by $n-j$ transpositions of rows and $n-i-1$ transpositions of columns, if $i<j$, and by $n-j-1$ transpositions of rows and $n-i$ transpositions of columns, if $i>j$. In any case they differ by a factor of $(-1)^{i+j+1}$; $D^{(n-1)}_{n,n-1}$ and $\Gamma_i{}^j$ accordingly differ by a factor of (-1). Now, all cross terms of the primary configuration function C have coefficients which are zero or negative, and it is easily shown that this remains true when C is partially rearranged into a sum of squares, as in Eq. (3·7). Since $D^{(n-2)}_{n-2,n-2}$ is positive, for any coherent network, it follows from Eq. (3·7) that $D^{(n-1)}_{n,n-1}\leq 0$, no matter how the junctions are ordered; the truth of Eq. (6·3) follows at once.

If the ith and jth junctions are not mechanically connected—if there are no paths between them in the network which do not pass through a fixed point—the coordinates of the two junctions will be statistically independent. There will then be no term in X_iX_j in Eq. (6·2), and $P_{ij}(X_i, X_j)$ will factor into independent probability density functions for X_i and X_j, in which the coefficients in the exponential will be $-3/2l^2\mathfrak{N}_i$ and $-3/2l^2\mathfrak{N}_j$, respectively, by Eq. (5·1). To exhibit the effect of mechanical coupling between the ith and jth junctions it is sometimes convenient to write Eq. (6·2) as

$$P_{ij}(X_i, X_j)=K'\exp\{-(3/2l^2)[(a/\mathfrak{N}_i)X_i{}^2+(b/\mathfrak{N}_j)X_j{}^2+(c/(\mathfrak{N}_i\mathfrak{N}_j)^{\frac{1}{2}})X_iX_j]\}. \quad (6\cdot4)$$

The constant c is necessarily zero or positive [see Eq. (6·3)]. When the junctions are not coupled, $c=0$, $a=b=1$. It is therefore possible to take c as a measure of the strength of the coupling between junctions of given $\mathfrak{N}_i$ and $\mathfrak{N}_j$. Comparing Eq. (6·4) with Eqs. (5·3) and (6·2), one finds

$$\left.\begin{aligned} a=b&=\Gamma_i{}^i\Gamma_j{}^j/\Gamma\Gamma_{ij}{}^{ij},\\ c&=2\Gamma_i{}^j\{\Gamma_i{}^i\Gamma_j{}^j\}^{\frac{1}{2}}/\Gamma\Gamma_{ij}{}^{ij}.\end{aligned}\right\} \quad (6\cdot5)$$

By the use of

$$\Gamma_i{}^i\Gamma_j{}^j-(\Gamma_i{}^j)^2=\Gamma\Gamma_{ij}{}^{ij}, \quad (6\cdot6)$$

a relation which can be proved in the same way as Eq. (3·3), it is easily shown that

$$c^2=4a(a-1). \quad (6\cdot7)$$

VII. FLUCTUATION OF RELATIVE COORDINATES OF TWO JUNCTIONS

To obtain the probability density function for the relative coordinate $\xi=x_i-x_j$ of the ith and jth junctions, one can integrate $P_{ij}(X_i, X_j)$ over X_j, say, while keeping ξ constant [see Eq. (1·15)]. Let

$$\xi_0=x_{0i}-x_{0j}, \quad (7\cdot1)$$

and

$$w=\xi-\xi_0=X_i-X_j. \quad (7\cdot2)$$

Equation (6·2) can be rewritten as

$$P_{ij}(w, X_j)=(3/2\pi l^2)\{\Gamma/\Gamma_{ij}{}^{ij}\}^{\frac{1}{2}}\times\exp\{-(3/2l^2)[(\Gamma_i{}^i-2\Gamma_i{}^j+\Gamma_j{}^j)/\Gamma_{ij}{}^{ij}][X_j+[(\Gamma_j{}^j-\Gamma_i{}^j)/\Gamma_i{}^i-2\Gamma_i{}^j+\Gamma_j{}^j)]w]^2\}\times\exp\{-(3/2l^2)(\Gamma/\Gamma_i{}^i-2\Gamma_i{}^j+\Gamma_j{}^j)w^2\}. \quad (7\cdot3)$$

with the aid of Eq. (6·6). Integration over X_j yields

$$R_{ij}(\xi)=\{(3/2\pi l^2)(\Gamma/[\Gamma_i{}^i-2\Gamma_i{}^j+\Gamma_j{}^j])\}^{\frac{1}{2}}\times\exp\{-(3/2l^2)(\Gamma/[\Gamma_i{}^i-2\Gamma_i{}^j+\Gamma_j{}^j)][\xi-\xi_0]^2\}. \quad (7.4)$$

The probability density function for the relative coordinate ξ is thus a Gaussian function about a mean value ξ_0.

The probability density function $R_{ij}(\xi, \eta, \zeta)$ is the product of three formally identical factors for the three variables. It can be written, in analogy to Eq. (5·1) as

$$R_{ij}(\xi, \eta, \zeta)=\{3/2\pi l^2\mathfrak{N}_{ij}\}^{\frac{1}{2}}\exp\{-(3/2l^2\mathfrak{N}_{ij})\times[(\xi-\xi_0)^2+(\eta-\eta_0)^2+(\zeta-\zeta_0)^2]\}, \quad (7\cdot5)$$

where

$$\mathfrak{N}_{ij}=(\Gamma_i{}^i-2\Gamma_i{}^j+\Gamma_j{}^j)/\Gamma. \quad (7\cdot6)$$

This important result implies that *in a thermally agitated Gaussian network the relative coordinates of any pair of junctions will fluctuate according to a Gaussian distribution about mean values* ξ_0, η_0, ζ_0. The mean values in question will depend on the coordinates of the fixed points, but the

breadth of the distribution, specified by $\mathfrak{N}_{ij}$, will depend only on the structure of the network.

It will be noted that

$$\mathfrak{N}_{ij}=\mathfrak{N}_i+\mathfrak{N}_j-2\Gamma_i^j/\Gamma, \tag{7·7}$$

or, by Eqs. (6·5) and (6·7),

$$\mathfrak{N}_{ij}=\mathfrak{N}_i+\mathfrak{N}_j-[2c/\{1+(1+c^2)^{\frac{1}{2}}\}](\mathfrak{N}_i\mathfrak{N}_j)^{\frac{1}{2}} \geq[\mathfrak{N}_i^{\frac{1}{2}}-\mathfrak{N}_j^{\frac{1}{2}}]^2. \tag{7·8}$$

For two statistically independent junctions

$$\mathfrak{N}_{ij}=\mathfrak{N}_i+\mathfrak{N}_j; \tag{7·9}$$

the breadth of the distribution of values for ξ, η, ζ is greater than that for the coordinates of either junction. Any coupling between the junctions reduces $\mathfrak{N}_{ij}$ below this maximum value, thus reducing the fluctuations in the values of ξ, η, ζ. There is a lower limit of $\mathfrak{N}_{ij}$ consistent with given values of $\mathfrak{N}_i$ and $\mathfrak{N}_j$. Very strong coupling of the junctions will, however, make $\mathfrak{N}_i$ approach $\mathfrak{N}_j$, and reduce this lower limit to zero; the fluctuations of values of ξ, η, ζ in a Gaussian network can be arbitrarily small.

VIII. ELASTIC THREAD MODEL EQIVALENT TO A GAUSSIAN NETWORK

The preceding sections have given a formally complete treatment of the statistical properties of a Gaussian network; the probability density functions have all been expressed (or can very easily be) as functions of the fixed-point coordinates and certain determinants involving the $N_{\tau\nu}$. The explicit evaluation of these determinants may, however, offer serious difficulties. It is, therefore, very useful to have an alternative method of evaluating the statistical parameters, one that is better adapted to the detailed treatment of special problems. This method is based on the consideration of a mechanical system equivalent to the given Gaussian network—a network of elastic threads. Each of the quantities x_{0i}, $c_{j\alpha}$, $\mathfrak{N}_i$, $\mathfrak{N}_{ij}$ which describe the statistical properties of the Gaussian network has its analog in the equivalent thread network: the x_{0i} and $c_{j\alpha}$ are the same, $\mathfrak{N}_i$ is related to the distortion produced by unit force applied to the ith junction of the thread network, and $\mathfrak{N}_{ij}$ to the distortion produced by equal and opposite forces applied to the ith and jth junctions. This reduction of the statistical problem to an equivalent mechanical problem makes applicable to its solution a quite different set of mathematical techniques, as will be illustrated in Section IX.

A Gaussian network can be defined by giving the equivalent number of links $N_{\tau\nu}$ in the segment connecting the τth and νth junctions or fixed points, for all pairs of indices. The equivalent thread network[9] has the same connectivity, with the $\tau\nu$-segment of flexible chain replaced by a classical elastic thread for which the stress-strain relation is given by

$$F=(3kT/l^2N_{\tau\nu})d, \tag{8·1}$$

F being the tension in the thread and d the total distance between its ends. In the configuration of static equilibrium of the thread network the $\tau\nu$-segment should run straight from the τth to the νth junction; that is, the threads are not to be looped over each other in a way incompatible with this condition. (This corresponds to neglect of steric hindrances in the Gaussian network.)

The potential energy of the thread network, as a function of the position of the fixed points and junctions, is

$$V_i(\mathbf{r}_\alpha, \mathbf{r}_\beta, \cdots \mathbf{r}_i, \mathbf{r}_j, \cdots)=(3kT/2l^2)\sum_{\tau>\nu}\sum(1/N_{\tau\nu}) \times[(x_\tau-x_\nu)^2+(y_\tau-y_\nu)^2+(z_\tau-z_\nu)^2]. \tag{8·2}$$

There is thus a relation between the number of configurations C accessible to the Gaussian network and the potential energy V_i of the equivalent thread network:

$$C(\mathbf{r}_\alpha, \cdots \mathbf{r}_i, \cdots) =K\exp\{-V_i(\mathbf{r}_\alpha, \cdots \mathbf{r}_i, \cdots)/kT\}. \tag{8·3}$$

The positions of the junctions which make C a maximum for the Gaussian network are those which make the potential energy of the thread network a minimum. It follows that when the thread network is in equilibrium its junctions will lie at the points (x_{0i}, y_{0i}, z_{0i})—the mean positions of the junctions of the corresponding network of Gaussian flexible chains. All the previously given relations for the $x_{0\tau}$ thus apply to the thread network; conversely, any method by which one can determine the equilibrium

[9] The usefulness of this model has already been noted in reference 1.

configurations of the thread network will supply information about the Gaussian network.

A constant external force applied to a junction of a Gaussian network will change the mean positions of this and other junctions of the network. It is easy to show that an equal force applied to the corresponding junction of the thread network will produce the same shift in the equilibrium positions of each junction. In either case an external force F_i in the x direction, acting on junction i, introduces into the problem a potential energy which may be written as

$$V_e(x_i) = -F_i x_i. \tag{8·4}$$

The potential energy of the thread network becomes $V_i + V_e$. In the presence of this external force the probability of occurrence of a given configuration of the junctions of the Gaussian network is not simply proportional to the configuration function C; it is proportional to

$$C(\mathbf{r}_\alpha, \cdots \mathbf{r}_i, \cdots) \exp\{-V_e(x_i)/kT\} = K \exp\{-(V_e+V_i)/kT\}. \tag{8·5}$$

The most probable positions of the junctions of the Gaussian network (still the mean positions) maximize the quantity on the right; the equilibrium positions of the junctions of the thread network are those which minimize $V_i + V_e$. Obviously, then, these remain the same.

When the force F_i acts on the ith junction of the Gaussian network, the probability density function for $\mathbf{r}_i$ is the probability density already derived [Eq. (5·1)], multiplied by the weight factor $\exp[-V_e/kT]$ and renormalized:

$$P_i'(\mathbf{r}_i) = K \exp\{-(3/2l^2\mathfrak{N}_i)|\mathbf{r}_i - \mathbf{r}_{0i}|^2 + F_i x_i/kT\}. \tag{8·6}$$

On rearrangement, this becomes

$$P_i'(\mathbf{r}_i) = K' \exp\{-(3/2l^2\mathfrak{N}_i) \times [(x_i - x_{0i} - (l^2\mathfrak{N}_i F_i/3kT))^2 + (y_i - y_{0i})^2 + (z_i - z_{0i})^2]\}. \tag{8·7}$$

The force F_i thus changes the mean value of x_i by an amount equal to $l^2\mathfrak{N}_i F_i/3kT$; by the result of the preceding paragraph this is just equal to the displacement X_{ii} of the ith junction of the thread network due to a force F_i applied to that junction. That is,

$$X_{ii} = l^2\mathfrak{N}_i F_i/3kT, \tag{8·8}$$

whence

$$\mathfrak{N}_i = (3kT/l^2)(X_{ii}/F_i). \tag{8·9}$$

Thus $\mathfrak{N}_i$ for the Gaussian network is proportional to the displacement X_{ii} produced by unit force applied to the ith junction of the corresponding thread network.

The $\mathfrak{N}_{ij}$ can be determined similarly. Let equal and opposite forces in the x direction, F_i and $F_j = -F_i$, be applied to junctions i and j, respectively, of corresponding thread and Gaussian networks. Since, with both types of network, displacements due to different forces are additive, these paired forces will produce equal changes $\Delta\xi_0$ in the relative coordinates of the thread-network junctions and in the mean-relative coordinates of the Gaussian network junctions. In the case of the Gaussian network the distribution of relative coordinates ξ, η, ζ is that already derived [Eq. (7·5)], multiplied by the weight factor

$$e^{-V_e/kT} = e^{F_i(x_i - x_j)/kT} = e^{F_i\xi/kT} \tag{8·10}$$

and renormalized. A derivation entirely parallel to that of Eq. (8·9) leads to the result that

$$\mathfrak{N}_{ij} = (3k\Gamma/l^2)(\Delta\xi_0/F_i); \tag{8·11}$$

$\mathfrak{N}_{ij}$ for the Gaussian network is proportional to the change in the relative coordinates of junctions i and j of the thread network produced by oppositely directed unit forces applied to these junctions. If we denote by X_{ij} the displacement of the ith junction produced by a force F_j applied to the jth junction, and so on, we can write also

$$\mathfrak{N}_{ij} = \frac{3kT}{l^2}\left\{\frac{X_{ii}}{F_i} - \frac{X_{ji}}{F_i} - \frac{X_{ij}}{F_j} + \frac{X_{jj}}{F_j}\right\}. \tag{8·12}$$

Finally, it should be noted that the Gaussian and thread networks exert equal forces on each fixed point. If the junctions of the thread network are allowed to take on their equilibrium positions, the potential energy becomes

$$V_0(\mathbf{r}_\alpha, \mathbf{r}_\beta, \cdots) = (3kT/2l^2)\sum_{\tau>\nu}\sum(1/N_{\tau\nu}) \times [(x_{0\tau} - x_{0\nu})^2 + (y_{0\tau} - y_{0\nu})^2 + (z_{0\tau} - z_{0\nu})^2]. \tag{8·13}$$

This is a function of the fixed-point coordinates only, since these determine all the $x_{0\tau}$, $y_{0\tau}$, $z_{0\tau}$; it is related to the total number of configurations

possible for the Gaussian network [Eq. (4·3)]:

$$\mathfrak{C}(\mathbf{r}_\alpha, \mathbf{r}_\beta, \cdots) = K_1 e^{-V_0/kT}. \quad (8\cdot14)$$

Now the mean x-component of force exerted on fixed point α by the thermally agitated Gaussian network is, by the usual methods of statistical mechanics,

$$kT(\partial/\partial x_\alpha)\ln\mathfrak{C} = kT(\partial/\partial x_\alpha)(-V_0/kT) = -\partial V_0/\partial x_\alpha. \quad (8\cdot15)$$

This is, of course, also the x-component of force exerted on fixed point α by the thread network in its equilibrium configuration.

IX. REGULAR CUBIC NETWORK

The regular cubic network is the simplest typical three-dimensional network. It will be discussed here both for its intrinsic interest[10] and as an illustration of the power of the methods described in the preceding section.

A regular cubic network will be defined to consist of segments all having the same number of links, connected together like the edges of a set of equal cubes filling a cubical region on the surface of which the fixed points of the network are regularly spaced. Let the network segments consist of M links each, and let there be N of these segments in each chain extending between opposite faces of the bounding cube. There will be in all $3(N-1)^2$ of these chains of MN links,

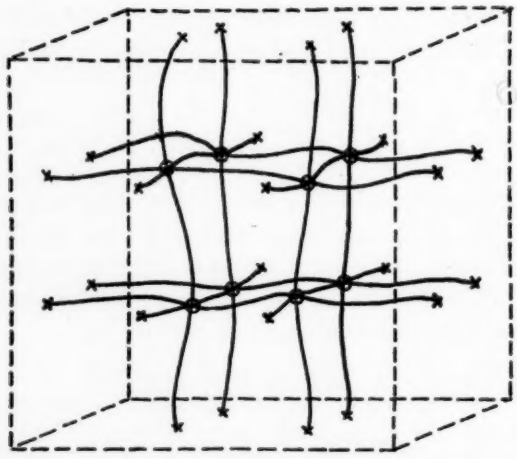

FIG. 2. Regular cubic network, $N=3$. Solid lines—Gaussian chains; ×—fixed points; ○—junctions.

[10] The results are employed by James and Guth, reference 8.

extending between fixed points

$[0, (m/N)L, (n/N)L]$ and $[L, (m/N)L, (n/N)L]$,

or

$[(m/N)L, 0, (n/N)L]$ and $[(m/N)L, L, (n/N)L]$,

or

$[(m/N)L, (n/N)L, 0]$ and $[(m/N)L, (n/N)L, L]$,

for all integral values of m and n from 1 to $N-1$. Such a network is illustrated in Fig. 2, for the case $N=3$.

The junctions of any cubic network are conveniently specified by three indices p, q, r, which give the number of segments lying between this junction and the planes $x=0$, $y=0$, and $z=0$, respectively. Let $N(r, s, t; u, v, w)$ be the number of links in the segment between the junctions (r, s, t) and (u, v, w). Then in the regular cubic network

$$\left.\begin{aligned} &N(r,s,t;u,v,w) = M, \\ &\text{if } u=r\pm1,\ v=s\pm1,\ w=t\pm1, \\ &N(r,s,t;u,v,w) = \infty, \text{ otherwise.} \end{aligned}\right\} \quad (9\cdot1)$$

Equation (9·1) defines the structure of the network; its state of extension is specified by giving the coordinates of the fixed points,

$$\left.\begin{aligned} x(r,s,t) &= (r/N)L, \\ y(r,s,t) &= (s/N)L, \\ z(r,s,t) &= (t/N)L, \end{aligned}\right\} \quad (9\cdot2)$$

where one of the three indices r, s, t, must be 0 or N.

By Eq. (8·1), the equivalent elastic-thread network consists of a cubic array of threads for each of which the stress-strain relation is given by

$$F = (3kT/Ml^2)d = \kappa d. \quad (9\cdot3)$$

The nature of the equilibrium configuration of this model is obvious:

$$\left.\begin{aligned} x_0(r,s,t) &= (r/N)L, \\ y_0(r,s,t) &= (s/N)L, \\ z_0(r,s,t) &= (t/N)L, \end{aligned}\right\} \quad (9\cdot4)$$

for all values of the indices. These are then the mean positions of the junctions of the Gaussian network.

The main problem to be considered is the calculation of $\mathfrak{N}(r, s, t)$ and $\mathfrak{N}(r, s, t; u, v, w)$, which

determine respectively the fluctuations of the coordinates of the junction (r, s, t) of the Gaussian network and the fluctuations of the relative coordinates of junctions (r, s, t) and (u, v, w) about their mean values. The determinants of the general theory are not easily calculated; we shall therefore apply the methods described in Section VIII. Specifically, we shall consider the effect of applying a unit force in the x direction to the junction (u, v, w) of the elastic thread network. This will produce a displacement $X(u, v, w; u, v, w)$ of this junction from its previous equilibrium position, and a displacement $X(r, s, t; u, v, w)$ of the junction (r, s, t). These displacements can be calculated by a method closely related to the normal-mode calculations for cubic crystals; the $\mathfrak{N}$'s can then be obtained by application of Eqs. (8·9) and (8·12).

Let any system of external forces $F(r, s, t)$, all having the x direction, be applied to the junctions of the thread network. They will produce a system of junction displacements $X(r, s, t)$, all having the x direction. The x component of the force exerted on junction (r, s, t) by the thread running to junction $(r+1, s, t)$ will be increased by

$$\Delta F=\kappa\{X(r+1, s, t)-X(r, s, t)\}, \quad (9\cdot5)$$

and similarly for the other threads entering this junction. The conditions for the static equilibrium of all junctions under the applied forces are thus

$$\begin{aligned}F(r, s, t)=\kappa\{&6X(r, s, t)\\&-X(r+1, s, t)-X(r-1, s, t)\\&-X(r, s+1, t)-X(r, s-1, t)\\&-X(r, s, t+1)-X(r, s, t-1)\},\end{aligned} \quad (9\cdot6)$$

$$r, s, t=1, 2, \cdots N-1.$$

For the fixed points,

$$X(r, s, t)=0, \text{ if } r \text{ or } s \text{ or } t=0 \text{ or } N. \quad (9\cdot7)$$

The quantities $X(r, s, t; u, v, w)$ in which we are particularly interested solve these equations for

$$F(u, v, w)=1,$$
$$F(r, s, t)=0 \text{ unless } r=u,\ s=v,\ t=w. \quad (9\cdot8)$$

It is easy to solve Eqs. (9·6) and (9·7) for a normal-mode distribution of forces given by

$$F_{abc}(r, s, t)=\sin(\pi ar/N)\sin(\pi bs/N)\times\sin(\pi ct/N). \quad (9\cdot9)$$

The indices a, b, c which distinguish the normal modes can each run from 1 to $N-1$. It is natural to expect that the normal-mode forces will produce proportional displacements of each junction:

$$X_{abc}(r, s, t)=h_{abc}\sin(\pi ar/N)\times\sin(\pi bs/N)\sin(\pi ct/N). \quad (9\cdot10)$$

The truth of this conjecture is easily proved by introduction of Eqs. (9·9) and (9·10) into Eq. (9·6); one finds that this is then satisfied for all r, s, t, provided only that

$$h_{abc}=\{4\kappa[\sin^2(\pi a/2N)+\sin^2(\pi b/2N)+\sin^2(\pi c/2N)]\}^{-1}. \quad (9\cdot11)$$

Since Eqs. (9·6), (9·7) form a linear system, any sum of solutions will be a solution. In particular, any sum of normal-mode distributions,

$$F(r, s, t)=\sum_{a, b, c} g_{abc}F_{abc}(r, s, t), \quad (9\cdot12)$$

will give rise to the displacements

$$X(r, s, t)=\sum_{a, b, c} g_{abc}X_{abc}(r, s, t). \quad (9\cdot13)$$

To solve the problem at hand it is only necessary to find constant g_{abc} such that the $F(r, s, t)$ are those specified by Eq. (9·8); the corresponding $X(r, s, t)$ are then given by Eq. (9·13).

The constants g_{abc} can be determined from Eqs. (9·8), (9·9), (9·12) by the usual method of Fourier analysis:

$$g_{abc}=(2/N)^3\sin(\pi au/N)\times\sin(\pi bv/N)\sin(\pi cw/N). \quad (9\cdot14)$$

Thus

$$X(r, s, t; u, v, w)=\frac{2}{\kappa N^3}\sum_{a, b, c}\frac{\sin(\pi au/N)\sin(\pi ar/N)\sin(\pi bv/N)\sin(\pi bs/N)\sin(\pi cw/N)\sin(\pi ct/N)}{\sin^2(\pi a/2N)+\sin^2(\pi b/2N)+\sin^2(\pi c/2N)}. \quad (9\cdot15)$$

By Eq. (8·9), one has then

$$\mathfrak{N}(r, s, t)=\frac{2M}{N^3}\sum_{a, b, c}\frac{\sin^2(\pi ar/N)+\sin^2(\pi bs/N)+\sin^2(\pi ct/N)}{\sin^2(\pi a/2N)+\sin^2(\pi b/2N)+\sin^2(\pi c/2N)}. \quad (9\cdot16)$$

Similarly, Eq. (8·12) yields

$$\mathfrak{N}(r,s,t;u,v,w)$$
$$=\frac{2M}{N^3}\sum_{a,b,c}\frac{[\sin(\pi ar/N)\sin(\pi bs/N)\sin(\pi cb/N)-\sin(\pi au/N)\sin(\pi bv/N)\sin(\pi cw/N)]^2}{\sin^2(\pi a/2N)+\sin^2(\pi b/2N)+\sin^2(\pi c/2N)}. \quad (9\cdot17)$$

To make clear the physical nature of these results it is necessary to evaluate the sums in Eqs. (9·16) and (9·17). In Eq. (9·16) it is convenient to replace $\sin^2\pi ar/N$ by $\frac{1}{2}(1-\cos 2\pi ar/N)$, and similarly for the other terms in the numerator. Let

$$I(r,s,t)=\frac{1}{N^3}\sum_{a,b,c}\frac{\cos(2\pi ra/N)\cos(2\pi sb/N)\cos(2\pi tc/N)}{\sin^2(\pi a/2N)+\sin^2(\pi b/2N)+\sin^2(\pi c/2N)}. \quad (9\cdot18)$$

One then has

$$\mathfrak{N}(r,s,t)=(M/4)\{I(0,0,0)-I(r,0,0)-I(0,s,0)-I(0,0,t)$$
$$+I(r,s,0)+I(r,0,t)+I(0,s,t)-I(r,s,t)\}. \quad (9\cdot19)$$

In a similar way one finds

$$\mathfrak{N}(r,s,t;u,v,w)=\mathfrak{N}(r,s,t)+\mathfrak{N}(u,v,w)-\frac{M}{2}\Big\{I\Big(\frac{r-u}{2},\frac{s-v}{2},\frac{t-w}{2}\Big)-I\Big(\frac{r+u}{2},\frac{s-v}{2},\frac{t-w}{2}\Big)$$
$$-I\Big(\frac{r-u}{2},\frac{s+v}{2},\frac{t-w}{2}\Big)-I\Big(\frac{r-u}{2},\frac{s-v}{2},\frac{t+w}{2}\Big)+I\Big(\frac{r+u}{2},\frac{s+v}{2},\frac{t-w}{2}\Big)$$
$$+I\Big(\frac{r+u}{2},\frac{s-v}{2},\frac{t+w}{2}\Big)+I\Big(\frac{r-u}{2},\frac{s+v}{2},\frac{t+w}{2}\Big)-I\Big(\frac{r+u}{2},\frac{s+v}{2},\frac{t+w}{2}\Big)\Big\}. \quad (9\cdot20)$$

It remains to evaluate the sums $I(r,s,t)$.

The sum $I(0,0,0)$ requires separate attention. When N is large—as will be assumed henceforward—the summand in $I(0,0,0)$ changes slowly with the indices a, b, c. The sum can then be approximated very closely by an integral:

$$I(0,0,0)\cong(2/\pi)^3\int_0^{\pi/2}dx\int_0^{\pi/2}dy\int_0^{\pi/2}dz$$
$$\times\{\sin^2x+\sin^2y+\sin^2z\}^{-1}$$
$$=(2/\pi)^2\int_0^{\pi/2}dx\int_0^{\pi/2}dy\{\sin^2x+\sin^2y\}^{-\frac{1}{2}}$$
$$\times\{1+\sin^2x+\sin^2y\}^{-\frac{3}{2}}$$
$$=(2/\pi)^2\int_0^{\pi/2}dx\{1+\sin^2x\}^{-1}$$
$$\times K(\{1+\sin^2x\}^{-1}), \quad (9\cdot21)$$

where $K(\ )$ is the complete elliptic integral. This integral has resisted evaluation in closed form; numerical integration shows that

$$I(0,0,0)\cong1, \quad (9\cdot22)$$

to within 1 percent. This may very well be the exact value.

All the quantities $I(r,s,t)$ except $I(0,0,0)$ are sums of terms with oscillating signs. They will all be smaller than $I(0,0,0)$, and the smaller the more rapid the changes in sign—that is, the larger $(r^2+s^2+t^2)^{\frac{1}{2}}$, so long as $r, s, t<N/2$. Thus, except for junctions very near one of the bounding surfaces, one can neglect all but the first term in Eq. (9·19), and write

$$\mathfrak{N}(r,s,t)\cong M/4. \quad (9\cdot23)$$

To compute the corrections to Eq. (9·23), wherever they are appreciable, it will suffice to compute $I(r,s,t)$ for r/N, s/N, $t/N\ll1$. The summand in $I(r,s,t)$ then changes slowly enough to permit replacement of the sum by an integral:

$$I(r,s,t)\cong\frac{1}{N^3}\int_0^N da\int_0^N db\int_0^N dc$$
$$\times\frac{\cos2\pi\frac{r}{N}a\cos2\pi\frac{s}{N}b\cos2\pi\frac{t}{N}c}{\sin^2\frac{\pi a}{2N}+\sin^2\frac{\pi b}{2N}+\sin^2\frac{\pi c}{2N}}. \quad (9\cdot24)$$

The integrand oscillates sinusoidally with a variable amplitude

$$[\sin^2(\pi a/2N)+\sin^2(\pi b/2N)+\sin^2(\pi c/2N)]^{-1}.$$

The integration over the regions in which a/N, b/N, or c/N are large, makes a very small contribution to the integral: the amplitude is there small and, more importantly, it changes so slowly that contributions of opposite sign to the integral from neighboring regions will very nearly cancel each other. The value of the integral is thus determined mainly by the integration over the regions of smaller a/N, b/N, c/N, where one can write with good accuracy

$$\sin^2(\pi a/2N)\cong(\pi a/2N)^2, \qquad (9\cdot25)$$

and so on; even for the larger a/N this is not a very bad approximation. It is thus a good approximation to write

$$I(r,s,t)\cong\frac{4}{\pi^2N}\int_0^N da\int_0^N db\int_0^N dc \times\frac{\cos 2\pi\frac{r}{N}a\cos 2\pi\frac{s}{N}b\cos 2\pi\frac{t}{N}c}{a^2+b^2+c^2}. \qquad (9\cdot26)$$

Extending the range of integration, we can also write

$$I(r,s,t)\cong\frac{1}{2\pi^2N}\int_{-N}^{+N} da\int_{-N}^{+N} db\int_{-N}^{+N} dc \times\frac{\exp\{(2\pi i/N)(ra+sb+tc)\}}{a^2+b^2+c^2}; \qquad (9\cdot27)$$

the sine parts of the complex exponentials contribute nothing to the integral when the range of integration is thus extended.

To evaluate this integral it is convenient to use polar coordinates. The radial coordinate will of course be

$$\rho=(a^2+b^2+c^2)^{\frac{1}{2}}. \qquad (9\cdot28)$$

As the polar axis we choose the direction of the vector

$$\mathbf{P}=r\mathbf{i}+s\mathbf{j}+t\mathbf{k}, \qquad (9\cdot29)$$

where $\mathbf{i}$, $\mathbf{j}$, $\mathbf{k}$, are unit vectors in the a, b, and c directions, respectively. Then

$$ra+sb+tc=(\mathbf{P}\cdot\boldsymbol{\rho})=(r^2+s^2+t^2)^{\frac{1}{2}}\rho\cos\theta. \qquad (9\cdot30)$$

We shall also replace the integration over a cubical region by integration over a sphere of equal volume. This change in the range of integration is of little importance, since it affects only a region that contributes little to the integral—how little will be made evident immediately. We have then

$$I(r,s,t)\cong\frac{1}{2\pi^2N}\int_0^{\pi}\sin\theta d\theta\int_0^{2\pi}d\varphi\int_0^{(6/\pi)^{\frac{1}{3}}N}d\rho \times\exp\{(2\pi i/N)(r^2+s^2+t^2)^{\frac{1}{2}}\rho\cos\theta\}. \qquad (9\cdot31)$$

Integration over the angle coordinates is simple; on a change of variable in the remaining integral, the result becomes

$$I(r,s,t)\cong\frac{1}{\pi^2}\frac{1}{(r^2+s^2+t^2)^{\frac{1}{2}}} \times\int_0^{(6/\pi)^{\frac{1}{3}}2\pi(r^2+s^2+t^2)^{\frac{1}{2}}}dx\frac{\sin x}{x}. \qquad (9\cdot32)$$

The asymptotic series for the integral on the right, for large values of the upper limit, is

$$\int_0^x dx(\sin x/x)=\pi/2-\cos x/x+\cdots, \qquad x\gg1. \qquad (9\cdot33)$$

Thus we have, to terms of the first order in the small quantity $1/2\pi(r^2+s^2+t^2)^{\frac{1}{2}}$,

$$I(r,s,t)\cong1/2\pi(r^2+s^2+t^2)^{\frac{1}{2}}, \quad r,s,t\ll N. \qquad (9\cdot34)$$

It will be noted that the approximation of neglecting higher order terms corresponds to extension of the integration of Eq. (9·31) over the whole of space; the smallness of the resultant change justified the change in limits which led to Eq. (9·31).

Since $\mathfrak{N}(r,s,t)$ is unchanged on replacing r by $N-r$, s by $N-s$, t by $N-t$, it will suffice to consider $\mathfrak{N}(r,s,t)$ when all three indices are less than $N/2$. By use of Eq. (9·34) one can then write Eq. (9·19) as

$$\mathfrak{N}(r,s,t)=\frac{M}{4}\left\{1-\frac{1}{2\pi}\left[\frac{1}{r}+\frac{1}{s}+\frac{1}{t}-\frac{1}{(r^2+s^2)^{\frac{1}{2}}} -\frac{1}{(r^2+t^2)^{\frac{1}{2}}}-\frac{1}{(s^2+t^2)^{\frac{1}{2}}}+\frac{1}{(r^2+s^2+t^2)^{\frac{1}{2}}}\right]\right\}. \qquad (9\cdot35)$$

This approximation appears to be good for all junctions, for which r, s, and t are all necessarily

1 or more. It does not apply to the fixed points (r, s, or $t=0$), for which the correct value is zero.

There is an important difference between Eq. (9·35) for a three-dimensional network and the corresponding equation for a single chain. Let us consider a single chain consisting of N segments, each containing M links. The value of $\mathfrak{N}$ for the rth junction is easily computed as follows. The chain can be treated as a network with one junction, the rth, linked to two fixed points by chains with $N_{1\alpha}=Mr$ and $N_{1\beta}=M(N-r)$ links, respectively. The network determinant Γ has a single element:

$$\Gamma=\gamma_{11}=N/Mr(N-r). \tag{9·36}$$

By Eq. (5·2),

$$\mathfrak{N}(r)=1/\gamma_{11}=Mr(N-r)/N, \tag{9·37}$$

since $\Gamma_1'=D^{(0)}=1$. In the three-dimensional network all junctions except those very near the fixed points have essentially the same value of $\mathfrak{N}$, and fluctuate about their mean positions with the same freedom. In the single chain, however, $\mathfrak{N}$ varies much more strongly along the chain, being proportional to r over a large range; the junction coordinates have a mean-square variation proportional to $r(N-r)$. It thus appears that there is danger in extending conclusions reached by considering the properties of a single Gaussian chain to three-dimensional networks.

An expression for $\mathfrak{N}(r, s, t; u, v, w)$ can now be written down by use of Eqs. (9·20), (9·34), and (9·35). We shall restrict our attention to pairs of junctions neither of which is close to a bounding surface—that is, to cases in which r, s, t, u, v, w are all large but not close to N. Then

$$\mathfrak{N}(r, s, t)\cong\mathfrak{N}(u, v, w)\cong M/4. \tag{9·38}$$

Furthermore, each of the I's in Eq. (9·20), except possibly $I[(r-u)/2, (s-v)/2, (t-w)/2]$, has at least one large argument and is negligibly small. Thus we have

$$\mathfrak{N}(r, s, t; u, v, w) \cong\frac{M}{2}\left\{1-\frac{1}{\pi}\frac{1}{[(r-u)^2+(s-v)^2+(t-w)^2]^{\frac{1}{2}}}\right\}, \tag{9·39}$$

valid for junctions far from the bounding surfaces but possibly near to each other. The correct value of $\mathfrak{N}(r, s, t; u, v, w)$ is of course 0 if $r=u$, $s=v$, $t=w$. Equation (9·39) seems to be very accurate in all other cases. The worst case is that of $|r-u|=1$, $s=v$, $t=w$, which requires the use of the approximate Eq. (9·34) for $I(\frac{1}{2}, 0, 0)$. It is, however, easy to show that the exact value of the integral $I(\frac{1}{2}, 0, 0)$ as given by Eq. (9·24) is $\frac{1}{3}$, in excellent agreement with the approximate value $1/\pi$ given by Eq. (9·34).

THE JOURNAL OF CHEMICAL PHYSICS VOLUME 15, NUMBER 9 SEPTEMBER, 1947

Theory of the Increase in Rigidity of Rubber during Cure

HUBERT M. JAMES
Purdue University, West Lafayette, Indiana

AND

EUGENE GUTH
University of Notre Dame, Notre Dame, Indiana

(Received May 5, 1947)

The rigidity of rubber, considered as a network of flexible molecules with Gaussian configuration functions, can be calculated for a particular sample if one is given a complete description of the molecular network or certain types of statistical description. In particular, it is sufficient to know the distribution of lengths and vector-mean extensions of the segments of the network, or only the latter distribution if it is of Gaussian form. The assumption that the vector-mean extensions have a Gaussian distribution corresponds to a similar postulate in the theory of Wall, and has been applied to a simplified network theory by Flory. In the complete theory it leads to calculation of the same proportionality between the rigidity of the material and the number G_a of segments, per unit volume, in the "active" part of the molecular network. However, consideration of the process of cure shows that this assumption cannot be expected to be correct, though it does lead to results of the right order of magnitude. An alternative approach to the problem is based on a study of the increase in rigidity of the material as cure proceeds. It uses a more realistic picture of the process of cure than those hitherto employed, and uses Gaussian distribution functions only where they can be logically justified. The final result is of the same form as that given by the previous theory, except that G_a is replaced by B_a, the number of bonds formed within the molecular network during cure. Since B_a is smaller than G_a by a factor of about two or more, the improved theory leads to the prediction of somewhat lower rigidities per bond formed. Available experimental results of Flory on Butyl rubber vulcanizates do not appear to give an adequate check on the quantitative features of the theory.

IN another paper on the network theory of rubber[1] we have shown that one can derive the form of the stress-strain relation for a unit cube of ideal soft rubber,

$$Z=KkT[L_z-1/L_z^2], \tag{1}$$

on the following assumptions:

(1) Soft rubber consists of a liquid-like mass of long, flexible molecules united into a network by a relatively few intermolecular bonds.

(2) The molecular network is isotropic on the average.

(3) Each segment of the network can take on a number of configurations which is a Gaussian function of the separation of its ends.

(4) The steric hindrances between the molecules (as opposed to the constraints implied by their union into a network) can be neglected.

(5) Compressibility and thermal expansion of the material are neglected. (More complicated forms arise when these factors are taken into account.)

Equation (1) is valid whatever the structure of the network. In this equation k is the Boltzmann constant. The constant K, which determines the rigidity of the material, will vary from sample to sample; to determine it theoretically one must know more about the network—whether there are few or many molecules involved in it, and so on. In particular, K for a piece of rubber will change as cure proceeds. It is the purpose of this paper to discuss the relation of K to the factors in terms of which one might specify the structure of a piece of rubber. It includes the calculation of K for a completely specified network, a discussion of the problem of determining K for a molecular network described only in a statistical sense, and the development of a third approach to the problem through a consideration of the process of cure in a more complete and more realistic way than has heretofore been attempted.

I. CALCULATION OF K FOR A COMPLETELY SPECIFIED NETWORK

A complete specification of the structure of a Gaussian molecular network will make possible calculation of the corresponding constant K.

[1] H. M. James and E. Guth, J. Chem. Phys. 11, 455 (1943).

For the purposes of the network theory of rubber, a complete description of the molecular network will include specification of (a) the "configuration function" for each segment of the network, (b) the connectivity of the network into which these segments are united, and (c) the positions of any points of the network which are subject to external constraints—the "fixed points" of the network. The configuration function for a network segment gives the relative number of configurations possible for the segment, as a function of the separation of its ends. If this is of Gaussian form—an approximation which has been thoroughly discussed in reference 1 and will be used throughout the present paper—it can be written as

$$c(N_{\tau\nu},\ |\mathbf{r}_\tau-\mathbf{r}_\nu|) = k_{\tau\nu}\exp\{-(3/2l^2N_{\tau\nu})|\mathbf{r}_\tau-\mathbf{r}_\nu|^2\}. \quad (2)$$

Here $\mathbf{r}_\tau$ and $\mathbf{r}_\nu$ are vectors specifying the positions of the end points of the segments, and $|\mathbf{r}_\tau-\mathbf{r}_\nu|$ is the distance between the end points. This is the form valid in the limit of small extensions for a chain of $N_{\tau\nu}$ independent links each of fixed length l; for other types of flexible chain it serves to define an effective number $N_{\tau\nu}$ of links in the segment. In the description of a network, l can be assigned the same value for every segment. If the network is considered as a system of junctions and fixed points joined by unbranching chain segments, its structure can then be specified completely by giving the number of links $N_{\tau\nu}$ in the segment connecting each such pair of points. Specification of the positions of the fixed points then completes the description of the network.

It has been shown elsewhere[2] how the number of configurations possible for a network of Gaussian segments can be expressed as a function of the $N_{\tau\nu}$ and the coordinates of the fixed points. Let the indices i, j, $\cdots$ refer to junctions, the indices α, β, $\cdots$ to fixed points, and the indices τ, μ, ν, $\cdots$ to points of both types; $\sum_i$ then indicates a sum over all junctions, $\sum_\alpha$ a sum over all fixed points, and $\sum_\tau$ a sum over all points of both types. The number of configurations possible for the network can then be written as

$$\mathfrak{C}=K_1\exp\Big\{-\frac{3}{2l^2}\sum\sum_{\tau>\nu}\frac{1}{N_{\tau\nu}}[(x_{0\tau}-x_{0\nu})^2 + (y_{0\tau}-y_{0\nu})^2+(z_{0\tau}-z_{0\nu})^2]\Big\}. \quad (3)$$

Here the double sum is over all pairs of junctions and fixed points, or over all segments of the network; if there is no segment of the network joining the points τ and ν, then $1/N_{\tau\nu}$ is to be taken as zero. The quantities x_{0i}, y_{0i}, z_{0i} are the mean values of the coordinates of the ith junction, whereas $x_{0\alpha}$, $y_{0\alpha}$, $z_{0\alpha}$ are identical with the fixed coordinates x_α, y_α, z_α of the fixed point α. The x_{0i}, y_{0i}, z_{0i} can be expressed in terms of the x_α, y_α, z_α as follows. Let

$$\left.\begin{aligned}\gamma_{\tau\nu}&=-1/N_{\tau\nu}, \quad \tau\neq\nu\\ \gamma_{\tau\tau}&=\sum_{\nu\neq\tau}1/N_{\tau\nu},\end{aligned}\right\} \quad (4)$$

and let Γ be the determinant of the coefficients γ_{ij}, with one row and column for each of the n junctions of the network:

$$\Gamma=\begin{vmatrix}\gamma_{11} & \gamma_{12} & \cdots & \gamma_{1n}\\ \gamma_{21} & \gamma_{22} & \cdots & \gamma_{2n}\\ \cdots & \cdots & \cdots & \cdots\\ \gamma_{n1} & \gamma_{n2} & \cdots & \gamma_{nn}\end{vmatrix}. \quad (5)$$

Let $\Gamma^{i\to x}$ be the determinant obtained by replacing the ith column of Γ by the column of constants $\sum_\alpha\gamma_{1\alpha}x_\alpha$, $\sum_\alpha\gamma_{2\alpha}x_\alpha$, $\cdots$; let $\Gamma^{i\to y}$ and $\Gamma^{i\to z}$ have the same form with y_α and z_α, respectively, replacing x_α. Then

$$\left.\begin{aligned}x_{0i}&=-\Gamma^{i\to x}/\Gamma,\\ y_{0i}&=-\Gamma^{i\to y}/\Gamma,\\ z_{0i}&=-\Gamma^{i\to z}/\Gamma.\end{aligned}\right\} \quad (6)$$

Equations (3) to (6) together give an explicit expression for $\mathfrak{C}$ in terms of the $N_{\tau\nu}$ and x_α, y_α, z_α.[3] The constant K_1 is of no interest.

In deriving Eq. (1) we may consider a molecular network which fills a unit cube when the material is unstretched; the fixed points lie on the surface of this cube with coordinates $x_\alpha^{(0)}$, $y_\alpha^{(0)}$, $z_\alpha^{(0)}$. To subject the material to a

[2] H. M. James, J. Chem. Phys. **15**, 651 (1947).

[3] A more compact expression is derived in reference 2, but it is of less interest for the developments of the present paper.

homogeneous deformation, the fixed points may be constrained to lie of the surface of a cuboid with edges L_x, L_y, L_z at points with coordinates

$$x_\alpha = x_\alpha^{(0)} L_x,$$
$$y_\alpha = y_\alpha^{(0)} L_y, \tag{7}$$
$$z_\alpha = z_\alpha^{(0)} L_z.$$

Then the x_{0i}, y_{0i}, z_{0i} are also proportional to L_x, L_y, L_z, respectively:

$$x_{0i} = x_i^{(0)} L_x,$$
$$y_{0i} = y_i^{(0)} L_y, \tag{8}$$
$$z_{0i} = z_i^{(0)} L_z,$$

where

$$x_i^{(0)} = -\Gamma^{i \to x^{(0)}}/\Gamma, \tag{9}$$

and similarly for $y_i^{(0)}$ and $z_i^{(0)}$. Then the number of configurations possible for the network becomes a Gaussian function of the external coordinates only:

$$\mathfrak{C}(L_x, L_y, L_z) = K_1 \exp\{-(K_x L_x^2 + K_y L_y^2 + K_z L_z^2)\}, \tag{10}$$

where

$$K_x = (3/2l^2) \sum\sum_{\tau>\nu} (1/N_{\tau\nu})(x_\tau^{(0)} - x_\nu^{(0)})^2, \tag{11}$$

and K_y and K_z have similar forms. If the unstretched material is isotropic on the average one must have $K_x = K_y = K_z$. Then Eq. (1) follows, with

$$K = (1/l^2) \sum\sum_{\tau>\nu} (1/N_{\tau\nu})[(x_\tau^{(0)} - x_\nu^{(0)})^2 + (y_\tau^{(0)} - y_\nu^{(0)})^2 + (z_\tau^{(0)} - z_\nu^{(0)})^2]. \tag{12}$$

This, together with Eq. (9), gives the desired explicit form for K.

II. CALCULATION OF K FOR A STATISTICALLY SPECIFIED NETWORK

In practice, one can only hope to know certain statistical properties of physically occurring networks. Any one of several statistical specifications of the network structure may serve to determine K; one of these is suggested by the results quoted in the preceding section.

We define the "vector-mean fractional extension" of a network segment as follows. The instantaneous vector extension of the network segment connecting the τth and νth junctions is (with arbitrary choice of sign)

$$\mathbf{E}_{\tau\nu} = \mathbf{r}_\tau - \mathbf{r}_\nu = \mathbf{i}(x_\tau - x_\nu) + \mathbf{j}(y_\tau - y_\nu) + \mathbf{k}(z_\tau - z_\nu), \tag{13}$$

where $\mathbf{i}$, $\mathbf{j}$, $\mathbf{k}$ are the usual unit vectors in the coordinate directions. The mean value of this vector, for all possible configurations of the network, is

$$\langle \mathbf{E}_{\tau\nu} \rangle_{Av} = \mathbf{i}(x_{0\tau} - x_{0\nu}) + \mathbf{j}(y_{0\tau} - y_{0\nu}) + \mathbf{k}(z_{0\tau} - z_{0\nu}). \tag{14}$$

The vector-mean extension of the segment is the magnitude of this vector; its vector-mean fractional extension, $\lambda_{\tau\nu}$, is this magnitude divided by $N_{\tau\nu} l$, the total length of the segment:

$$\lambda_{\tau\nu} = [(x_{0\tau} - x_{0\nu})^2 + (y_{0\tau} - y_{0\nu})^2 + (z_{0\tau} - z_{0\nu})^2]^{\frac{1}{2}}/N_{\tau\nu} l. \tag{15}$$

In terms of vector-mean fractional extensions the number of configurations possible for the network becomes simply

$$\mathfrak{C} = K_1 \exp\left\{-\tfrac{3}{2} \sum\sum_{\tau>\nu} N_{\tau\nu} \lambda_{\tau\nu}^2\right\}. \tag{16}$$

Similarly, we have from Eq. (12)

$$K = \sum\sum_{\tau>\nu} N_{\tau\nu} [\lambda_{\tau\nu}^{(0)}]^2, \tag{17}$$

where

$$\lambda_{\tau\nu}^{(0)} = [(x_\tau^{(0)} - x_\nu^{(0)})^2 + (y_\tau^{(0)} - y_\nu^{(0)})^2 + (z_\tau^{(0)} - z_\nu^{(0)})^2]^{\frac{1}{2}}/N_{\tau\nu} l \tag{18}$$

is the vector-mean fractional extension of the $\tau\nu$-segment when the material is unstretched. The sum in Eq. (17) is over all segments in a unit volume of the network; *each segment contributes to the rigidity of the material an amount proportional to the product of the number of its links and the square of its vector-mean fractional extension when the material is unstretched.* This result is independent of the detailed structure of the network.

It is thus evident that K can be determined without knowledge of the detailed structure of the network: it will suffice to know how many segments there are per unit volume of the network having any given number of links and any given value of $\lambda^{(0)}$. Let $F(N)dN$ be the

number of segments per unit volume for which the number of links lies between N and $N+dN$, and let $G(N, \lambda)d\lambda$ be the fraction of these segments which have a vector-mean fractional extension between λ and $\lambda+d\lambda$ when the material is unstretched. Then Eq. (17) becomes

$$K = \int_0^\infty dN \int_0^1 d\lambda F(N) G(N, \lambda) N \lambda^2. \quad (19)$$

This determines K in terms of two distribution functions, $F(N)$ and $G(N, \lambda)$; it will be shown later that under certain circumstances it is not even necessary to know the form of $F(N)$.

It is possible to consider as part of the network chain segments that are not actually linked into it. For such unattached segments all orientations of the vector $\mathbf{E}_{rr}$ are equally probable, and $\langle \mathbf{E}_{rr} \rangle_N$ and λ_{rr} are zero. It follows from Eqs. (17) and (19) that such unattached segments do not contribute to the rigidity of the material. The same is true of more complicated structures that are not attached to the network or to a fixed point; it is also true of all "loose ends"—segments and complex structures joined to the rest of the network at only one point. Only when a segment is subject to constraints that cause its ends to have different *mean* positions does it contribute to the rigidity of the material. It is easily seen that this requires that the segment lie on a non-retracing path through the network from one fixed point to another. The term "active network" will be applied to the aggregate to these segments.

One can hope to determine K by establishing the forms of $F(N)$ and $G(N, \lambda)$—perhaps by reference to general principles, perhaps by considering the process by which the molecular network is formed. One approach to the problem is the following. We may picture milled uncured rubber as a mass of unconnected Gaussian molecular chains which form a liquid-like mass, rather than a coherent network. In this liquid each chain segment can take on any orientation with equal probability; the vector-mean fractional extension of each segment is zero, and K is zero—the system may be very viscous, but it has no fixed form. Now let us consider the instantaneous distribution of extensions of the molecular segments in this liquid. The probability that a segment of N links has an extension r is proportional to the number of configurations of the segment consistent with that extension. The number of configurations of the *ends* of the segment consistent with separation r is proportional to r^2; the number of configurations of the segment consistent with a given configuration of the ends is given by Eq. (2). Thus the probability that the segment will have an *instantaneous* extension r, an *instantaneous* fractional extension λ_i, is proportional to

$$f(N, r) = r^2 \exp\{-(3/2l^2N)r^2\}$$
$$= N^2 l^2 \lambda_i^2 \exp\{-\tfrac{3}{2}N\lambda_i^2\}. \quad (20)$$

It would be quite in accord with some current ideas to picture the process of cure as the instantaneous introduction of bonds which convert these originally unconstrained segments into a coherent network, and to suppose that the distribution of instantaneous fractional extensions of the segments at the moment of cure is the same as the distribution of vector-mean extensions in the completed network. In that case $G(N, \lambda)$ for the network will differ from the expressions in Eq. (20) only by a normalizing factor:

$$G(N, \lambda) = (4/\pi^{\frac{1}{2}})(3N/2)^{\frac{3}{2}}\lambda^2 \exp\{-\tfrac{3}{2}N\lambda^2\}. \quad (21)$$

Then

$$K = \int_0^\infty dN \cdot NF(N) \int_0^\infty d\lambda 4/\pi^{\frac{1}{2}}$$
$$\times (3N/2)^{\frac{3}{2}}\lambda^4 \exp\{-\tfrac{3}{2}N\lambda^2\}, \quad (22)$$

whence

$$K = \int_0^\infty dN F(N) = G. \quad (23)$$

Thus K is found to be equal to G, the total number of segments per unit volume in the network, whatever may be the form of the distribution function $F(N)$.[4]

It should be emphasized at once that we do not consider this to be an acceptable solution of the problem. It is thus, however, that one must

[4] It should be noted that the integration over λ in Eq. (22) extends to infinity. The Gaussian distribution is only an approximation for any chain of finite length, and does not exclude values of λ greater than 1. The error resulting from the integration over these fictitious fractional extensions is completely negligible if N is large.

translate into terms of the complete network theory of rubber the theories of Wall[5] and of Kuhn[6] which are not explicitly network theories, and a calculation of Flory and Rehner[7] which employs a specialized and incompletely developed network theory. Wall derives an equation of the form

$$Z = GkT[L_x - 1/L_x^2] \tag{24}$$

by a formalism that, as it stands, cannot be interpreted as a network theory. One can, however, bring his calculation into correspondence with the network theory outlined in the preceding paragraph by modifying his method of counting configurations in a way that does not affect the final result for Z, and then reinterpreting his formalism. In particular, it is necessary to interpret G, which in Wall's paper is the number of molecules per unit volume, as the number of segments of the active network per unit volume. Influenced by Wall's theory, Flory and Rehner have also obtained Eq. (24) by assuming mean segment extensions which would follow from Eq. (21).

In relating his formalism to the network theory of rubber Kuhn employs the idea that the network junctions are essentially fixed in space. (We shall emphasize elsewhere how poor an approximation this is to the actual case.) If the molecules of Kuhn's theory are identified with the segments of the network, and are considered to be constrained only at the ends, then one obtains[8] Eq. (23). As thus applied, the theory assumes that the fixed (and therefore the vector-mean) extensions of the segments have the distribution given in Eq. (20). Kuhn's original formalism yielded instead

$$K = 7/3G_0, \tag{25}$$

where G_0 is the original number of molecules per unit volume. This result differs from Eq. (23) because it corresponds to a different picture of the process of cure. In effect, Kuhn treats each molecule as though its ends were converted into fixed points during the process of cure, the instantaneously existing extensions in the rubber liquid being converted into fixed extensions of the solid. These extensions would have the distribution of Eq. (21). Next, the midpoints of these molecules are suddenly converted into fixed points which divide each of the molecules into two segments. These segments will not have had distributions of extensions described by Eq. (20), since they are not portions of a *completely unconstrained* molecule; thus the resulting distribution of fixed extensions of these segments will not be given by Eq. (21). Finally, the quarter-points are suddenly converted into fixed points, each original molecule thus being divided into four segments, with a distribution of extensions different from that of Eq. (21), but related to it. If Eq. (25) is rewritten in terms of the number of segments of the completed model it becomes

$$K = 7/12G. \tag{26}$$

Kuhn has interpreted G_0 as the number of segments between points of chemical bonding, and G as the number of segments into which the network is divided by chemical bonds and "steric junction points." In any case, the G segments in question are treated as extending between fixed points, and the difference between the constant coefficients in Eqs. (23) and (26) is due to the different distributions of segment extensions implicit in the formalisms in the two cases.

All derivations of Eq. (24), with its specific value of K, depend on the assumed identity of two distribution functions: (1) the distribution of extensions of molecular segments in solid unstretched rubber, and (2) the distribution of instantaneous extensions which these same segments would have if they were completely unconstrained. This hypothesis appears to have been considered to be self-evident by its proponents, and no justification for it has been proposed.[9] It is, however, open to very serious criticism, and it appears to us that it cannot be relied upon. Our objections to it are connected with the fact that physically occurring networks

[5] F. T. Wall, J. Chem. Phys. **10**, 485 (1942).

[6] W. Kuhn, Kolloid Zeits. **76**, 285 (1936). Kuhn's original formalism is brought into closer correlation with the network theory of rubber in his recent papers; see particularly W. Kuhn, J. Polymer Sci. **1**, 380 (1946).

[7] P. J. Flory and J. Rehner, Jr., J. Chem. Phys. **11**, 512 (1943).

[8] This was first shown by L. R. G. Treloar, Trans. Faraday. Soc. **39**, 36 (1943).

[9] It is not always clearly stated that the extensions considered in the solid are the vector-mean extensions, but this interpretation is required if the result is to be understood in terms of the network picture.

are not formed all at once, but by a process of gradual growth and reinforcement which we shall now describe.

The first stage in the cure of a liquid of rubber molecules is that of gel formation. Flory[10] has shown how this occurs as long flexible molecules are bonded together. First these molecules are linked together into more complicated molecules containing two, three, or more chains. With increasing number of bonds, the more complicated molecular species occur with increasing frequency. When the number of bonds becomes sufficiently large there suddenly appears an essentially infinite molecule—a gel, or network extending throughout the material. This is at first a very tenuous structure, with low tensile strength and very small rigidity.

The second stage of cure, in which the gel is built up into a tough and relatively rigid material, is that with which we are here concerned. The amount of material in the network is increased when bonds are formed between the network and previously unattached material. Formation of these bonds does not increase the rigidity of the material, for a structure linked to the network by a single bond is only a "loose end"; it is the formation of bonds between pairs of elements within the network that increases the rigidity of the system. These bonds may link two points of the active network, thus increasing its rigidity but not the amount of material involved in it; or they may link a loose end to the active network at a second point, or to another loose end, thus incorporating new material into the active network. All these processes increase both K and the number of segments in the network, though not evidently in the same ratio. Formation of a bond between two points in the same loose end increases neither the amount of material in the active network nor the value of K.

Our objections to the assumption of Eq. (21) are then the following:

(1) The rubber network is built up by processes which involve segments constrained by their inclusion in the network—segments to which the distribution of Eq. (20) does not apply. In fact, it is only the formation of intra-network bonds that causes an increase in K.

(2) The mean extension of a molecular segment in the network is not likely to be equal to its instantaneous extension at the moment when it was incorporated into the network. The mean extension after union may be greater or less than that at the moment of union; one can reasonably expect it to be less, on the average, since the chain is not being linked to a rigid framework but to points of a yielding structure, which it can pull toward each other.

(3) Even if the segments had extensions described by Eq. (21) immediately after their incorporation into the network, they would often be subdivided into smaller segments as the process of cure continues. It is easily seen that after such subdivision has occurred the distribution of extensions of the resulting segments will not be that of Eq. (21). For example, Kuhn's theory, which can be interpreted in terms of such successive subdivisions of molecular chains, does not lead to Eq. (23).

In view of these factors it seems evident that Eq. (21) predicts segment extensions that are of the right order of magnitude, but that it would be rash to assume any higher degree of validity for that equation. Correspondingly, Eq. (24) should be right as to order of magnitude, but subject to change in the numerical factor. We have therefore re-examined the problem from a point of view which avoids these difficulties.

III. CHANGE OF K BY BOND FORMATION

The essential features of our calculation of K as it depends on cure are (a) its use of the more realistic picture of the process of cure, as outlined in the preceding section, and (b) the application of the distribution of Eq. (20) only where this is logically justified—that is, in the case of *unconstrained* molecular segments. Our fundamental assumptions are as follows: At any time during cure the material will consist of a molecular network and unattached material. We shall assume that:

(1) The network can be treated as a Gaussian network, as defined in reference 2. In particular, it will be assumed that every unbranching chain segment of the network—and of the unattached material—has a configuration function described by Eq. (2). This assumption limits our discussion to the ideal soft rubbers for which Eq. (1) can be

[10] P. J. Flory, J. Am. Chem. Soc. **63**, 3096 (1941).

deduced. It then follows from the preceding analysis (and will appear again in our further development of the theory) that the rigidity of the material is increased during cure only when a bond is formed between two elements within the network.

(2) The probability that a bond will be formed between two bondable elements of the system is proportional to the probability that these two elements, during the thermal agitation of the material, will lie in the same small volume in space. This latter probability can be derived, for arbitrary pairs of elements of the general Gaussian network, using results of reference 2.

It appears that these two assumptions, together with an assumption as to the lengths of the unbranching molecular chains in the material before cure, should completely determine the solution of the problem; in particular it should determine K as a function of the total number of bonds formed in the material during cure. The complete analysis of this problem offers formidable mathematical difficulties connected with the division of the complete network into the "active network" and "loose ends." Our more limited approach yields a relation between K and the number of bonds formed between elements of the network—not the completed network, but the network as it exists at the time of bond formation. This is a fraction of the total number of bonds that we can only estimate.

Our analysis proceeds in three steps, as follows:

(a) We consider the network as it exists at any stage in the process of cure, and compute the relative probability that the next bond to be formed within the network will be formed between any two given points of the network. This is found to be a simple function of two parameters that give a sufficient description of the relation of the two elements: ρ, the separation of their mean positions in the material, and $\mathfrak{N}_{ij}$, which determines the variability of their separation.

(b) We next compute the change in entropy of the system which would result from the formation of such a bond. This again depends essentially on ρ and $\mathfrak{N}_{ij}$.

(c) Finally, we compute the average change in K per bond formed between elements of the network, at this stage of the cure. The averaging process requires the assumption of a distribution function $g(\rho, \mathfrak{N})$ such that

$$dn = g(\rho, \mathfrak{N}) d\rho d\mathfrak{N} \tag{27}$$

in the relative number of bondable element pairs in the whole network characterized by parameter values ρ to within $d\rho$, and $\mathfrak{N}$ to within $d\mathfrak{N}$. Fortunately, because of the special characteristics of Gaussian networks, it turns out that the result of the averaging process is the same for all distribution functions $g(\rho, \mathfrak{N})$ of a large class; it is the same in the opposing limits of very small and very large network constraint, and it is essentially the same for intermediate cases when the network is of regular structure.

One is thus led with considerable assurance, though not with mathematical certainty, to the conclusion that the average change in K, per bond formed within the network, is equal to 1, and this independently of the detailed structure of the network or the state of cure of the material. It follows that

$$K = B_a, \tag{28}$$

where B_a is the total number of bonds which, during the process of cure, were established between pairs of elements in the network as it then existed, but exclusive of those established between elements of the same loose end. Discussion of the differences between this result and Eq. (23) will be deferred to Section IV. We now indicate the calculation in more detail.

A. Probability of Bond Formation Between Elements of a Gaussian Network

Let ξ, η, ζ be the relative Cartesian coordinates of network elements i and j:

$$\xi = x_i - x_j, \quad \eta = y_i - y_j, \quad \zeta = z_i - z_j. \tag{29}$$

In reference 2 it has been shown that the probability that these relative coordinates have values ξ to $\xi + d\xi$, η to $\eta + d\eta$, ζ to $\zeta + d\zeta$ is

$$dR = R_{ij}(\xi, \eta, \zeta) d\xi d\eta d\zeta, \tag{30}$$

where the probability density function R_{ij} is given by

$$R_{ij}(\xi, \eta, \zeta) = \left\{\frac{3}{2\pi l^2 \mathfrak{N}_{ij}}\right\}^{\frac{3}{2}} \exp\left\{-\frac{3}{2l^2}\frac{1}{\mathfrak{N}_{ij}} \times [(\xi - \xi_0)^2 + (\eta - \eta_0)^2 + (\zeta - \zeta_0)^2]\right\}. \tag{31}$$

In this expression ξ_0, η_0, ζ_0 are the mean and most probable values of ξ, η, ζ, and $\mathfrak{N}_{ij}$ is a parameter which determines the breadth of the distribution of the actual fluctuating values ξ, η, ζ about these mean values. Given a complete description of the network, the values of ξ_0, η_0, ζ_0, $\mathfrak{N}_{ij}$ can be calculated by methods described in reference 2.

The probability that the element i will lie in a small volume ΔV about the element j—in a volume ΔV about the point $\xi=\eta=\zeta=0$—is

$$dR=R_{ij}(0,0,0)\Delta V=\left[\frac{3}{2\pi l^2\mathfrak{N}_{ij}}\right]^{\frac{3}{2}} \times\exp\left\{-\frac{3}{2l^2}\cdot\frac{1}{\mathfrak{N}_{ij}}[\xi_0^2+\eta_0^2+\zeta_0^2]\right\}\Delta V. \quad (32)$$

The values of ξ_0, η_0, ζ_0 will depend upon the state of stretch of the material. Cure will of course be carried out when the material is unstretched, and the values of ξ_0, η_0, ζ_0 are ξ_{00}, η_{00}, ζ_{00}, respectively. According to our second fundamental assumption, the relative probability that a bond will be formed between these elements is then

$$A(\rho,\mathfrak{N}_{ij})=\left\{\frac{3}{2\pi l^2\mathfrak{N}_{ij}}\right\}^{\frac{3}{2}}\exp\left\{-\frac{3}{2l^2}\frac{\rho^2}{\mathfrak{N}_{ij}}\right\}, \quad (33)$$

where

$$\rho=[\xi_{00}^2+\eta_{00}^2+\zeta_{00}^2]^{\frac{1}{2}} \quad (34)$$

is the distance between the mean positions of the elements when the material is unstretched.

B. Change of Entropy by Bond Formation

Before introduction of a bond between elements i and j of the network, the relative coordinates ξ, η, ζ of these junctions can take on all values. Introduction of a bond restricts the possible configurations of the network to those in which ξ, η, ζ lie in a small range of values near zero, of total volume ΔV in (ξ,η,ζ)-space. Now $R_{ij}(\xi,\eta,\zeta)$ is proportional to the number of configurations of the network consistent with the indicated values of the relative coordinates of the two elements. Introduction of a bond between elements i and j will thus change the number of configurations possible for the network by a factor

$$q=R_{ij}(0,0,0)\Delta V\Big/\int_{-\infty}^{+\infty}d\xi\int_{-\infty}^{+\infty}d\eta\int_{-\infty}^{+\infty}d\zeta R_{ij}(\xi,\eta,\zeta). \quad (35)$$

The resultant change in the entropy of the system is

$$\Delta S=k\ln q=k\ln\left\{\left(\frac{3}{2\pi l^2\mathfrak{N}_{ij}}\right)^{\frac{3}{2}}\Delta V\right\} -\frac{3k}{2l^2}\frac{1}{\mathfrak{N}_{ij}}[\xi_0^2+\eta_0^2+\zeta_0^2]. \quad (36)$$

The difference in the entropy of the network with the bond and without the bond falls into two parts. The first term on the right of Eq. (36) is independent of the form of the material; the second depends on the form of the material through the quantities ξ_0, η_0, ζ_0. It follows from Eq. (8) that

$$\xi_0=\xi_{00}L_x,\quad \eta_0=\eta_{00}L_y,\quad \zeta_0=\zeta_{00}L_z. \quad (37)$$

Thus

$$\Delta S=k\ln\left[\left(\frac{3}{2\pi l^2\mathfrak{N}_{ij}}\right)^{\frac{3}{2}}\Delta V\right] -\frac{3k}{2l^2}\frac{1}{\mathfrak{N}_{ij}}[\xi_{00}^2L_x^2+\eta_{00}^2L_y^2+\zeta_{00}^2L_z^2]. \quad (38)$$

Only the second, shape-dependent term in the entropy will be of further interest to us, since it alone contributes to the rigidity of the material

C. Average Change in K per Bond Formed

We have now to find the average change in the shape-dependent entropy of the material, and the corresponding change in K, per bond formed in the material.

First of all, we restrict our attention to element pairs with the same values of $\mathfrak{N}$ and ρ^2. These element pairs will have all orientations in space with equal probability when the material is unstretched. Averaging over all these element pairs, we have then

$$\langle\xi_{00}^2\rangle_{Av}=\langle\eta_{00}^2\rangle_{Av}=\langle\zeta_{00}^2\rangle_{Av}=\tfrac{1}{3}\rho^2. \quad (39)$$

It follows that the average change in the shape-

dependent entropy of the material, per bond formed between element pairs with the same values of $\mathfrak{N}$ and ρ, is

$$\langle \Delta S \rangle_{Av} = -(k/2l^2)(\rho^2/\mathfrak{N})[L_x^2+L_y^2+L_z^2]. \quad (40)$$

The corresponding change in the stress Z required to produce unilateral stretch of a unit cube at constant volume is

$$\langle \Delta Z \rangle_{Av} = (\rho^2/l^2\mathfrak{N}) \cdot kT[L_z - 1/L_z^2]. \quad (41)$$

Comparison with Eq. (1) shows that the average change in K, per bond formed between elements with given $\mathfrak{N}$ and ρ, is

$$\Delta K = \rho^2/l^2\mathfrak{N}. \quad (42)$$

Equation (42) shows that certain types of bonds will give $\Delta K = 0$ and will make no contribution to K. Bonding of one piece of unattached material to another, or to the network, makes no contribution to K because the bonded elements were previously subject to no constraints on their relative motion: $\mathfrak{N} = \infty$. Bonds within the same piece of unattached material, or between elements in the same loose end of the network, will not contribute to K because the bonded elements had previously the same mean position: $\rho = 0$. In the calculation of K one is thus primarily interested in bonds formed between elements of the network, exclusive of those formed between elements of the same loose end; only these bonds contribute to K. The total number of such bonds introduced during cure, per unit volume of the material, we denote by B_a; this can be expected to be nearly equal to the total number of bonds formed between elements of the network. B will denote the total number of bonds formed in unit volume of the material, without regard to whether or not they contribute to K. In a similar way we shall distinguish two distribution functions, $g(\rho, \mathfrak{N})$ and $g_a(\rho, \mathfrak{N})$. The function $g(\rho, \mathfrak{N})$ describes, as shown in Eq. (27), the distribution of values of ρ and $\mathfrak{N}$ for all element pairs in unit volume of the material; $g_a(\rho, \mathfrak{N})$ describes the distribution of ρ and $\mathfrak{N}$ among element pairs within the network only, exclusive of those in the same loose end—in short, pairs of elements such that a bond between them would increase K and B_a.

We can now compute the average change in K per bond formed in a unit cube of the material: $\langle dK/dB \rangle_{Av}$. The relative probability that the bond will be formed between elements with given ρ and $\mathfrak{N}$ is equal to the product of the number of such element pairs in the material, as described by the distribution function $g(\rho, \mathfrak{N})$, and the probability per element pair that a bond will be formed, as given by Eq. (33). Then the required average is

$$\langle dK/dB \rangle_{Av} = \frac{\int_0^\infty d\rho \int_0^\infty d\mathfrak{N} g(\rho, \mathfrak{N}) A(\rho, \mathfrak{N}) \langle \Delta K \rangle_{Av}}{\int_0^\infty d\rho \int_0^\infty d\mathfrak{N} g(\rho, \mathfrak{N}) A(\rho, \mathfrak{N})}, \quad (43)$$

or

$$\langle dK/dB \rangle_{Av} = \frac{1}{l^2} \frac{\int_0^\infty d\rho \int_0^\infty d\mathfrak{N} g(\rho, \mathfrak{N}) \rho^2 \mathfrak{N}^{-5/2} \exp\{-(3/2l^2)(\rho^2/\mathfrak{N})\}}{\int_0^\infty d\rho \int_0^\infty d\mathfrak{N} g(\rho, \mathfrak{N}) \mathfrak{N}^{-3/2} \exp\{-(3/2l^2)(\rho^2/\mathfrak{N})\}}. \quad (44)$$

Similarly, one has

$$\langle dK/dB_a \rangle_{Av} = \frac{1}{l^2} \frac{\int_0^\infty d\rho \int_0^\infty d\mathfrak{N} g_a(\rho, \mathfrak{N}) \rho^2 \mathfrak{N}^{-5/2} \exp\{-(3/2l^2)(\rho^2/\mathfrak{N})\}}{\int_0^\infty d\rho \int_0^\infty d\mathfrak{N} g_a(\rho, \mathfrak{N}) \mathfrak{N}^{-3/2} \exp\{-(3/2l^2)(\rho^2/\mathfrak{N})\}}. \quad (45)$$

Equation (45) will be more useful to us than Eq. (44), because of the simpler form of $g_a(\rho, \mathfrak{N})$. The function $g(\rho, \mathfrak{N})$ differs from $g_a(\rho, \mathfrak{N})$ in that it applies not only to the element pairs within the network, but also to a large number of element pairs with $\rho=0$ or $\mathfrak{N}=\infty$, because of the presence of unattached material and loose ends. One can reasonably expect $g_a(\rho, \mathfrak{N})$ to be a smoothly-varying function of its arguments; $g(\rho, \mathfrak{N})$ differs from $g_a(\rho, \mathfrak{N})$ by the addition of integrable infinities at $\rho=0$ and $\mathfrak{N}=\infty$. The numerators in Eqs. (44) and (45) are identical, since $g(\rho, \mathfrak{N})$ and $g_a(\rho, \mathfrak{N})$ differ only at points where other factors in the integrand vanish; the denominators differ by a factor $\langle dB_a/dB\rangle_{Av}$. In the early stages of cure, when a relatively small fraction of the material is included in the network, this factor will be small; in the later stages, as more and more unattached material and loose ends are incorporated into the active network, it will approach the value 1. To avoid a discussion at this point of the distribution of material between the active network, unattached material, and loose ends, we shall concentrate our attention on Eq. (45).

If the form of $g_a(\rho, \mathfrak{N})$ is regarded as subject to arbitrary choice one can make the right-hand side of Eq. (45) take on any chosen value. On the other hand, complete statistical analysis of the process of cure should lead to a definite prediction of the form of g_a at each stage of the cure, and a corresponding value of $\langle dK/dB_a\rangle_{Av}$. In default of this complete analysis, we have been lead to consideration of a number of special models. It is a surprising fact that these models, though they represent quite different limiting cases, lead to the same value of $\langle dK/dB_a\rangle_{Av}$—a value which can therefore be regarded with some assurance as representing the result of a more complete analysis, at least approximately. We turn now to a consideration of these special models.

D. Special Forms of the Distribution Function

In physically occurring networks the mean positions of the network elements will be distributed through space with uniform average density. Correspondingly, one would expect that the relative coordinates ξ_{00}, η_{00}, ζ_{00} of pairs of these mean positions will be uniformly distributed. This is not strictly true if the system contains loose ends and unattached material which contribute a disproportionate number of element pairs with $\xi_{00}=\eta_{00}=\zeta_{00}=0$. It is easily shown, however, that it is true for the active part of any random Gaussian network, and it remains true if loose ends are randomly attached to such a network, so long as one does not count pairs of elements in the same loose end. Thus we must expect a uniform distribution of values of ξ_{00}, η_{00}, ζ_{00} among the element pairs described by the distribution function $g_a(\rho, \mathfrak{N})$. The corresponding distribution of values of ρ is proportional to ρ^2. Physically reasonable forms of g_a must then all have the property that

$$P(\rho)=\int_0^\infty d\mathfrak{N} g_a(\rho, \mathfrak{N})=c\rho^2, \tag{46}$$

where c is a constant.

Independent Elements. The first limiting case to be considered is that in which all bondable elements take on their positions essentially independently of each other. This limit is approached by a network formed of very long molecular chains bonded together at a relatively few points. Each element of such a network will be surrounded for the most part by elements of other chains—elements which can be reached only by a relatively long path through the network. The relation of these chain elements is then almost the same as if they were separate molecules in an ordinary liquid: the probability that element i will be found in a given position is independent of the position of element j, except as this may be affected by the direct steric hindrances that come into play only when the elements are immediately adjacent. In neglecting the relatively small probability of bond formation between elements of the same network segment, and the very small correlations between the motions of elements of different segments of the network, one obtains the limiting case of independent elements.

It is shown in reference 2 that the probability distribution for the coordinates of the ith element of a Gaussian network is of the form

$$P_i(x_i, y_i, z_i)=\left\{\frac{3}{2\pi l^2\mathfrak{N}_i}\right\}^{\frac{3}{2}} \exp\left\{-\frac{3}{2l^2}\frac{1}{\mathfrak{N}_i} \times[(x_i-x_{0i})^2+(y_i-y_{0i})^2+(z_i-z_{0i})^2]\right\}, \tag{47}$$

where $\mathfrak{N}_i$ is a parameter which determines the breadth of the distribution of the coordinates x_i, y_i, z_i in the same way that $\mathfrak{N}_{ij}$ does that of the relative coordinates ξ, η, ζ of the ith and jth junctions. A similar parameter $\mathfrak{N}_j$ describes the breadth of the distribution of coordinates of the jth junction. It can be shown (reference 2, Section VII) that when the ith and jth junctions are independent (the limiting case of weak coupling), then

$$\mathfrak{N}_{ij}=\mathfrak{N}_i+\mathfrak{N}_j, \tag{48}$$

whatever may be the value of ρ. The value of $\mathfrak{N}_i$ will vary from element to element, and $\mathfrak{N}_{ij}$ will vary from pair to pair, but there will be no correlation between the values of $\mathfrak{N}_{ij}$ and ρ: the distribution of values of $\mathfrak{N}_{ij}$ will be the same for all ρ. This, together with Eq. (46), shows that for this limiting case

$$g_a(\rho, \mathfrak{N})=\rho^2 f(\mathfrak{N}), \tag{49}$$

where $f(\mathfrak{N})$ is a function of still undetermined form. On substituting Eq. (49) into Eq. (45) and carrying out the integration over ρ, one finds

$$\langle dK/dB_a\rangle_{Av}=\int d\mathfrak{N} f(\mathfrak{N})/\int d\mathfrak{N} f(\mathfrak{N})\equiv 1, \tag{50}$$

whatever the form of the function $f(\mathfrak{N})$.

Strongly Coupled Elements. We next consider the opposite case to the preceding, that of pairs of elements as strongly coupled as is consistent with the separation of their mean positions. The strongest possible correlation in positions is shown by elements of the same chain segment. We therefore consider first a single Gaussian chain of N links, with ends fixed at the points $(0, 0, 0)$ and $(0, 0, L)$. Let elements i and j of this chain be separated by a segment of n links. It is easily shown (see, for instance, Section IX, reference 2) that for this pair of elements

$$\rho=(n/N)L, \quad \mathfrak{N}_{ij}=n(N-n)/N. \tag{51}$$

If the chain is very long, $N\gg n$, then

$$\mathfrak{N}_{ij}/\rho\cong N/L. \tag{52}$$

To this approximation the value of $\mathfrak{N}/\rho$ for the strongly coupled pairs of elements in the chain is independent of ρ, just as the value of $\mathfrak{N}$ is independent of ρ in the case of independent elements.

In a network consisting of many long segments the ratio $\mathfrak{N}/\rho$ will vary from segment to segment. There will then be a distribution of values of $\mathfrak{N}/\rho$ for pairs of elements within the segments, but it will be the same distribution for all values of ρ. (Strictly this will be true only so long as ρ is less than the extensions of the long segments. Since only pairs of elements with small ρ are likely to be bonded together, this limitation is of little importance.) If we pass to the limit of strong coupling by assuming this to be true for all element pairs in the material, we have

$$g_a(\rho, \mathfrak{N})=\rho f(\mathfrak{N}/\rho); \tag{53}$$

the form of the multiplying factor in ρ is determined by Eq. (46). On introducing this expression into Eq. (45), changing the variables of integration to

$$x=\mathfrak{N}/\rho, \quad y=\rho^2/\mathfrak{N}, \tag{54}$$

and integrating over y, one finds

$$\langle dK/dB_a\rangle_{Av}=\int dx f(x)/\int dx f(x)\equiv 1, \tag{55}$$

whatever the form of $f(x)$.

A generalized form of Eq. (53) leads to the same result. If the distribution of values of $\mathfrak{N}/\rho^n$ is independent of ρ, then

$$g_a(\rho, \mathfrak{N})=\rho^{2-n} f(\mathfrak{N}/\rho^n). \tag{56}$$

If $n\neq 2$, introduction of the variables

$$x=\mathfrak{N}/\rho^n, \quad y=\rho^2/\mathfrak{N}, \tag{57}$$

and integration over y leads again to Eq. (55). For $n=2$ the integrals do not converge.

Regular Cubic Network. The relation between the limiting cases treated above becomes especially clear on consideration of a special network —the regular cubic network discussed in detail in reference 2, Section IX. This consists of segments, all of M links, connected into a network with the connectivity of a cubic lattice. This network extends between the faces of a cube with edges of length L, on which the fixed points of the network are regularly arranged; the faces of the cube will be taken to be the planes $x=0$, $x=L$, $y=0$, $y=L$, $z=0$, $z=L$. The number N of segments in each chain extending between opposite faces of the cube will be assumed to be large. Each junction of the network will be distinguished by three indices, r, s, t, which give the number of network segments

lying between that junction and the planes $x=0$, $y=0$, $z=0$, respectively. Each of these indices can range from 1 to $N-1$.

It is shown in reference 2 that the mean coordinates of junction (r, s, t) are $(rL/N, sL/N, tL/N)$. The separation of the mean positions of junctions (r, s, t) and (u, v, w) is thus

$$\rho(r, s, t; u, v, w) = (L/N)[(r-u)^2 + (s-v)^2 + (t-w)^2]^{\frac{1}{2}}. \quad (58)$$

The parameter $\mathfrak{N}_i$ of Eq. (47) is essentially the same for all junctions except those very near the fixed points on the bounding surfaces:

$$\mathfrak{N}(r, s, t) \cong M/4. \quad (59)$$

The parameter $\mathfrak{N}_{ij}$ for junctions (r, s, t) and (u, v, w), not too near the bounding surfaces, is

$$\mathfrak{N}(r, s, t; u, v, w) \cong \frac{M}{2}\left\{1 - \frac{1}{\pi}\frac{1}{[(r-u)^2+(s-v)^2+(t-w)^2]^{\frac{1}{2}}}\right\}. \quad (60)$$

For the junctions of this network one has then the relation

$$\mathfrak{N} = M/2\{1-(1/\pi N)(L/\rho)\}. \quad (61)$$

If the junctions of this network were independent one would have, by Eq. (48), $\mathfrak{N}=M/2$. Thus Eq. (60) shows that the coupling of immediately adjacent junctions of the network has an appreciable effect on the distribution of their relative coordinates, reducing $\mathfrak{N}$ by some 30 percent. This coupling, however, decreases rapidly with increasing difference in the ordinal numbers of the junctions; junctions more than a few segments removed from each other take on their positions almost independently. This is true whatever the values of L and N. The condition for effective independence of two elements is thus that $\rho \gg L/N$. If L is relatively small—that is, if the network is not greatly extended—junctions with small ρ will nevertheless be essentially independent. On the other hand, it is clear from Eqs. (33) and (60) that bonding is likely to occur even between elements with $\rho > \{Ml^2\}^{\frac{1}{2}}$, which is the r.m.s. separation of the ends of an unconstrained chain segment of M links. Thus most of the bonds introduced at random into this network will link essentially independent elements if

$$L/N \ll \{Ml^2\}^{\frac{1}{2}}; \quad (62)$$

the network elements can be treated as independent if the network constraints are so small that the segments have vector-mean fractional extensions small compared with the ordinary r.m.s. average extensions they would have if they were unconstrained.

It is easily shown that $\mathfrak{N}$ for two elements in the same segment of a regular cubic network approaches the number of intervening links as this number becomes small. In this limit one finds

$$\mathfrak{N} = n, \quad \rho = (n/M)\cdot(L/N). \quad (63)$$

Such elements are strongly coupled in the sense already discussed. If

$$L/N \gg \{Ml^2\}^{\frac{1}{2}}, \quad (64)$$

bonds introduced at random will for the most part link such strongly coupled element pairs; the limiting case of strongly coupled elements is approached by a regular cubic network in which the network constraints are strong and result in large vector-mean extensions of the segments.

The intermediate case,

$$L/N \cong \{Ml^2\}^{\frac{1}{2}} \quad (65)$$

probably corresponds more closely to physically occurring networks than either of the limiting cases. It can be discussed as follows. Equation (61) strictly applies only to pairs of network *junctions*, for which ρ is not a continuous variable, and is never less than L/N. If we consider all element pairs, $\mathfrak{N}$ must be a continuous function proportional to ρ when this becomes small. The relation

$$\mathfrak{N} = \frac{M}{2}\left\{\frac{\rho}{\rho + L/N\pi}\right\} \quad (66)$$

approximates Eq. (61) very well wherever that equation is applicable. For small ρ it gives $\mathfrak{N} \cong \pi/2(MN/L)\rho$, whereas Eqs. (63) show that for element pairs in the same segment one should have $\mathfrak{N} \cong (MN/L)\rho$; nevertheless it can be expected to be a good representation of the situation in a regular cubic network when all element pairs, whether in the same or in different network segments, are taken into account.

The form of g_a corresponding to Eq. (66) is

$$g_a(\rho, \mathfrak{N}) = \rho^2 \delta\left(\mathfrak{N} - \frac{M}{2}\left\{\frac{\rho}{\rho + L/N\pi}\right\}\right), \quad (67)$$

where δ is the usual singular function which gives unit integral over any range including the origin but vanishes except when the argument is zero. Equation (45) then becomes

$$\langle dK/dB_a \rangle_{Av} = \frac{1}{l^2} \frac{\int_0^\infty d\rho \rho^4 [(\rho+a)/c\rho]^{5/2} \exp\{-(3/2l^2)\rho^2(\rho+a)/c\rho\}}{\int_0^\infty d\rho \rho^2 [(\rho+a)/c\rho]^{3/2} \exp\{-(3/2l^2)\rho^2(\rho+a)/c\rho\}}, \quad (68)$$

where

$$c = M/2, \quad a = L/N\pi. \quad (69)$$

On changing the variable of integration to y, with

$$y^2 = (3/2l^2c)\rho(\rho+a), \quad (70)$$

and introducing the parameter

$$b = \{3a^2/2cl^2\}^{\frac{1}{2}} = \{3L^2/\pi^2N^2Ml^2\}^{\frac{1}{2}}, \quad (71)$$

one obtains

$$\langle dK/dB_a \rangle_{Av} = \tfrac{2}{3} \frac{\int_0^\infty dy y^4 \exp[-y^2]\{1+[b/(b^2+4y^2)^{\frac{1}{2}}]\}}{\int_0^\infty dy y^2 \exp[-y^2]\{1+[b/(b^2+4y^2)^{\frac{1}{2}}]\}}. \quad (72)$$

In the limit of independent elements, $b \to 0$, or strongly coupled elements, $b \to \infty$, the last factor in the two integrals of Eq. (72) becomes constant over the range of integration, and one obtains the results already noted in Eqs. (50) and (55). For other positive values of b this factor decreases monotonely from 2 to 1 as y increases from 0 to ∞. The presence of this factor decreases the numerator by a larger factor than it does the denominator, since the larger values of y contribute relatively more to the numerator. Thus, one can easily prove,

$$\langle dK/dB_a \rangle_{Av} \leq 1 \quad (73)$$

for all positive values of b. The intermediate case described by Eq. (65) corresponds to $b \cong \frac{1}{2}$, for which numerical evaluation of Eq. (72) yields $\langle dK/dB_a \rangle_{Av} \cong 0.96$. The minimum value of this quantity, ~ 0.92, is obtained with $b \cong 1.5$.

It thus appears to be a good approximation in any case, and a safe upper limit, to take $\langle dK/dB_a \rangle_{Av} = 1$. Integration of this equation with respect to B_a yields the already stated result of this approach to the problem:

$$K = B_a. \quad (28)$$

IV. COMPARISON OF THE THEORETICAL RESULTS

We have now to discuss the relation between the result of Wall's theory, $K = G$, and the result obtained by us in the preceding section.

Let the system to be considered consist originally of N unbranching molecular chains. Each bond introduced into the system will increase the total number of chain segments by two: a bond formed between two different segments (or chains) will divide each segment into two, and a bond formed between two elements of a single segment will divide this into three. If B bonds are introduced, the total number of segments in the system will become

$$G = 2B + N. \quad (74)$$

If Wall's postulate concerning the distribution of extensions of molecular segments [Eq. (21)] is to be introduced into the network theory, it must certainly apply only to the vector-mean extensions of the segments of the active network; all other segments, whether of loose ends or unattached material, have $\lambda = 0$ and contribute nothing to K. Let the active network, stripped of all loose ends, contain G_a segments, and let there be J junctions in this network. Each of

these junctions will form the end point of either three or four segments. It is then clear that

$$\tfrac{3}{2}J<G_a<2J<2B. \tag{75}$$

Each chain attached to the network will include at least two segments, the terminal segments, which are not part of the active network. If all chains are attached to the network one has also

$$G_a<G-2N=2B-N. \tag{76}$$

The degree of inequality will depend on the nature of the network; the difference will be large if loose ends make up a considerable part of the structure.

The quantity B_a of Eq. (28) is unlike G_a in that it cannot be determined by observation of the completed network. B_a is the number of bonds introduced as intra-network bonds *when they were formed;* examination of simple cases will show that a given network can be built up by alternative processes for which B_a has different values. One may term G_a a "structural" quantity, since it can be determined from the network structure, and B_a a "historical" quantity, since to determine it one must know the history of the network—that is, the process by which it is formed. The relation between B_a and G_a, like that between B_a and K, or G_a and K, is thus only a statistical relation.

Concerning the relation between B_a and G_a, the following remarks can be made. A bond formed between different loose ends will contribute 1 to B_a, and 1 or *more* to G_a; the increase in G_a may be large if the loose-end structures are complicated. A bond formed within a single segment of the active network will increase B_a by 1, but will not change G_a; the loop thus formed in the segment is a loose end, and when it is stripped off the added bond will not subdivide the original segment. A bond formed between two different segments of the active network, or between a loose end and a segment of the active network, will increase B_a by 1, and G_a by two or more. Processes of the last types will certainly dominate in the latter stages of network formation, and it is reasonable to expect

$$G_a\cong 2B_a. \tag{77}$$

It thus appears that our theory predicts a value of K which is less by a factor of about 2 than that given by Wall's theory, amended by replacing G by G_a.

A comparison of theory with experiment has been carried out by Flory.[11] Flory treats the inequality of Eq. (76) as an equality, but finds for a series of Butyl rubber vulcanizates that the

---

[11] P. J. Flory, Chem. Rev. **35**, 51 (1944). In this review article Flory makes a number of incorrect or misleading statements about our work which we take this opportunity to correct.

(1). Flory states that Eq. (3.3) of reference 1 is in error by a factor of 3. Actually it is correct, and in agreement with the result which he gives in his own paper. As was noted in our explanation of Eq. (2.5), $\langle L^2\rangle_{Av}$ is, in the three-dimensional case, the mean-square value of a *component* of the extension of the chain; in Flory's notation it is $1/2\beta^2$.

(2). As concerns a very simple network model introduced in reference 1 for purposes of visualization, Flory seriously misstates the justification given for its use and gives a false idea of the importance to be attached to its introduction. Instead of presenting as a justification the quite trivial observation indicated by Flory, we gave an extensive analysis of the behavior of a general network of Gaussian flexible chains. Along with other results, this led to the conclusion that the entropy forces exerted by an arbitrary network, and hence the entropy itself, was the same as that for a very simple "network" of independent chains from which cross linkages were entirely absent. For illustrative purposes in certain derivations we used this simple model, but all results hold for the general model with Gaussian chains.

(3) In speaking of our use of "springs" Flory apparently expresses a distaste for a discussion of the problem in terms of average forces rather than of thermodynamic functions. In statistical mechanics these methods are of course equivalent.

(4) Flory states that certain equations relating to this model are dimensionally incorrect. Actually they are correct, though the notation may disguise this fact. M is the effective number of chains crossing unit area in the unstretched material; its dimensions are reciprocal length squared. N is the number of links per unit length of molecular chain in the unstretched state of the material; it has the dimensions of reciprocal length. In equations involving this model $\langle L^2\rangle_{Av}=\frac{1}{3}Nl^2$ has therefore the dimensions of length. The physical significance of M and N is discussed in the Appendix to reference 1, p. 481.

(5) After noting that almost all the chains of a well-cured piece of rubber will be linked to the network, Flory indicates that this result is in contradiction to our estimate that 25 percent of the total material is "actively involved" in the network. We do not wish to attach undue significance to our estimate, which was admittedly rough. It is, however, necessary to note that Flory's estimate and ours do not apply to the same quantity. Flory's statistical theory lumps together all material of all chains connected into the network, whether by one bond or by many. In the "active part of the network," with which we were dealing, one has to do only with portions of chain which contribute to the forces. A molecule linked to the network by only one bond does not contribute at all to the active part; molecules linked at two points contribute, on the average, about half their length.

(6) Our failure to arrive at a definite value of K in reference 1 was not due to such use as we made of the independent chain network, but to our desire to avoid unjustifiable postulates. One can introduce special postulates which lead to a value of K into that model quite as readily as into any other model. We prefer the approach to the problem given in this paper.

theoretically predicted rigidity, with $K=G_a$, is less than the observed rigidity by a factor of about 2.1. If Flory's results are correct there is then a discrepancy of a factor of about 4 between observation and the theory of Section III.

Flory has suggested several possible origins for this discrepancy between theory and his observations. He suggests that entanglements—that is, steric hindrances of the sort neglected in the theory of Gaussian networks—may have the same effect as bond formation. In a paper now in preparation we shall discuss the effect of such entanglements. It appears to us that their effect should be small when the network segments are long and the material is but little stretched; their effect should be greater in more highly cured materials, and at greater extensions. The fact that Flory's observations are made at 300 percent elongation would favor increased importance of these steric hindrances. On the other hand, Flory's stress-strain curves have essentially the form of Eq. (1), whereas steric hindrances would modify this form; furthermore, the discrepancy between experiment and theory is less for the more highly cured materials, rather than greater, as we would expect if the effect is one of steric hindrances.

We attach greater importance to another point made by Flory, concerning a peculiarity of Butyl rubber—the limited number of points at which cross linking can occur. Our theory has assumed that there are so many points of bonding that all relative positions of bondable elements occur with equal probability. If the bondable elements in the chains are widely scattered the small values of ρ will be relatively few. In such a case, the average increase in K per bond formed may be much greater than that given by our theory. For instance, a treatment of the regular cubic network of Section III, with the assumption that only the junction elements are bondable, leads to calculation of a value of $\langle dK/dB_a \rangle_{Av}$ which may be much larger than 1 if the junction points are not close together. A repetition of Flory's experiments, with other types of rubber, is much to be desired.

It seems also to be possible that Flory's estimate of the number of bonds introduced during cure is in error by a considerable factor. Flory has determined this quantity by use of the theory of gelation. Walling[12] has attempted to check the theoretical predictions of Stockmayer[13] as to the point of gelation, in the case of the systems methyl methacrylate-ethylene dimethacrylate and vinylacetate-divinyladipate. Walling succeeds in checking the qualitative features of Stockmayer's formulas but notes that "observed extents of reaction at the gel-point are in general found to be several times those calculated, particularly in experiments in which early gel-points are to be anticipated." If such a discrepancy is present in Flory's observations, his estimate of the number of bonds formed in cure of his materials may be several-fold too low. This factor alone would go far toward accounting for the discrepancy between theory and experiment.

[12] C. Walling, J. Am. Chem. Soc. **67**, 441 (1945).
[13] W. H. Stockmayer, J. Chem. Phys. **12**, 124 (1944).

Letters to the Editor

THIS section will accept reports of new work, provided these are terse and contain few figures, and especially few halftone cuts. The Editorial Board will not hold itself responsible for opinions expressed by the correspondents. Contributions to this section should not exceed 600 words in length and must reach the office of the Managing Editor not later than the 15th of the month preceding that of the issue in which the letter is to appear. No proof will be sent to the authors. The usual publication charge ($4.00 per page) will not be made and no reprints will be furnished free.

Thermodynamics of Crystallization in High Polymers

II. Simplified Derivation of Melting-Point Relationships[1,2]

PAUL J. FLORY
The Goodyear Research Laboratory, Akron, Ohio
July 24, 1947

RECENT attempts to treat crystallization in polymers by statistical thermodynamical methods, have yielded several relationships between the melting temperature and polymer constitution. The melting-point composition relationship derived for copolymers, for example, is analogous to the freezing-point composition relationship for ideal mixtures of simple molecules (see Eq. (4) below). As is also shown by x-ray studies, the structural units of polymers occupy a role corresponding to the molecules of simple substances. While a comprehensive treatment covering various complicating circumstances which may be anticipated in crystaliine polymers is somewhat cumbersome, the essentials devoid of these complications can be presented briefly as follows.

A chain polymer containing identical units A will be considered, these units are capable of forming a crystal lattice. Other units B, unable to enter the crystal lattice characteristic for A, also may be present. It will be assumed that the structure of the liquid can be described in terms of a pseudo-lattice, each cell of which is occupied by a polymer segment. (The configurational segment is assumed to be identical with the structural unit in the present treatment.) The formation of a crystallite composed of σ-chains in its cross section and ζ-units in length, requires first of all the location of a planar array of σ-cells each occupied by type-A units. Each of these A units must be succeeded by an uninterrupted sequence of $\zeta-1$ additional A units if the array is to be acceptable as a nucleus for the formation of a crystallite of the prescribed length. The probability of such a constellation will be $W_\zeta{}^\sigma$, where W_ζ is the probability of a sequence of ζ A segments in a given chain, starting with an arbitrarily selected unit. The corresponding entropy term will be $k\sigma \ln W_\zeta$.

It is further required that the segments (units) involved become aligned in perfect array, packed in the more dense arrangement of the crystal lattice. The entropy associated with this step wiil be assumed, as an approximation, to be proportional to the number of units, i.e., the entropy change will be expressed as $-\sigma\zeta s_u$, where s_u is the entropy of fusion per unit when $W_\zeta-1$. Actually, the configurational entropy contribution, which may account for the major part of the entropy of fusion, should be taken proportional to $\zeta-1$ (see Eq. (8) of reference 3).

The total entropy change involved in the formation of the crystallite will be

$$-\Delta S_f=\sigma(R \ln W_\zeta-\zeta s_u), \tag{1}$$

where ΔS_f represents the total entropy of fusion expressed in molar units. The free energy of fusion is correspondingly

$$\Delta F_f=\sigma\zeta[h_u-Ts_u+(RT/\zeta) \ln W_\zeta]. \tag{2}$$

In the case of a random copolymer containing a "mole" fraction X_A of A units, $W_\zeta=X_A{}^\zeta$. Hence,

$$\Delta F_f=\sigma\zeta(h_u-Ts_u+RT \ln X_A). \tag{3}$$

The equilibrium condition at which $T=T_m$, the temperature ("melting point") for complete disappearance of crystallinity, may be applied by differentiating with respect to either σ or ζ and equating to zero, giving

$$1/T_m=s_u/h_u-(R/h_u) \ln X_A.$$

Setting $s_u/h_u=1/T_m{}^0$ where $T_m{}^0$ refers to the melting point for the polymer composed exclusively of A units,

$$1/T_m-1/T_m{}^0=-(R/h_u) \ln X_A. \tag{4}$$

Corresponding expressions may be derived similarly for the melting points of non-random copolymers as functions of their compositions and the kinetic factors governing order along the chain.

If the polymer chains are composed exclusively of A units, but are limited in length, $W_\zeta=(x-\zeta+1)/x$, where x is the number of repeating units per molecule. Substituting in Eq. (2) and proceeding as above, there is obtained in the limit of vanishing ζ

$$1/T_m-1/T_m{}^0=R/xh_u.$$

However, the more detailed treatment leads to an additional term arising from the increased concentration of ends of molecules in the liquid phase. Thus,

$$1/T_m-1/T_m{}^0=(R/xh_u)(1+1/z), \tag{5}$$

where z is the number of configurational segments per structural unit. If the molecules are of random length such that the probability of continuation of the chain from one unit to the next is p,

$$1/T_m-1/T_m{}^0=(R/h_u)[-\ln p+(1-p)/z], \tag{6}$$

which is approximately equivalent to Eq. (5) if x is replaced by its number average $\bar{x}_n$.

A direct measurement of the heat of fusion of a high polymer invariably yields a value dependent on the degree of crystallinity, the latter being difficult to determine. By means of the above relationships the latent heat (and the entropy) for the transformation from totally crystalline to amorphous polymer may be deduced readily from mere melting-point measurements on polymers of known constitution.

[1] The work on which this paper is based comprises a part of a program of fundamental research on rubber and plastics being carried out under contract between the Office of Naval Research and the Goodyear Tire and Rubber Company.
[2] Contribution No. 142 from the Goodyear Tire and Rubber Company Research Laboratory.
[3] P. J. Flory, J. Chem. Phys. **10**, 51 (1942).

Thermodynamics of Crystallization in High Polymers

III. Dependence of Melting Points of Polyesters on Molecular Weight and Composition[1,2]

ROBERT D. EVANS, HAROLD R. MIGHTON, AND PAUL J. FLORY
The Goodyear Research Laboratory, Akron, Ohio
July 24, 1947

ALTHOUGH fairly definite melting points have been assigned to a number of crystalline polymers and to a few copolymers, no adequate systematic study has been carried out either on the effects of molecular weight or on the influence of copolymer composition on the melting point. Recently we have undertaken in this laboratory a comprehensive investigation of the dependence of melting point and crystallinity on polymer constitution. Linear condensation polymers are especially well suited for this purpose and we have chosen the polyester, decamethylene adipate, for the preliminary experiments reported here.

Various copolymers have been prepared in which a portion of the decamethylene or the adipate residue is replaced by another glycol or dibasic acid radical. Decamethylene adipate polymers, varying in molecular weight and in the nature of the end groups have been prepared also. Melting points of these polymers and copolymers can be reproducibly measured using a micro-melting point apparatus, consisting of a low power microscope equipped with an electrically heated hot stage. The sample, located in the hot stage, is observed between crossed Polaroid sheets using transmitted light while the temperature is raised slowly. So long as crystallinity remains, the sample appears bright in a dark field. The fairly sharp disappearance of this manifestation of depolarization marks the "melting point," corresponding to complete disappearance of crystallinity.

The melting points of decamethylene adipate copolyesters in which 20-mole percent of the glycol or acid residues was replaced by the indicated comonomer residue, are presented in Table I. The same molar percentage of each of the first three comonomers lowers the melting point by the same amount in accordance with the theory presented in the preceding communication.[3] The melting-point depression for the copolymer containing sebacate units, however, is appreciably less, indicating that the sebacate unit may occur within the crystallites.

When the proportion of the co-ingredient is varied, a plot of $1/T_m$ *vs.* $\ln X_A$, where X_A is the mole fraction of decamethylene adipate units, is linear in agreement with theory.[3] Eutectic compositions can be located in analogy with simple binary mixtures. From the slope of the $1/T_m$ *vs.* $\ln X_A$ plot a heat of fusion of 3800 calories per decamethylene adipate unit is computed from Eq. (4) of the preceding paper.[3]

TABLE I. Melting points of decamethylene adipate copolyesters.

Comonomer group	η in poises at 218°C	m m. pt. (°C)
None	6800	81 –81.5
Isophthalate	600	64.5–65.5
cis-quinitol	310	66.5–67.5
Resorcinol	160	64 –65
Sebacate	770	72 –75

TABLE II. Effect of molecular weight on the melting point of decamethylene adipate.

$\bar{x}_n$	η in poises at 109°C	m m. pt. (°C)	m. pt. (°C) calc from Eq. (7)
2.5	0.171	42.5–45.5	45.3
5.05	0.616	62 –64	62.0
7.6	1.60	67 –68	67.8
15.75	18.1	72.5–74	71.2
19.75	31.3	74 –75	74.0
85 est.	6800*	81 –81.5	80.0

* Viscosity determined at 218°C.

The dependence of the melting point on the average number of structural units (the unit consisting of one decamethylene and one adipate radical) is shown in Table II for polymers terminated with benzoate groups. In agreement with Eqs. (5) and (6) of the preceding communication,[3] $1/T_m$ varies linearly with $1/\bar{x}_n$; i.e.,

$$1/T_m - 1/353 = 7.69 \times 10^{-4}/\bar{x}_n, \qquad (7)$$

from which the melting points given in the last column of Table II have been computed. Comparing Eq. (7) with (6)[3]

$$h_u/(1+1/z) = 2600 \text{ cal.},$$

which, in conjunction with the above value for h_u, leads to a not unreasonable value between 2 and 3 for z.

Decamethylene adipates having hydroxyl or carboxyl (or both) end groups, melt higher than benzoate terminated polymers of the same degree of polymerization. Occurrence of these smaller end groups within the crystal lattice affords a likely explanation for this observation.

We have concluded from these preliminary experiments that melting points of polymers depend in a systematic fashion on polymer constitution and that quantitative relationships can be traced. The results appear to be in accord with the theory outlined above.

[1] The work on which this paper is based comprises a part of a program of fundamental research on rubber and plastics being carried out under contract between the Office of Naval Research and the Goodyear Tire and Rubber Company.
[2] Contribution No. 143 from the Goodyear Tire and Rubber Company, Research Laboratory.
[3] See Paul J. Flory, J. Chem. Phys. 15, 684 (1947).

Resonance Energies from Thermal Data

T. L. COTTRELL AND L. E. SUTTON
Physical Chemistry Laboratory, Oxford, England
July 3, 1947

IN a recent paper Dewar[1] discussed the discrepancy between the values for resonance energies of benzene derivatives found by the Pauling-Sherman method from heats of combustion and by the Kistiakowsky method from heats of hydrogenation, and suggested that it is due to differences in internal kinetic energy between cyclic and open-chain compounds. In particular, he predicted that the heat of formation of cyclohexane should be greater than that calculated from the bond-energy sum by an amount equal to the difference between the resonance energy of benzene obtained by the two methods.

Recent data show that in fact the heat of formation of cyclohexane is the same as that calculated from bond energies obtained from the normal paraffins. The discrepancy between the two ways of obtaining resonance

energies of benzene derivatives proves to be due to the use of incorrect bond-energy values. No special explanation in terms of differences in stability between cyclic and open-chain structures is necessary, since the required bond energies may be derived from open-chain compounds.

The bond energies in the normal paraffins reach constant values with increasing chain length. From Rossini's data[2] for the heats of formation of the paraffins, and values of 126.3 and 51.71 kcal. as the heats of formation per gram atom of carbon and hydrogen, respectively, in their standard states from monatomic gases at 298.1°K[3], the the C−C and C−H bond energies are found to be 60.3 and 87.1$_5$ kcal. The sum of these bond energies gives the heat of formation of *n*-hexane exactly, and using them we obtain 1407.6 kcal. for the heat of formation of cyclohexane from atoms, which is in very good agreement with the value of 1407.8 obtained from Rossini's data.[4]

With the above C−C and C−H values, that for the C=C energy may be obtained from Rossini's data[5] for the heats of formation of the monoölefin hydrocarbons, which were obtained by combining heats of hydrogenation with specific heat and heat of combustion data. For olefins with the double bond in the 1 position, this tends to a constant value of 101.2 kcal. With these bond energies, the apparent resonance energy of benzene is 41 kcal., in disagreement with hydrogenation result of 36. If, however, the heats of formation of the isomeric olefins are considered, and the other bond energies taken as constant, the C=C energy is found to vary from, for example, 101.3 in 1-henene to 107.2 in 2,3-dimethyl-2-butene. This is, of course, the well-known substitution effect noted by Kistiakowsky,[6] which persists to a considerable extent at 0°K.[7] The hexene in which the double bond most nearly resembles that found in an unsubstituted ring is clearly *cis* 3-hexene, for which the C=C energy is found to be 102.9 kcal. Using this C=C value, we obtain for the resonance energy of benzene 36 kcal. in agreement with the hydrogenation value. Similarly for 0-xylene, two of the C=C bonds may be taken as equivalent to that in 2-methyl-2-butene, and the third as equivalent to that in *cis* 3-hexene, which reduces the derived resonance energy by 12 kcal. to 34. Again, with Rossini's value for the heat of combustion of styrene,[8] and appropriate C=C energies obtained from non-cyclic compounds as before, the resonance energy of styrene obtained by the two methods agrees. That it is legitimate to consider the double bond in a ring structure as similar to a *corresponding* double bond in an olefin is shown by the fact that the heat of hydrogenation of non-cyclic compounds of the type CHR=CHR (*cis*) is the same as that of cyclohexene.

We should point out that while for convenience we have assumed that bond-energy differences are localized in the C=C bond, this is a purely formal treatment; some change may occur in other bond energies.

[1] Trans. Faraday Soc. **42**, 767 (1946).
[2] Prosen and Rossini, J. Research Nat. Bur. Stand. **34**, 263 (1945).
[3] Coates and Sutton, to be published.
[4] Prosen, Johnson, and Rossini, J. Research Nat. Bur. Stand. **37**, 51 (1946).
[5] Prosen and Rossini, J. Research Nat. Bur. Stand. **36**, 269 (1946).
[6] Kistiakowsky *et al.*, J. Am. Chem. Soc. **58**, 137 (1936).
[7] Rossini, Chem. Rev. **27**, 1 (1940).
[8] Prosen and Rossini, J. Research Nat. Bur. Stand. **34**, 59 (1945).

The Detection of Free Radicals in Hydrogen Atom Reactions

G. M. Harris and A. W. Tickner
Department of Chemistry, University of Saskatchewan, Saskatoon, Saskatchewan, Canada
July 2, 1947

A LARGE number of investigations of reactions of hydrogen atoms with various substances have been made making use of the discharge tube method of Wood and Bonhoeffer.[1] With organic vapors, the mechanisms of such reactions have invariably been explained in terms of free organic radical chains.[2] However, no direct evidence for the existence of free radicals in such reacting mixtures has heretofore been reported. The Paneth-Rice technique for the detection of free radicals,[3] successfully applied in the past to photo-chemical and thermal decomposition reactions, has been recently adapted by the present authors to the hydrogen atom reaction problem.

A mirror of metal known to be insensitive to atomic hydrogen but sensitive to free organic radicals was deposited by condensation in a vacuum on a water-cooled glass finger, and introduced into the reaction chamber of the apparatus. Bismuth was adopted as the mirror metal in our work because of the ready availability (from uranium extraction residues) of its radioisotope of atomic weight 210, the activity of which is eminently suitable for tracer use. Preliminary experiments confirmed the non-removal of a radioactive bismuth mirror in the presence of atomic hydrogen alone, thus eliminating the possibility of the formation of a stable volatile hydride under the conditions of our experiments.

A volatile compound known to be easily decomposed at room temperature by atomic hydrogen, dimethyl mercury, was selected for trial. Previous work[4] had suggested a free radical mechanism to explain the products, which are free mercury and a methane-ethane mixture. It was readily demonstrated that no direct reaction occurred between the dimethyl mercury vapor and the bismuth mirror in the absence of atomic hydrogen within the temperature range 20° to 45°C. With the mirror maintained at 20°C, which was about 5° cooler than the prevailing room temperature, the presence of the hydrogen atom-dimethyl mercury reaction mixture resulted in a rapid clouding up of the mirror with condensed mercury vapor, and within a few minutes it was completely concealed by mercury droplets. Radioactivity measurements indicated that part of the bismuth was transported to a trap cooled in liquid air, some distance removed from the reactor, and recoverable from this trap as a volatile compound. However, after 20 minutes treatment most of the bismuth still remained on the cooled finger, apparently amalgamated with the mercury.

The experiment was repeated, this time maintaining the bismuth mirror at a temperature of 45°C. In this case, the mirror disappeared almost completely within the 20-minute reaction period, and the resulting volatile bismuth compound was shown to have been transported to the liquid air trap by means of radioactivity measurements, as before. The mercury formed in the reaction condensed as a grayish fog on the surrounding walls of the reactor, which were at

room temperature, and consequently about 20° cooler than the bismuth mirror.

Our experiments thus prove that a volatile bismuth compound, presumably the trimethyl, is formed when dimethyl mercury is decomposed by atomic hydrogen in the vicinity of thin deposits of metallic bismuth. The fact that the mercury produced in the reaction was prevented from amalgamating with the mirror metal when the latter was slightly warmer than the reactor walls, provides strong evidence that the dimethyl mercury-hydrogen atom reaction was a gas phase process, and not merely a heterogeneous reaction on the surface of the bismuth deposit. The volatile bismuth compound must result, therefore, from direct reaction between alkyl radicals and the mirror. Full details of our technique and of correlative experiments now under way in this laboratory will be published elsewhere at a later date.

[1] G. Glocker and S. C. Lind, *The Electrochemistry of Gases and Other Dielectrics* (John Wiley & Sons, Inc., New York, 1939), p. 115.
[2] E. W. R. Steacie, *Atomic and Free Radical Reactions* (Reinhold Publishing Corporation, New York, 1946).
[3] F. Paneth and W. Hofeditz, Ber. **62B**, 1335 (1929); F. O. Rice and K. K. Rice, *The Aliphatic Free Radicals* (Baltimore, 1935).
[4] G. M. Harris and E. W. R. Steacie, J. Chem. Phys. **13**, 559 (1945).

Absorption by Hydrogen Sulfide in the 3.5μ–4.5μ Region*

EARL A. WILSON, JR. AND PAUL C. CROSS
Brown University, Providence, Rhode Island
July 24, 1947

THE percent absorption by 90 cm of H_2S at 1-atmosphere pressure is plotted against wave number in Fig. 1. This spectrum was obtained with a fluorite prism

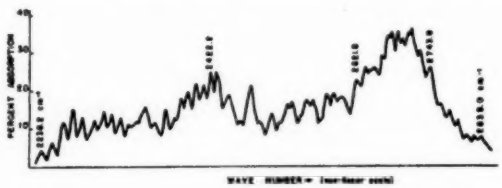

FIG. 1. Absorption by 90-cm atmos. of hydrogen sulfide in the 3.5μ–4.5μ region.

spectrometer which had a resolution of about 6 cm^{-1} in this region.

Theoretically, it is possible for three vibrational transitions (ν_σ, ν_π, and $2\nu_\delta$) to contribute to this absorption. It is especially noteworthy that considerable absorption is observed in the region 2620 cm^{-1} – 2450 cm^{-1}, where the *P*-branch of ν_σ may be expected to appear according to the calculations of Hainer and King,[1] but contrary to the reports of Nielsen and co-workers.[2]

A detailed tabulation of the absorption peaks at this resolution would be of little use unless accompanied by an analysis of the band envelope. A complete analysis will probably require new measurements at higher resolution.

* This work was performed under a contract between Brown University and the Office of Naval Research.
[1] R. M. Hainer and G. W. King, J. Chem. Phys. **15**, 89 (1947).
[2] H. H. Nielsen and E. F. Barker, Phys. Rev. **37**, 727 (1931); A. D. Sprague and H. H. Nielsen, J. Chem. Phys. **5**, 85 (1937); R. H. Nobel and H. H. Nielsen, Phys. Rev. **71**, 484 (1947).

The Magnitude of the Experimental Error in the Adsorption of Nitrogen at 78°K on Various Surfaces

W. V. LOEBENSTEIN AND V. R. DEITZ
National Bureau of Standards, Washington, D. C.
July 7, 1947

THE adsorption isotherms of nitrogen at −195°C have been widely used in recent years to determine the surface areas of solids. The published values for the surface areas have covered the range from about 2000 square meters per gram to about 0.1 square meter per gram. If the surface area is large, a small sample of about one gram is sufficient in the experimental procedure for the adsorption measurements. However, for materials of small surface areas, it is necessary to take large samples and, hence, use adsorption tubes with comparatively large dead spaces. It is the purpose of this note to ascertain that part of the experimental error which may result from the use of the various sized adsorption tubes which are necessary to accomodate adsorbents of widely varying surface areas.

Assuming the perfect gas laws to apply to the gas phase measurements, the following expression gives the number of moles, n, of gas adsorbed for a given initial point in an adsorption measurement.

$$n = p_i V_B/300R - p_e V_B/300R - p_e V_D/78R, \qquad (1)$$

where p_i = initial pressure of nitrogen introduced into the buret system.
p_e = equilibrium pressure of nitrogen after exposure to sample at 78°K.
V_B = volume of nitrogen (S.T.P.) in the buret system.
V_D = volume of nitrogen (S.T.P.) in the dead space of the adsorption tube.
R = gas constant (in appropriate units).

Room temperature is taken as 300°K and the temperature of the liquid nitrogen as 78°K.

If δn be the variation in the number of moles adsorbed, then the general expression for the percentage error is:

$$\frac{100\delta n}{n} = 100\left[\frac{(V_B)p_i + (V_B - 3.85V_D)\delta p_e + (p_i - p_e)\delta V_B + (3.85p_e)\delta V_D}{V_B(p_i - p_e) - 3.85p_e V_D}\right] \qquad (2)$$

where δp_i, δp_e, δV_B, and δV_D are the corresponding variations in p_i, p_e, V_B, and V_D, respectively. It is to be noted,

TABLE I.

	Sample (g)	B.E.T. Surface area (m^2/g)	V_L (ml)	δV_D (ml)	Pressures (mm Hg) initial p_i	Pressures (mm Hg) equilibrium p_e	V_B (ml)	Percentage error $\frac{100\delta n}{n}$
Cement*	21.5	1.5	15.3	0.15	104.0	39.2	123.	1.1
Cotton*	31.1	0.7	121.	1.21	184.7	34.6	125.	10.4
Bone char (1)	1.92	121.	7.0	0.07	562.	156.	150.	0.20
Bone char (2)	1.92	121.	7.0	0.07	428.	0.4	47.	0.27
Glass spheres	12.29	0.93	16.3	0.16	232.8	67.6	50.1	1.9
Activated cocoanut shell charcoal	0.71	1720.	5.7	0.06	392.7	0.3	149.8	0.12
Titanium oxide	1.08	9.9	4.1	0.04	131.4	78.9	49.9	2.1

* Data kindly furnished through the courtesy of R. L. Blane of this Bureau.

since variations may be positive or negative, that all the signs in the numerator of the above fraction are taken to be positive in order to obtain the maximum percentage error. The expression for the pressure drop, $p_i - p_e$, will always be positive.

An accuracy of ±0.1-mm Hg may be readily attained in the range of pressure measurements that are dealt with. Hence, δp_i and δp_e may each be set equal to 0.1. An accuracy of ±0.1 milliliter in V_B may also be easily realized, since a calibration of the buret space with mercury is possible before the apparatus is assembled. Therefore, $\delta V_B = 0.1$. The dead space volume is generally determined by a calibration with helium. A reasonable value in the accuracy of such a measurement is 1 percent. The value for δV_D may be determined, consequently, by multiplying the value for V_D by 0.01.

The data contained in Table I were observed in a number of different adsorption tubes. These calculations were made for the first point of each isotherm. The calculation for subsequent points becomes more complicated, and the equation above is not directly applicable. It is obvious that the error in obtaining subsequent points is cumulative. Nevertheless, it is felt that the treatment above is indicative of the relative accuracy of this type of measurement.

It should be noted that the absolute accuracy of the surface determination includes other factors than those treated here. These other quantities are dependent on the validity of the assumptions in the B.E.T. theory and on the density of packing of the adsorbed nitrogen molecules. Since the dead space is obtained by a helium calibration, the above consideration shows that it is necessary to make this calibration with an accuracy adequate to the particular application.

The Formation of Per-Compounds in Relation to Electronegativities

A. D. WALSH
Laboratory of Physical Chemistry, Cambridge, England
July 3, 1947

IT is pertinent to add to the letter of M. Haissïnsky,[1] under the above title, the following remarks. They are largely taken from recent communications[2] in which we have surveyed some of the many factors that determine bond strengths.

It is clear that the electronegativity of the groups at either end of a bond is a very important factor in determining the strength of the bond. The bond strength commonly increases with the electronegativity of the bonded groups. Examples are numerous[2, 3] and the point has recently been stressed by Gordy[3] who has given an empirical relation between bond strength and the product of the electronegativities of the groups concerned. It is equally clear, however, that the increase of bond strength with electronegativity of bonded groups can only be true up to a certain point: if the electronegativities are too great there will be insufficient electron density in the 'shared' region between the nuclei that is all important for bonding purposes. In other words, high bond strength also requires adequate atomic orbital overlap, and too high an electronegativity of the bonded groups may result in reduced overlap. We therefore expect the rule of increasing bond strength with increasing electronegativity product to break down when we come to consider bonds between highly electronegative groups. Thus it is not surprising that Gordy's relation fails for the OO bond in H_2O_2 and probably for the FF bond.[2] As regards the OO bond the indications[2, 4] are that the strength *increases* with substitution of *less* electronegative groups for H. Similarly, the FF bond is *weaker* than the FCl bond, FF is weaker than FH, OO weaker than OH, and NN weaker than NH. If we accept the structure (*I*) advocated by Ingold and Ingold[5] for N_2O_4, the dissociation energy of the NN bond is 13 kcal./mole. The bond energy (E) must be distinguished from the dissociation energy[2, 6] but is likely also to be very low since the stretching force constant (k) is only 1.5×10^5 dyne/cm. In hydrazine,[2] however, E(NN) appears to be ~64 kcal./mole, with k(NN) $=3.6\times10^5$ dyne/cm. The great reduction of NN strength in N_2O_4 relative to N_2O_4 can be explained as caused by reduced overlap in the NN bond of N_2O_4 consequent

(*I*)

upon the high dipole $\begin{pmatrix}\delta+\delta-\\ NO_2\end{pmatrix}$ in each NO_2 group. Glyoxal affords a similar example,[2] the CC bond strength appearing to be considerably weaker than considerations of the conjugation between its two C=O groups alone would indicate.

The conclusion of M. Haissïnsky that elements whose electronegativities are smaller than a certain amount form per-compounds while those whose electronegativities are greater than this amount do not form per-compounds finds a natural explanation in terms of this factor of reduced atomic orbital overlap consequent upon too great an electronegativity. It is an important point of peroxide chemistry that the OO bond, to be strong, needs groups of *low* electronegativity attached to it.

[1] M. Haissïnsky, J. Chem. Phys. **15**, 152 (1947).
[2] Walsh, J. Chem. Soc., in press (2 papers).
[3] W. Gordy, J. Chem. Phys. **14**, 305 (1946).
[4] Walsh, Trans. Faraday Soc. **42**, 264 (1946).
[5] Ingold and Ingold, Nature, **159**, 743 (1947).
[6] Walsh, Trans. Faraday Soc. **43**, 60 (1947).

Addendum: A Relation between Bond Order and Covalent Bond Distance

[J. Chem. Phys. **15**, 284 (1947)]

H. J. BERNSTEIN
Division of Chemistry, National Research Council, Ottawa, Canada

THE paper, by G. N. Copley,[1] presenting the same model for obtaining multiple carbon bond distances as that which appeared in the appendix of this paper, has just come to my attention. Copley treats CC, CN, CO bonds and requires an empirical correction factor to his relation between bond order and bond distance.

[1] G. N. Copley, Chem. Ind. 663 (1941).

Structure-Optical Studies

I. X-Ray Diffraction by Addition Compounds of Halogens with Hydrophilic Organic Polymers

C. D. WEST
Polaroid Corporation, Cambridge, Massachusetts
July 14, 1947

IODINE, bromine, and iodine bromide can be incorporated in high concentrations in films or fibers of many hydrophilic organic high polymers, crystalline and amorphous, natural and artificial. Examples are starch, cellulose, polyvinyl alcohol (PVA), the polyamides called Nylon (not previously reported), and many of their derivatives. These polymers are all transparent in the visible, while the halogens by themselves absorb light in this region. It is easy to show that an increase in the absorption coefficient of the halogen generally accompanies its incorporation into the polymer, indeed a well-defined new, strong band often appears in the visible (blue starch-iodine). By a high concentration of, e.g., iodine on PVA, is meant about 30 percent by weight of free iodine, accompanied by an amount of hydrogen or alkali iodine which may be varied between wide limits. The presence of halogen in these preparations in the known orthorhombic, or any other three-dimensional crystal form, is readily excluded by x-ray diffraction study.

The polymers named (save starch), including such substantially amorphous PVA derivatives as the borate and the commercial butyral can be put into well-oriented uniaxial states by methods involving unidirectional stretching, if they do not naturally occur in this state. When the halogen is incorporated into such well-oriented preparations, then strong uniaxial positive dichroism accompanies the enhanced light absorption.[1]

We have photographed, by monochromatic x-ray diffraction under widely varying conditions, many such dichroic preparations and find, nearly without exception, a single constant characteristic feature on the pictures: a pair of diffuse continuous layer lines, which are also observable in the second and third orders under favorable conditions. This can only indicate diffraction by independent line gratings, which are here extended straight chains of halogen atoms all lying parallel to the orientation or absorption direction. The periodicities of the halogen chains are substantially independent of the original periodicity of the oriented organic polymer (if any) and are for iodine 3.10, for bromine 2.70, for iodine bromide 2.90A, with individual values possibly varying up to 0.15A from these figures. Besides these characteristic diffractions, accessory diffractions in other directions and varying to some extent with the mode of preparation are not uncommon, e.g., with PVA-iodine; these, however, need not affect the present arguments. Only rarely are the characteristic diffractions absent when they would be expected, such exceptions could be accounted for by picturing the halogen chains as short, or crooked, or both. With *unoriented* preparations, including those of starch-iodine, a diffuse halo corresponding in position to the first characteristic continuous layer line can usually be seen; by themselves such haloes can prove little in the present problem, but they do have a certain confirmatory interest.

The foregoing periodicities are much shorter than the unbonded separations of halogen atoms (4.3A for I—I, etc.) and are somewhat greater than the single bond separations (2.7A for I—I, etc.). Shortened distances between known atom pairs, AB, usually mean either a hydrogen bond between A and B, or the bonding of both A and B to a central atom C, or a direct bond of some kind between A and B. The foregoing data suggest that only the third possibility comes into question here; the halogens in these preparations form bonds with each other at 180°, weaker than single covalent bonds but much stronger than van der Waals attractions, they are therefore properly called linear polymeric halogens or polyhalogens for short. Such a picture is consistent with the observed small fugacity of halogen in these preparations, and with the observed optical properties. Concerning the probable mode of interaction (if any) between halogens and oxygen or nitrogen atoms in the organic polymer, which confer hydrophilic properties on the latter, one can for the present only speculate within two limitations: first, such interaction cannot depend on any crystalline or long-range order of the ligher atoms; second, the incorporation of the halogen does not affect the infra-red absorption spectrum of the organic polymer over the range 3–15 mu, so far as we are able to determine.

The several previous explanations for these addition compounds, of which the latest was made by Rundle and coworkers,[2] require revision to account for the characteristic x-ray diffractions which we consider to be the single most important clue to their structure.

[1] E. H. Land and C. D. West in J. Alexander, *Colloid Chemistry* (Reinhold Publishing Corporation, New York, 1946), Volume 6, Chapter 6, pp. 160–90.
[2] R. Rundle, J. Foster, and R. Baldwin, J. Am. Chem. Soc. **66**, 2116 (1944).

Activation in Unimolecular Reactions*, **

O. K. RICE[1]
Clinton Laboratories, Oak Ridge, Tennessee
July 9, 1947

THE decomposition of nitrogen pentoxide remains first order to extremely low pressures, of the order of 0.01 mm. Kassel[2] has shown that to account for this it is necessary, using the most probable model for the system of oscillators comprising the molecule, to suppose that the diameter for collisional activation and deactivation is about 20×10^{-8} cm. Recently Ogg** has made an ingenious suggestion which appears to account for this characteristic of the reaction, as well as a number of other features, without any excessive collision diameters. It is supposed that the equilibrium

$$N_2O_5 \rightleftarrows NO_2+NO_2$$

is established, and that the dissociated products of this equilibrium can occasionally react

$$NO_3+NO_2 \rightarrow NO_2+O_2+NO$$

to give the decomposition. Working out this mechanism shows that the reaction should be first order to arbitrarily low pressures; the apparent observed falling off in the

rate constant at very low pressures presumably indicates that an appreciable fraction of the N_2O_5 is dissociated.

A brief historical note, which will indicate where this explanation stands in relation to the theory of unimolecular reactions, may be in order. In the early days of the discussion of these reactions it was supposed that the equilibrium fraction of activated molecules would be given by the simple exponential $e^{-Q/RT}$, where Q is the activation energy. The rate of activation could not be faster than the rate of deactivation which would occur if there were no reaction and consequently no draining away of activated molecules. This in turn would be equal to the number of collisions made by the activated fraction of molecules, $e^{-Q/RT}$, with other molecules. It was in general impossible, on this basis, to account for a sufficiently rapid rate of activation to maintain the reaction. It was soon pointed out,[3] however, that in the case of a molecule with many internal degrees of freedom, the fraction of molecules with energy greater than Q is much greater than $e^{-Q/RT}$. All this energy may be considered as activation energy if the molecule is capable of transferring energy between the internal degrees of freedom, and in particular to the bond which is to break in the reaction. Thus it is possible to account for much larger rates of activation. This comes about because there are many ways in which the excess energy necessary for activation can be distributed among the various oscillators of the molecule, thus increasing the probability, or the entropy, of the activated molecules. Anything which increases this entropy may increase the rate of activation. For example, if the energy levels of an activated molecule are much closer together on the average than those in the normal state of the molecule, the rate of activation is increased. This can be important when the number of degrees of freedom is small.[4]

It is now apparent how Ogg's suggested mechanism fits into the scheme. The activated state of the molecule is actually the separated pair NO_2+NO_3 which has an extremely high entropy. The rate of activation can, therefore, be large. In fact, the difference in entropy between the activated and normal states increases with decreasing pressure in such a way as to render the rate of activation independent of the pressure. But the assumption that activation occurs while the parts of the molecule are separated is essentially a device for increasing the rate of activation.

* This document is based on work performed under Contract No. W-35-058-eng-71 for the Atomic Energy Project at the Clinton Laboratories.

** A remark on the note, "The Mechanism of Nitrogen Pentoxide Decomposition," by R. A. Ogg, Jr., J. Chem. Phys. **15**, 337 (1947).

[1] On leave 1946–47 from the University of North Carolina.

[2] L. S. Kassel, *The Kinetics of Homogeneous Gas Reactions* (Reinhold Publishing Corporation, New York, 1932) p. 182.

[3] G. N. Lewis and D. F. Smith, J. Am. Chem. Soc. **47**, 1514 (1925); J. A. Christiansen, Proc. Camb. Phil. Soc. **23**, 438 (1926); C. N. Hinshelwood, Proc. Roy. Soc. London **113A**, 230 (1926); O. K. Rice and H. C. Ramsperger, J. Am. Chem. Soc. **49**, 1617 (1927); see also Kassel, reference 3, p. 94.

[4] O. K. Rice, J. Chem. Phys. **9**, 258 (1941).